CZECH TECHNICAL UNIVERSITY IN PRAGUE

Faculty of Civil Engineering

Experimental Centre

Geopolymer based composite
as a new material in underground building industry

DOCTORAL THESIS

Ing. Alexey Manaenkov

Doctoral degree program: Civil engineering

Branch of study: Physical and material engineering

Supervisor: Doc. Ing. Jiri Litos, Ph.D.

Consultant: Doc. Ing. Jiří Němeček, Ph.D.

Prague, 2020

Prohlášení

Jméno doktoranda: Alexey Manaenkov

Název disertační práce: Geopolymer based composite as a new material in underground building industry

Prohlašuji, že jsem uvedenou dizertační práci vypracoval samostatně pod vedením školitete Doc. Ing. Jiri Litos, Ph.D.

Použitou literaturu a další materiály uvádím v seznamu použité literatury.

V Praze dne 30. 7. 2020   _____

Alexey Manaenkov

Acknowledgements

Table of contents

List of Abbreviations

GP   Geopolymer

Geopolymer (Z)   Zlosyn sand based geopolymer composite

Geopolymer (K)   Kaznejov sand based geopolymer composite

XRPD   X-ray powder crystallography

FTIR   Fourier transform infrared spectroscopy

CTU   Czech Technical University

UHPC   Ultra-high-performance concrete

GGBFS   Ground granulated blast-furnace slag

SS   Sodium silicate

SH   Sodium hydroxide

CLUZ   Ceske Lupkove Zavody

List of Figures

List of Tables

1. Literature review

1.1.   *Introduction*

Building materials, such as hardened clay, gyps, quicklime, and others were used in the civil and building engineering as binder materials by humanity for many millenniums. One of them - unrivaled Portland cement called such name in the middle of the XVI century, is widely applied in the building industry until now. It has an excellent reputation thanks to environmental resistant effect and good strength characteristics. However, in the middle of the last century, new competitive material was discovered. Its name is a geopolymer.

Geopolymer was named in the 1970s, when Joseph Davidovits, a French chemistry expert, determined the alkali-activated aluminosilicates. In 1972 he registered the first patent dealing with kaolin polycondensation, and at the end of the 80s, he started to publish articles on his invent. However, the first alkali-activated aluminosilicate research results were published in the 50s of the 20th century by Pavel Krivenko from Gluchovskij University in Kyiv, USSR. Since the beginning of the 2000s, scientists from all over the world started to carry out geopolymer research actively, which significantly extended its concept.

Among the benefits of the geopolymer belong the fact, that greenhouse gas emissions could be significantly reduced by approx. 80 % during geopolymer production in comparison with the ordinary Portland cement manufacturing. Meanwhile, various types of pollutants can be stabilized by means of geopolymer, and the product is also durable, chemically resistant to an aggressive environment and can withstand high temperatures. That is why, with every passing month, the number of scientists involved in geopolymer research increases from all over the world.

A detailed study of this subject showed, that despite its enormous popularity in the scientific field, geopolymer is uncommon in the building industry. This could be attributed to the fact that some of building companies are afraid to use a new and insufficiently explored building material because it carries significant practical and

economic risks. Therefore, the first step that need to be done is establish the dependence of physical and chemical geopolymer properties on mixture composition. Based on the obtained mixture, different composite types are needed to be tested in various exploitation conditions. Simultaneously, it is necessary to figure out the applications for which geopolymer will be the most suitable and, besides if it has economic and technical benefits in comparison with the ordinary Portland cement in practice.

1.2. The current status of issue

1.2.1. Geopolymer concept

Term Geopolymer [Davidovits J., 1991] has been used for the first time by Joseph Davidovits for the metakaolin based amendment binder explains, which hardening activation was supported by means of alkali-silicate solutions [Davidovits J., 2002]. Later, this scientist and other researches had determined, that geopolymerization process can be performed in many materials. At present, geopolymer term is used for alkali-activated binders with aluminosilicates-based materials, such as slag, ash, rocks etc. [Davidovits J., 1994] In perspective, these materials are considered as a Portland cement alternative [Davidovits J., 2002; Davidovits J., 1994A; Davidovits J., 1994B]. Scientific literature is mainly focused on material that could be called GP and geopolymerization process research. However, this is not the only field being discussed [Davidovits J., 1994; Škvára F., 2007; Chen J.J., 2004].

By J. Davidovich's determination, geopolymer is artificially synthesized inorganic materials which has polymer structure with chains of silicon, Al and O atoms. There are three basic geopolymer framework formations categorized according to their Si:Al ratios: sodium polysialate sodalite framework, potassium polysialate-siloxo leucite framework and potassium polysialate disiloxo sanidine framework (*Fig. 1.*). As hardening activators sodium hydroxide and sodium or potassium metasilicates with the addition of alkali were used [Davidovits J., 1999; Davidovits J., 2002; Davidovits J., 2005].
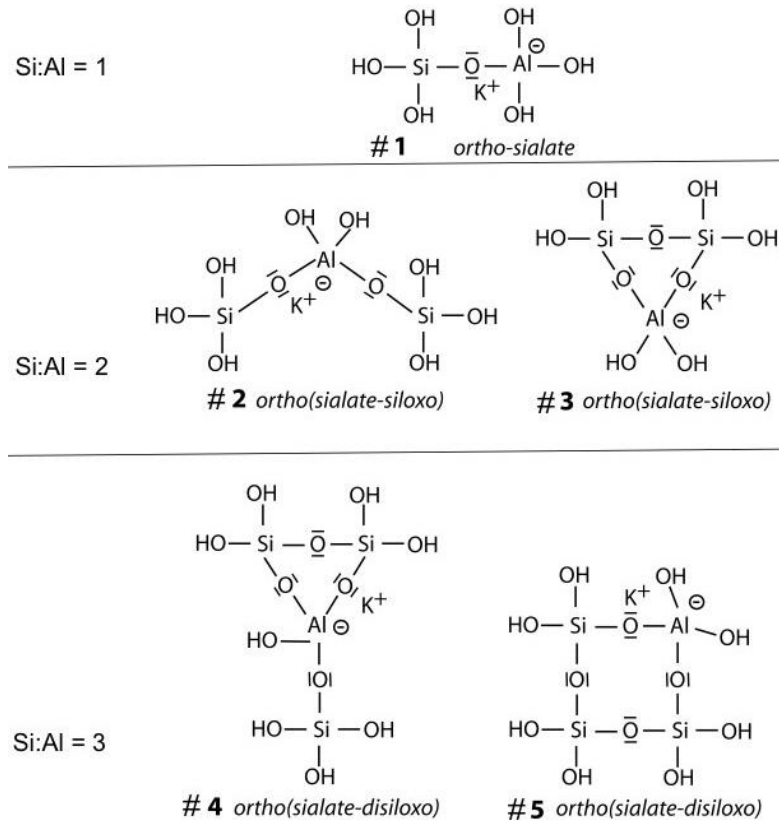
Fig. 1.: Geopolymer framework formations [Davidovits J., 2017]

As a product of geopolymerization reaction amorphous gels are obtained. Solidification of these gels via polycondensation releases water as the one secondary reaction product. Gel structure transforms into polymeric chains supporting each other to porous amorphous system, which appears as homogeneous solid phase. Unit cell of Al-Si inorganic polymer is called poly-disiloxo-sialate.

The main source of aluminium silicate is metakaolin. However, other sources with high amount of reactive Al-Si units are also available, e.g. ashes and slags. Under certain conditions of chemical activation complex composite system made of polycondensed binder and excess amount of surface reactive particles is formed from the sources mentioned earlier. Geopolymer microstructure depends on used Al-Si sources while macroscopic properties such as appearance, strength and texture are the same. [Davidovits J., 1994]

1.2.2. Geopolymer in a historical context

Geopolymer name consists from two words. The first one is *Geo* which indicates the mineralogical origin of the feedstock and the second one is *Polymer* which indicates specific grades in concrete in which the inorganic and mineral components form various kinds of polymers.

A long time ago for mineral components binding and asphaltic concrete production bonding materials was used. Organic additives were used for building mortar production with particularly outstanding properties in ancient times. In the British Encyclopedia article on cement a mortar made of quicklime, which consisted of sheep cheese, milk and egg white is mentioned. By the way, according to the article cement from quicklime and whipped egg whites was used in the 18th century for gluing broken ceramic, porcelain and glass products together. Interestingly, for the same purpose juice of the grated in the mortar garlic was used. As other organic additives used in the manufacture of cement and mortar, this encyclopedia also names resin, wax and a wheat flour suspension in water. However, in those cases use of various additives in building mixtures is mentioned, but not the geopolymer itself. [Gabovich E., 2004]

According to the Ten Books on Architecture of Marcus Vitruvius Pollio pozzolan was used as a base of ancient cement [Hanzlíček T., 2004]. The cement from which the monuments of Roman architecture that have been preserved so far have been built. Most likely as the pozzolan deposits of volcanic origin from the Vesuvius mountainside were used. According to the technology mentioned by Vitruvius, most likely it was about a unique chemical composition of substances that contained both fine-grained amorphous silicon dioxide in the form of high alkali porous glass and natural metakaolin with tetrahedral coordinated aluminium. Burning and decaying of clays and their minerals probably took place in deeply buried layers at the foot of Vesuvius, where this raw material was mined and are still mined near Puteoli (today Pozzuoli), near Naples. Solidification was going under initiation caused by aqueous suspension of calcium hydroxide in a paste form slaked lime.

For scientists who are engaged in geopolymer research it is very important to admit or even promote the hypothesis of building the oldest and largest pyramid

monuments using artificial stone. Their belief in the possibility of large blocks manufacturing in opposition to the previously recognized theory is usually based on the geopolymer laboratory experience. Indeed, with the right main component choice the reaction of geopolymer solidification is very simple. This is the main idea of using geopolymer for monumental construction from *in-situ* produced monoliths. Unequivocally the idea has not been proved yet. An indirect evidence according to microscopic images [Barsoum M. W. et al., 2006] is the texture difference of the extracted limestone samples, authentic pyramid material and Davidovits geopolymer composite with limestone filler. The first hypothesis was presented by J. Davidovits [Davidovits J., 1984]. This hypothesis is based on his own laboratory experience and on criticism of the existing representation of passive blocks transport. Other scientific conclusions [Demortier G., 2004] rely on comparison of reference and authentic samples in addition to the visual study of the masonry composition. The statement is supported by wall paintings which demonstrate block production. For such a fundamental changes of existing opinion, it is necessary to obtain sufficient evidences that could be accepted by scientific community and Egyptologists especially [Škvára F., 2008]. Davidovits has been making efforts to get the evidences during his life. However, conservative building engineering hypotheses and petrology of authentic stone are recognized [Müller-Römer F., 2008; Liritzis I. et al., 2008]. No sampling procedures of the above-mentioned compared samples is officially recognized [Ancient concrete rises again, 2006]. However, there is more and more public attention being given to the idea of artificially produced pyramid blocks and the question of used technology.

Nowadays, geopolymer is commonly mixed with various types of cement. Since the 1990s cement manufacturer Lone Star Industries applied Pyrament (geopolymer and cement mixture) for fast underground and road constructions [Husbands T. B. et al., 1994]. For example, these roads were used for the military purposes or also in hydroelectric facilities. However, the Pyrament material application was suspended in 1996. Currently, geopolymer is used to repair sewer pipes in the US [Allouche E., Montes C., 2010]. The HT Troplast department in Germany which is engaged in the industrial production of foamed parts of TROLIT molds from geopolymers was closed shortly after its commissioning [Liefke E., 2002]. List of companies applying geopolymer is showed below in *Tab. 1*. It should be noted that in the past five years,

the geopolymer has been actively used in India. Proof of this is a large number of scientific publications and companies that have begun to actively engage in the sale of geopolymer components, for example Kiran Global.

Tab. 1.: List of companies applying geopolymer and its applications

Company	Country	Application
Renotech Oy	Finland	Refractory geopolymer-based adhesive
camfil	Sweden	Air filter probably based on geopolymers
Pyromeral Systems	France	Various special geopolymer-based products
N. STRAŠECI ČESKÉ LUPKOVÉ ZÁVODY	Czech Republic	Geopolymer manufacturer
F.Willich Isoliersysteme GmbH & Co KG	Germany	Exhaust gas pipes insulation products probably GP based on geopolymers
Analyse Entscheidung Lösung B.P.S. Engineering GmbH	Germany	Consolidation and immobilization of toxic or radioactive residues by geopolymers
MC BE SURE. BUILD SURE.	Germany	Acid-resistant surface coating and repair mortar for the wastewater sector in sewage plants, probably based on geopolymers
WAGNERS	Australia	Eco Friendly Concrete (EFC) based on geopolymer binder system

	Country	Description
THE Zeobond GROUP	Australia	E-Crete™ is Zeobond's proprietary geopolymer technology product
Q QUADEX REPAIR MATERIALS	USA	Quadex Lining Systems
KIRAN GEOPOLYMER ULTIMATE GREEN CONCRETE	India	Pavers, breakwaters, supporting structures
indiamart	India	Online store that sells geopolymer concrete blocks
Zauba Corp www.zaubacorp.com	India	Manufacturer of geopolymer concrete blocks since 2008
T E R R A	Canada	Promising private company since 2012 engaged in the research and sale of geopolymer components
GEOKAST	USA	Manufacturer of a specially formulated admix for the production of geopolymer concrete pipe, box culvert and manholes. Available for sale since 2018
Alibaba.com	China	The largest online store, which sell both geopolymer components and finished products
Milliken Infrastructure	Canada	Applied geopolymer mortar to rehab CMP culvert

	Germany	Manufacturer of PCI Geofug® for hygienic treatment of surfaces in bathroom and kitchen
	Australia	Manufacturer of geopolymer materials in commercial scale production since the early 2000s
	United Kingdom	Manufacturer and distributer of banahCEM® since 2008 in building industry

These data show that geopolymer is more than popular and is actively used in various branches of the building industry around the world, especially in developing countries. In accordance with the latest market forecasts, the popularity of geopolymer in the industry will only grow and attract more and more investment and attention [www.imarcgroup.com].

1.3. Conditions of geopolymer preparation

Geopolymers are aluminosilicate-based materials which can be primarily prepared from heat-activated kaolinite. Kaolinite belongs to the group of minerals with a typical formula $Al_2O_3 \cdot 2SiO_2 \cdot 2H_2O$. As can be seen in *Fig. 2*, this group of minerals is composed of one octahedral and one tetrahedral mesh, together forming 0.7 nm layer. [Kubátová D., 2004]
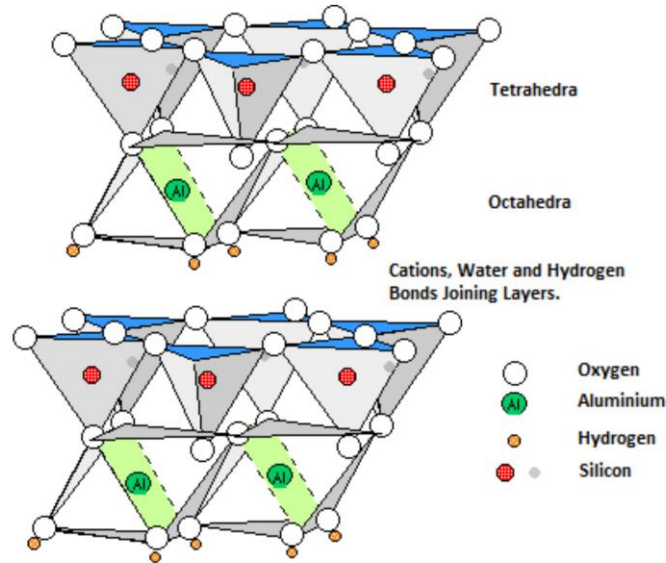
Fig. 2: The crystal structure of kaolinite. The diagram details the tetrahedral sheets of silicon bound via oxygen to the octahedral aluminium sheets [Deer W. A. et al., 2013]

The octahedral mesh is formed by two planes of the smallest atom arrangement, creating octahedral spaces occupied by Al^{3+} cations. To maintain the network electroneutrality, two Al^{3+} cations are needed to be occupied with three octetric positions. [Kubátová D., 2004]

The tetrahedral mesh is formed by SiO_4 tetrahedra, which are connected with the mesh by three atoms of oxygen and it forms a hexagonal arrangement. The fourth oxygen which is called the peak forms a connection with the octahedral network, respectively in the case of kaolinite with octahedral mesh.

Geopolymer matrix formation occurred by means of elemental aluminum and silicon building units in an aqueous alkaline activated solution. There are reactive groups of four oxygen atoms placed around silicon, SiO_4 tetrahedra, and tetrahedra formed by four oxygen atoms around aluminium, AlO_4. These reactive base units, theoretical monomers, are hydrated at the generation moment and form clusters (*Fig. 3.*), which are stoichiometrically described as poly (disiloxo-sialates). [Hanzlíček T., Steinerová M., 2002]
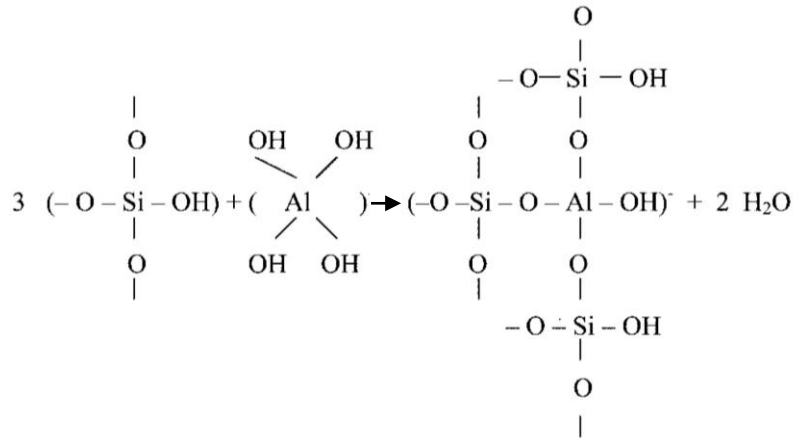
Fig. 3.: Disiloxo-sialates formation [Hanzlíček T., Steinerová M., 2002]

The SiO_4 monomers are available in the form of alkali metal stabilized silicate solution (with Na^+ or K^+) also known as water glass. Aluminum monomers are most readily available by metakaolin hydrolysis in a strongly alkaline solution. Metakaolin also provides SiO_4 monomers in a 1:1 ratio to Al^{3+}, based on the original kaolinite mineral stoichiometry. Its crystal lattice deforms because of dehydroxylation temperature and becomes reactive [Puyam S. Singh et al., 2005] *(Fig. 4.)*.

Kaolinite dehydroxylation and metakaolin activation occurs by changing the bridging angle bonds between the Al and Si layers and changing of the coordinate number of Al.

From a crystalline kaolinite under the suitable condition's thermal activation forms x-ray amorphic structure that can be dissolved in aqueous solution of alkali hydroxides [Sanz J. et al., 1988]. This activation is caused by a change of aluminum coordination in the metakaolin structure. The distribution of aluminum atoms in kaolinite crystals is based on the its octahedral coordination surrounded by six oxygen atoms in the central crystal structure layer of this two-layer mineral.

a. Kaolinite

b. Unstable metakaolin
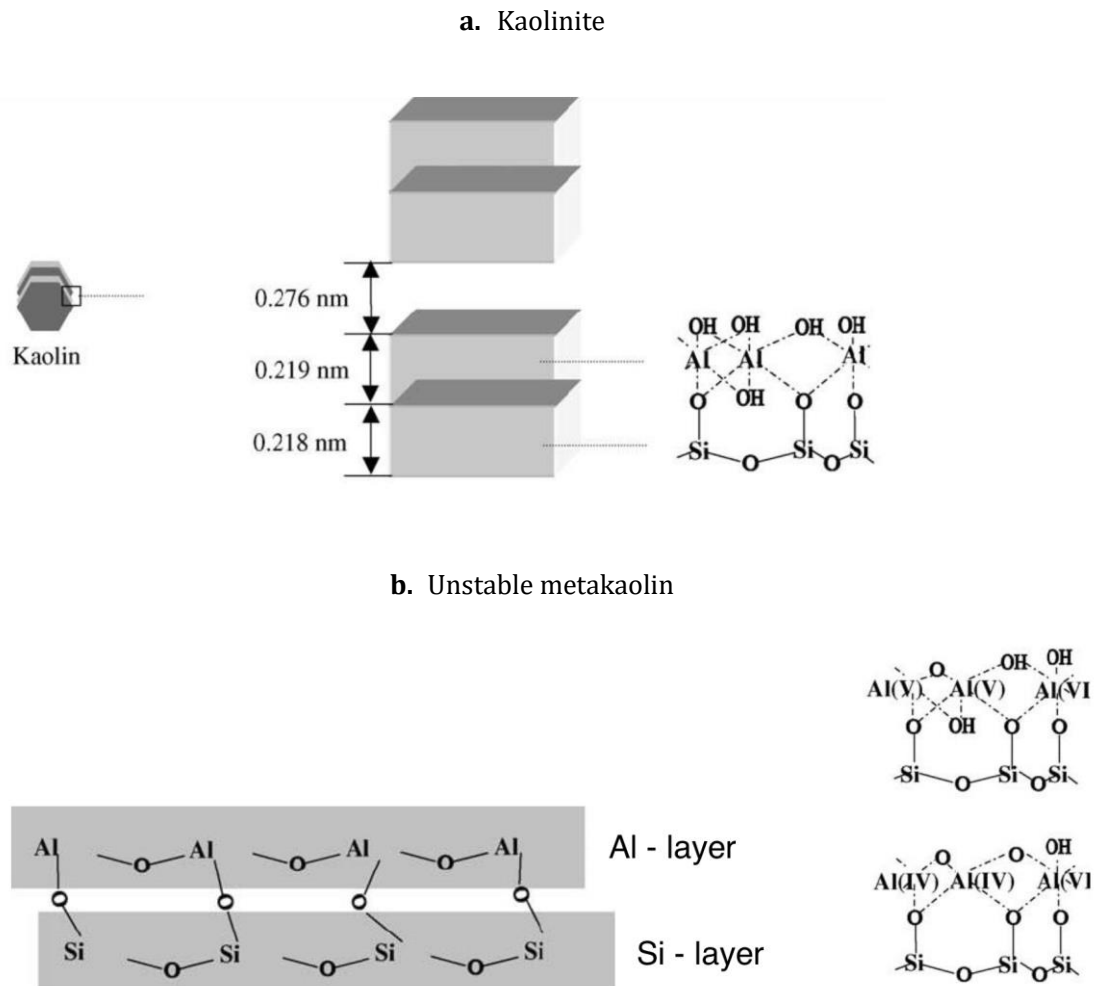
Fig. 4.: Scheme of kaolinite dihydroxylation **(a)** and metakaolin activation **(b)** by changing the bridging angle bonds between the Al and Si layers and changing the coordinate number Al [Šatava Vl., 1986]

Thermal activation contributes not only deformation and crystalline grids destruction, but oxygen deficiency and reduction of aluminum hexacoordinated atoms to penta- and tetra-coordination [Sanz J. et al., 1988]. Subsequent chemical activation by alkaline hydroxides impacts the decomposing of metakaolin unstable structure. Free bonds remaining after the water evaporation are hydrated and parts of the crystalline structure in the form of monomer get into the solution. Aluminum coordination number decreases because of breaking bonds between AlO_6 groups and therefore oxygen deficiency. Negatively charged aluminum hydroxide tetrahedron $[Al(OH)_4]^-$ interacts with alkali cation. Released monomer units simultaneously form

new formations while two the closest hydratated ends of adjacent monomers form bridge through oxygen. One H_2O molecule is released during the formation.

Reaction mixture is formed thought concentrated sol-gel. Polycondensation process leads to gel formation which reflects as viscosity growth. At the moment when yield strength is reached, whole structure turns into which solidifies very fast gel [Šatava Vl., 1986]. Then structure turns into a solid phase via polycondensation in one moment in whole volume of the gel. Released water is excluded on the surface of the product [Hanzlíček T., Steinerová M., 2005]. Scheme of the geopolymer formation is shown in *Fig. 5*.
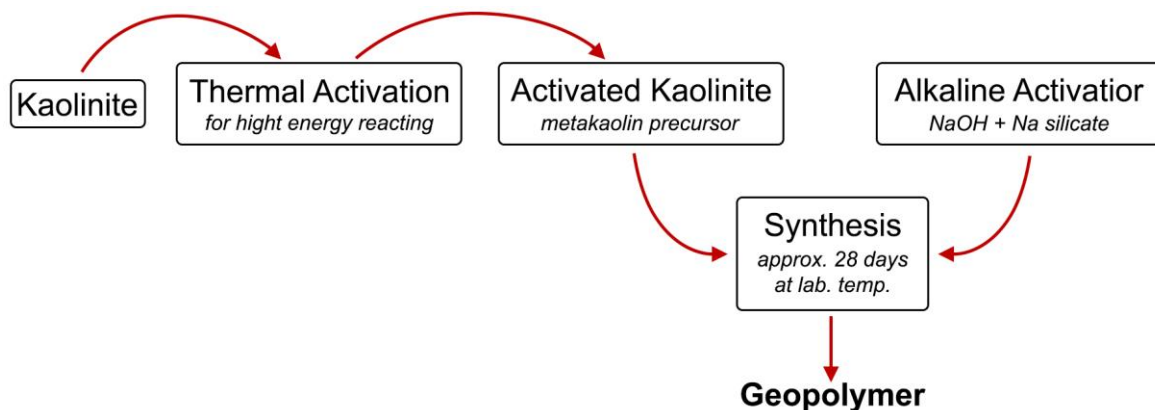
Fig. 5.: Scheme of geopolymer formation

1.3.1. Comparison between geopolymers and zeolites

The product of the described geopolymerization reactions is homogeneous solid phase, matrix, that keeps gel arrangement and remains amorphous. Zeolites are formed by similar reaction [Grutzeck M., 2004] with water excess. Because of lower concentration, distance among particles in the sol-gel is higher. Therefore, particles are able to form regular structure which depends on Al-Si ratio and energy-efficient organization of the Al a Si tetrahedra in crystalline structure [Dědeček J. et al., 2001]. During geopolymer formation, there is no enough room neither time for regular structure formation. Random arrangement of the geopolymer is somehow freezed as a gel matrix. This is the reason, why core authors use the word gel in their publications

for geopolymer matrix, even if it is solid material [Duxson P. et al., 2006]. Hence geopolymer composite appears as a gel with filler.

1.4.   Properties and characteristics of geopolymers

Geopolymers belong to inorganic polymers and form a group of inorganic binders. GP main benefit is reduced emission of greenhouse gases during manufacturing. In compare with the ordinary Portland cement production, amount of these gases may be lower by 80 % [Steinerová M., 2007]. Geopolymer gel consistency is similar to Portland cement and after hardening it is water resistant. After Portland cement solidification it has porous with a nm and μm pore size as well as geopolymer. But due to crystalline portlandite in these pores, the particles in contact with air are covered with a $CaCO_3$ layer as a result of carbonation [Škvára F., 2008].

After drying, the water in the Portland cement remains in the form of calcium-silicate-hydrate gel and in the hydroxyl groups partly. In the geopolymer water is in the form of hydroxyl group appearing on the surface of pores and cracks (*Fig. 6.*) [Brindley G. W., Nakahira M., 1957]. This water gradually evaporates when the matrix is heated to temperatures above 400 °C. Restructuring is accompanied by contraction, cracks formation and approximately 15 % loss of weight due to water evaporation [Barbosa V.F.F., MacKenzie K.J.D., 2003]. Water stops evaporating at temperatures above 600 °C. At a certain or higher temperature geopolymer drastic changes do not occur. At temperatures above 800 °C and close to 1000 °C, nepheline starts to form [Duxson P. et al., 2006]. At temperatures above 1000 °C gradual compaction occurs due to the disappearance of micropores and sintering which causes significant contraction (by 5-15 %). From 1100 °C the matrix melts. Beside water no gases are formed. It could be said, that the geopolymer matrix-based composite is resistant to high temperatures with the use of suitable additives.
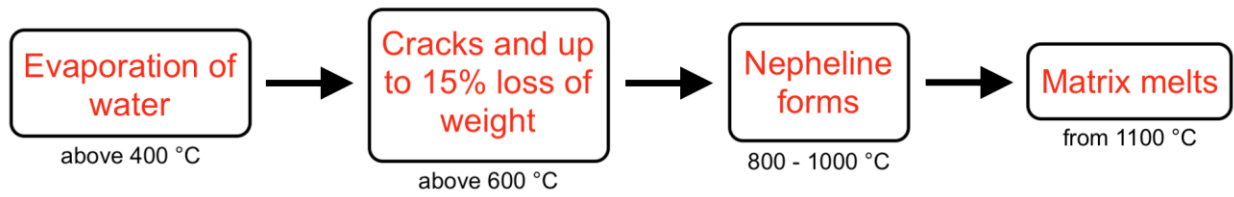
Fig. 6.: Geopolymer concrete phase changes in the process of heating to a temperature above 1000 °C

Macroscopic properties of various sources of aluminosilicates may not differ. In practice, however, their microstructure and properties may differ mainly due to the material source. For example, the structure of a geopolymer with slag differs from a metakaolin and fly ash based geopolymer. The existence of latent hydraulic substances containing calcium impacts the chemical reaction and the emerging microstructure as a product of this solidification type can be considered as an inorganic binders' group. It is similar with metakaolin or fly ash based geopolymers that also belong to the alkali-activated aluminosilicate group. Alkali-activated slag-based aluminosilicates need to be given special attention since they are a very complex system consisting of a complex of crystalline and amorphic elements. It is worth noting that for many years metakaolin is added to Portland cement as an improving additive. [Steinerová M., 2009]

The fly ash based geopolymers contain fine glassy particles in droplet are formed from the coal combustion. Considering the small size and the large surface area of these particles, they participate in the hydrolysis of alkali hydroxides. Glassy particles surface-corrode [Hanykýř V., Kutzeddörfer J., 2002] and provide the precursors for the geopolymerization reaction. After coal burning silt particles that were in it in presence of reactive aluminosilicates start behaving like metakaolin.

Ordinary volcano minerals such as pozzolan are based on the same principles. During Plinian eruption dispersed particles of melted rock were erupted under steam pressure instead of liquid lava. Produced volcanic dust and ash have fine grain and high amount of enamel.

Geopolymer composites have wide spectrum of properties including high compressive strength, low contraction during solidification, fire resistance, acid environment resistance, and low thermal conductivity. Also, was found out that matrix can preserve sludge's containing radionuclides, toxic heavy metals and hydro-carbons with good long-term structural, chemical and microbial stability satisfying high standards of contaminant retention. [Hermann E. et al., 1991]

However, it is worth noting that the geopolymer is not only cement substituting material or a universal binder for waste disposal, but also a specific material for various aaplications. Geopolymer technology is able to suggest tailored material by precise selection of input stocks and conversion conditions. Financial efficiency of expensive regular projects can also be improved by geopolymer usage. [Duxson P. et al., 2006]

1.5.   Ecology

The development of alternative astringents is currently undergoing a revival period. The reasons for this are, on the one hand, the increase in the cost of primary raw materials (or its regional deficit), and, on the other hand, the growing awareness of environmental problems. From the environmental point of view, there are also various restrictions. In the leading industrialized countries, through emission trading, reducing of CO_2 emissions from cement production is a priority. In the new developing countries, such as India and China, no adequate ways of recycling industrial waste have been developed. Therefore, in these countries ways of recycling in a connection with intensive accumulation of ash and slag are being investigated. The use of a binder based on geopolymers creates possibility of preventing the mass burial of ash and slag with the appropriate protection of raw materials. As well as a significant reduction of the amount of greenhouse gas emissions compared to the production of binders on a cement basis. [Weil M., 2011]

An intensive analysis of raw materials was carried out to develop the main recipes for geopolymer concretes as a mass building material. Fifty-eight types of primary and secondary raw materials were examined for their suitability [Weil M. et

al., 2007]. The selection of raw materials included various mineral wastes, ash, slag, clay and volcanic deposits. To identify the most promising materials, in addition to technical parameters, economic and environmental aspects including health effects were also taken into account [Weil M. et al., 2005; Weil M. et al., 2006]. To determine the technical suitability with all raw materials necessary tests such as dissolving the silicate and aluminate monomers in an alkaline solution, measuring the compressive and flexural strength were carried out [Buchwald A., 2005].

The results of the research showed the technical capability of geopolymers in various applications. In comparison with cement-bound concrete systems, both technical and economic conditions are fulfilled and the negative impact on the environment can be reduced [Weil M. et al., 2010]. Potential environmental benefits arise primarily from the secondary raw materials using, such as blast-furnace slags or fly ash, and also probably due to increasing lifetime in various applications. However, due to the limited availability of recycled materials in industrialized countries, widespread application of the technology is questionable, because of existing recycling technology especially in the building sector. In the developing countries such as India and China investigation of recycling solution for a large mass of slag and ash is carried out. The most promising way is using of geopolymer [Weil M., 2011].

1.6. Geopolymers structure analysis

1.6.1. X-ray powder diffraction (XRPD)

X-ray diffraction method is the main investigation source on the matter structure at the atomic level. From the crystal structure point of view, as well as the nature of the radiation interaction with matter, X-ray diffraction of crystal powder is most informative. The diffraction pattern of a powder sample includes information about the symmetry and size of an elementary cell, the coordinates of atoms, thermal parameters, etc. [Friedrich W. et al., 1912; Bragg, W.l., 1913]

It is always possible to isolate a certain minimal volume in the parallelepiped form in a crystal, three-dimension repetition of which builds a crystal in space. Such parallelepiped is called the elementary crystal cell. The cell may contain one or several molecules of matter.

The strict order of the molecule arrangement makes it a convenient object for studying the molecules structure. Only in the crystal there are billions of molecules equally located with respect to the incident ray and giving the same scattered rays that amplify each other. When an X-ray interact with a crystal, very intense scattered rays appear in certain directions. At the same time, there are many spatial directions in which the scattered rays do not amplify but extinguish each other.

X-ray powder diffraction is a method for the study of crystalline and partially crystalline solid-state materials, defects and stresses. In this method fine powdered sample is irradiated with X-rays with wavelength ranging from 0.07 to 0.2 nm. These rays are scattered (diffracted) on the edges of crystal lattice of the sample according to the Bragg's law:

$$\lambda = 2d \cdot sin\theta \quad (1)$$

where d is interplanar distance [nm], λ is wavelength of X-rays [nm] and θ is glancing angle. Due to different crystal lattice size (d), diffracted angles are different and are usually denoted as 2θ (2theta). The detector of diffracted X-rays is moving round the sample and measuring of the intensity of the rays *(Fig. 7.)*. [Murty B.S., 2013]
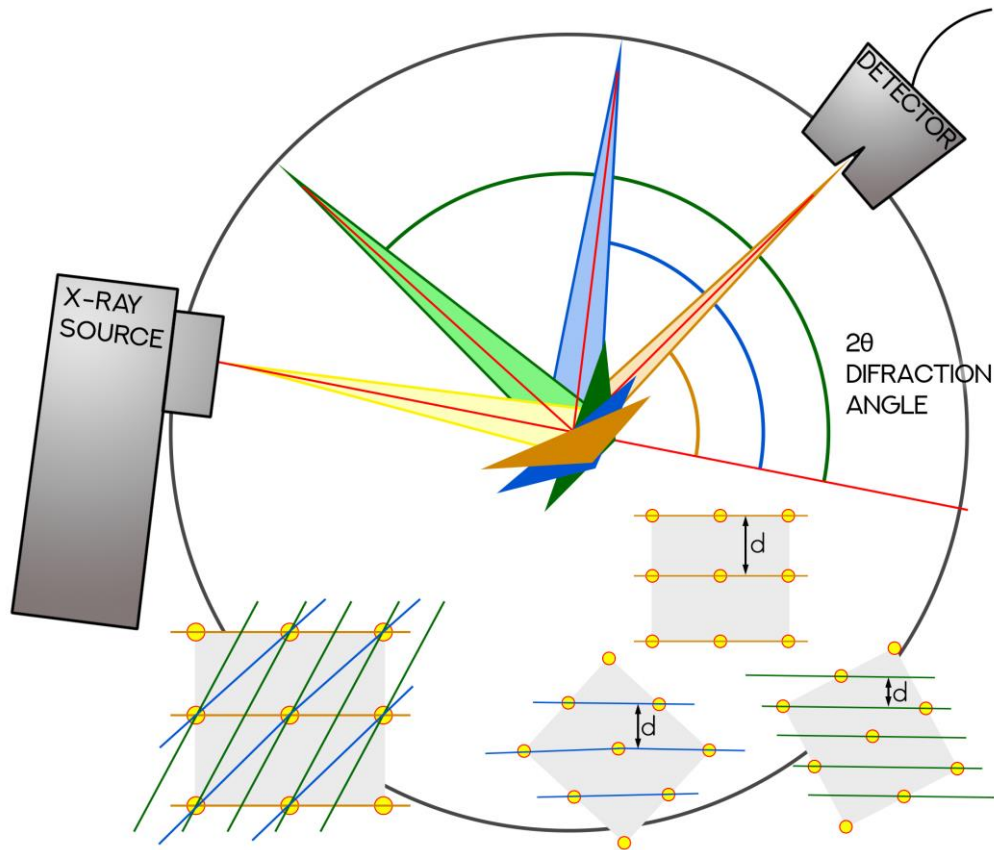
Fig. 7.: Principle scheme of X-ray powder diffraction measurements, showing importance of powdered sample with multi-oriented atomic planes [Theory of XRD, 2019]

As a result of the measurement is a diffractogram, where *x*-axis is angle theta/2theta and *y*-axis is intensity of diffracted X-rays. Each crystal lattice has its own diffracting angle where intensity is not equal to 0 *(Fig. 7.)*. For this method the sample must be well powdered because it ensures uniform chaotic orientation of crystals in the sample to avoid directional orientation. Directional orientation results in high intensity of some peaks (refracted from the side irradiated with x-rays) and very low intense of other peaks (refracted from the side hidden from x-ray beam). It appears during monocrystal measurements. In this case evaluation is not reliable. In the case of amorphous materials X-rays will be scattered in many directions leading to a large bump distributed in a wide range (2theta) instead of high intensity narrow peaks.

Investigation of the geopolymer structure using XRD is necessary when optimizing its composition and reaction parameters. This equally applies to metakaolin

and fly ash geopolymers, whose crystalline admixtures background (especially mullite and quartz) from fly ash is relatively unchanged even in the geopolymer and dissolution therefore only concerns the amorphous, vitreous fly ash component.

The geopolymer matrix can be expected to be amorphous. The original metakaolin obtained by the dihydroxylation of kaolinite under optimal thermal activation conditions is an X-ray amorphous [Paiva, 2016]. The geopolymer made from it, while maintaining the optimal reaction parameters, is also amorphous and the XRD diffractogram has a typical hump-shaped curve, like glass.

1.6.2. Fourier Transformed Infra-Red spectroscopy (FTIR)

For Fourier transform infrared spectrometry (FTIR), an interferometer-derived signal is converted to infrared spectrum by a mathematical operation named Fourier transformation. The basis of the FTIR spectrometer is, for example, the Michelson interferometer *(Fig. 8., gray zone)*. The radiation from the source comes to a semipermeable beam splitter that passes one half of the beams to the moving mirror, the other to the fixed mirror. The beams are reflected back from the two mutually perpendicular mirrors and the beams are either added or subtracted according to the position of the movable mirror on the beam splitter, so the interference occurs. As the optical path difference of both beams' changes, the signal falling on the detector generates an interferogram *(Fig. 8.)*. When recombinated beam passes through the sample matter, vibrational motions of molecules or their individual fragments are excited. In this case, the intensity of light transmitted or reflected from the sample is weakened. However, absorption does not occur in the entire spectrum of the incident radiation, but only at those wavelengths whose energy corresponds to the excitation energies of the vibrations in the studied molecules. Consequently, the wavelengths (or frequencies) at which the maximum IR radiation absorption is observed can indicate the presence of certain functional groups and other fragments in the sample molecules, which is widely used in various fields of chemistry to establish the structure of compounds. [Böcker J., 2009; Ramer G., 2013]

The attenuated total reflection (ATR) technique is the most frequently used sampling technique for infrared (IR) spectroscopy. IR light traveling in an optically denser medium is totally reflected at the interface to an optically rarer medium. Through this evanescent field, the light can interact with samples placed at the interface, making absorption measurements possible *(Fig. 8., diamond zone)*. The technic allows quick and robust measurements of solid as well as of liquid samples. The most common wavelength used for FTIR is the MIR region and is usually defined as the wavenumber region from 4000 to 400 cm^{-1} (from 2.5 to 25 µm). [Ramer G., 2013, Thermo Fisher Scientific, ATR]
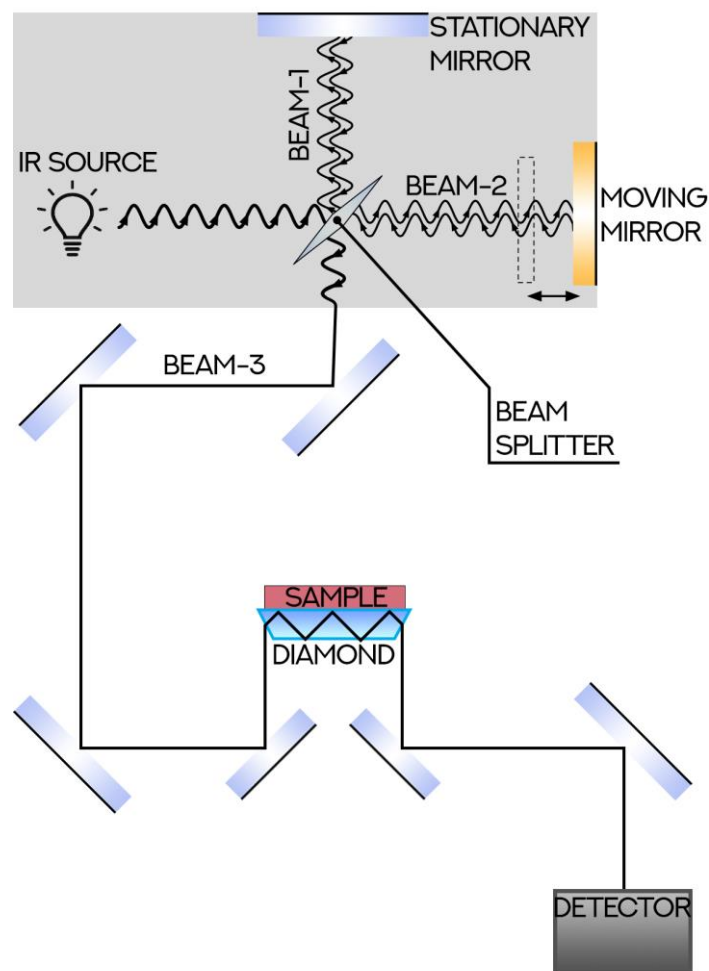
Fig. 8.: Principle scheme of FTIR-ATR spectrometer. IR beams in Michelson interferometer (gray zone) are demonstrated as waves in order to show interference of monochromatic beam due to moving mirror. Beam-1 is splitted beam, beam-2 is delayed splitted beam, beam-3 is recombined beam taking part in further measurements.

FTIR is a complementary tool for determining the molecular bonds and their proportion into geopolymer matrix formation. Since the geopolymer matrix is understood to be a macromolecular system, FTIR can study the matrix microstructure as a polymer analogue. The matrix is a solid, and only vibration modes are used in FTIR spectroscopy when absorbing IR. The radiation absorption energy corresponds to the respective vibrational transitions and occurs in all present bonds and is manifested in dependence on the frequency and type of vibration. [Ksandr Z., 2017] The bond between the tetrahedra of SiO_4 and AlO_4, in the free molecules of water and OH groups, is always present in metakaolin and fly ash geopolymers. The most pronounced bonds vibrations are vibrations of OH bonds and T-O-T oxygen bridge bonds between tetrahedra, where T corresponds to Al and/or Si. In the geopolymer matrix, these bonds are asymmetric, their absorption band are the strongest in the spectrum, the valence symmetrical vibrations T-O-Si and the deformation vibrations of the oxygen bonds are less pronounced.

In the aluminosilicate and silicate spectrum, the absorption band of the bridging O bonding tetrahedrons Si, which occurs in the 900 to 1100 cm^{-1} (main band) region, always appears as the main feature. Its position on the wave line is assigned wave numbers depending on the chemical environment type of this bond. Unlike the crystalline forms, the geopolymer matrix, as in the case of glass, is a broad band composed of individual bands of the bonding present types. For example, for kaolinite, the major band is determined by a wavelength of 925-1130 cm^{-1}, composed of four maxima corresponding to the bridged oxygen bonds of the crystal lattice. After pyroprocessing kaolin to metakaolin, the absorbent band converging in a broad band with a single peak at about 1070 cm^{-1}, the band width indicating crystalline lattice decay. [Prost R., 1989; Tironi, 2012]

When transitioning metakaolin into a geopolymer, the main band of valence asymmetric T-O-T bonds vibrations changes due to the geopolymer reaction. The wave number of about 3425 cm^{-1} is assigned to OH groups, 1680 cm^{-1} to molecular water. "Fingerprint" spectrum region 1500 – 400 cm^{-1} besides main band includes asymmetric valence vibrations bands of the TO-Si (Si-O-Si, Al-O-Si) with 1100 cm^{-1} wave number (for metakaolin) and 1110 cm^{-1} (for geopolymer) and other vibration

bands. These metakaolin and geopolymer bands correspond to asymmetric valence vibration of the Al-O-Si bond at 826 and 837 cm^{-1} and scissor-vibration at 469 cm^{-1}, respectively at 457 cm^{-1}. In an appropriately arranged experiment solidification process could be tracked via FTIR based on the characteristic bands shift. [Steinerová M., 2009; Prost R., 1989; Tironi, 2012]

1.7. Mechanical properties of geopolymers

Geopolymer research has not focused on the relationship understanding between composition, processing, microstructure and physical properties, such as mechanical strength [Duxson P. et al., 2005] yet. So far, the mechanical property analysis has been focused on the study of conditions needed to achieve as high compressive strength as possible or has been used as a tool for determination of the conversion degree with respect to the compressive strength achieved. The microstructure was also less studied, because most of the previously published works on geopolymer systems were focused on fly ash and blast furnace slag composites, making it difficult to evaluate material from a non-homogeneous aluminosilicate source. Therefore, to understand the microstructure of the geopolymer products, it is more convenient to use metakaolin as a starting material. Such comparison of the microstructure based on mechanical properties, especially on the Young's elastic modulus, was performed as a dependence on the different matrix composition relative to the Si/Al ratio. [Duxson P. et al., 2007 B; Duxson P. et al., 2007 C] It turns out that geopolymers have a microporous system with a characteristic pore size depended on the alkaline cation typ. The liquid precursor transforms into the solid phase of the gel and the mechanisms of its compaction is influenced by structure formation. During gel formation via hydrolysis and polycondensation of aluminum and silicon units water is released, but simultaneously retained in the gel and, after hardening, remained in the pores.

The elasticity modulus is a mechanical property of magnitude characteristic of each composition. Greater standard deviation of the compressibility implies that the fracture mechanism significantly influences the compression strength, especially at higher Si/Al ratios (*Fig. 9.*). Therefore, observed compressive strength values should

be judged with the respect to the value result range than to be considered as individually verifiable. The geopolymer compressive strength increases linearly about 4 times depending on the Si/Al ratio from 1,15 to 1,9 before it begins to fall again at the highest ratio Si/Al = 2,15. Young's elasticity modulus is constant in the Si/Al area of 1,65 and indicating that the strength and elasticity modulus in the Si/Al = 1,15-1,9 area is related but not directly proportional.
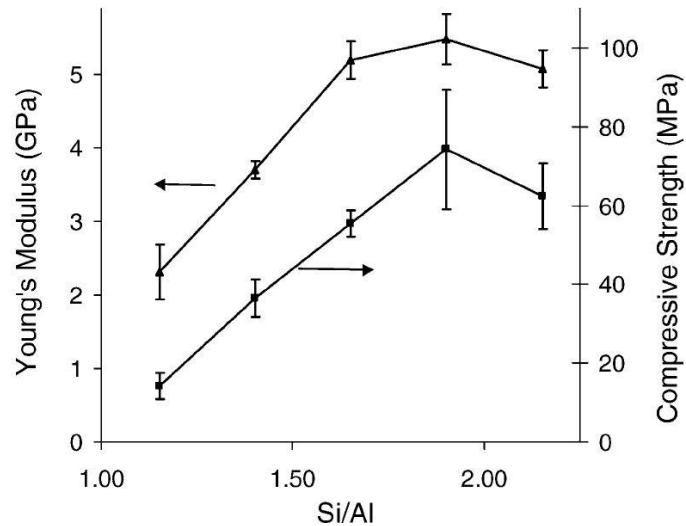
Fig. 9.: Young's elastic modulus and flexural strength of geopolymers. Young's elasticity modulus (▲) and compressive strength (■) of geopolymers. Perpendicular lines indicate an average deviation from the average of the 6 measured samples [Duxson P. et al., 2005]

The GP elasticity modulus depend mainly on the structure strength, i.e., the aluminosilicate chains crosslinking. Due to a small pore size the material behaves as a one-component system with 20 nm mesoporous, which are a part of homogeneous microstructure. During polycondensation new T-O-T bonds deforms due to the mutual position of the terminal hydroxyls presented in the formed clusters. These deformations contribute to the state of the binding stress [Duxson P. et al., 2007 A]. As a result, internal stresses in the matrix adversely affect the mechanical properties of the geopolymer product.

1.8. Frost resistance of geopolymers

Frost-resistance means the material ability to resist repeated freezing and thawing in a water-saturated state [Pytlík P., 2000]. Chemically bounded water does not turn into ice. Gel water passes in ice only at low temperatures of -73 °C. In capillaries, pore water passes in ice at 0.5 °C and less. It depends on its composition since the water could have different concentrations of a dissolved substances solution form.

The volume of freezed water increases by 1/11, i.e., 9% of the original volume [Pytlík P., 2000]. First, it freezes in the largest pores. Destruction influence occurs when the large pores are occupied by ice, but the temperature inside the composite decreases further until the water is freezed even in small pores. Water in the large pores, when changing the state, uses the closest space, such as smaller capillaries, where ice crystals start to form. The impact caused by crystal growing generates stress that can exceed the material structural strength. Crystalline ice pressure could be greater than 200 MPa. Ice first appears on the material surface and presses it to the center according to the material cooling rate. After ice melting the material retains up to 1/3 of increased volume because of freezing. These changes in practice have an impact on tensile strength and material flexibility modulus. Due to ice pressure, the material structure is changed by volume increases, which cannot be done without micro cracks creating. This leads to material strength reduction, but also trigger degradation processes. The frost resistance measurements, therefore, focus on strength reducing after a certain number of freezing cycles.

The frost effect depends on several factors. The first is climatic factor, consisting of changing of the freezing and thawing periods [Petránek J., 1963]. The second one is technological [Slížková Z., 2007] and relies on the material diversity composition, mainly on the texture, i.e., size and ratio of capillaries and pores [Teplý B., Rovnaník P., 2007]. After freezing water, which flows to the smallest cracks creates cracked ice. During repetitive melting and frosting, water flows into expanding cracks and breaks the strongest rocks.

The amorphous and isotropic material strength is a function of the number of variables such as material structure, internal temperature stress, surface condition, body shape, external force origin, temperature, the relative humidity of the environment, etc. The microstructure is defined by the phases volume fraction, crystalline, amorphous and pores, their character, size distribution, orientation, and the phase interfaces behavior. The rough estimation of the fragile isotropic material theoretical strength can be described by the relation [Hanykýř V., Kutzeddörfer J.,2002]:

$$\sigma_{th} = \left(\frac{E\gamma_0}{a}\right)^{\frac{1}{2}} \quad (2)$$

where is the theoretical strength, is γ_0 the surface energy, a is the inter-atomic distance, E is the modulus of elasticity.

The strengths are much smaller because the microstructure contains micro-cracks. It is clear that the frost damage mechanism is material microstructural dependent in terms of the crack's presence which, on the one hand, reduce the material structural strength and, on the other hand, forms the anlages of cracked ice destruction.

The frost resistance tests are carried out according to the concrete frost resistance determination, ČSN 73 1322 [ČSN 73 1322, 1969]. It is tested by alternating water-saturated beams freezing and defrosting with a certain cycle's numbers. For 50 cycles, the minimum number of test specimens is 9, up to 12, 3 or 6 of which are freeze-dried, others serve as reference specimens for assessing the strength or weight loss. To verify 150 cycles, 15 or 24 samples are required, according to the evaluation stages number of 25 or 50 cycles.

The specimens freezing and defrosting is carried out in freezing cycles at a temperature of -15 to -20 °C. One freezing cycle consists of 4 hours of freezing and 2 hours of defrosting in the water at 20 °C. After 25 or 50 freezing cycles, the samples are dried, the bulk density is measured, and the flexural and compressive strengths are tested. Non-freeze specimens are also tested. The test is completed after either the prescribed cycle conduction or the weight loss is more than 5 %. The test results in each step are evaluated through the frost resistance coefficient based on weight loss in

%, flexural and compressive strength. The frost resistance coefficient is defined as the frozen beam measured strength arithmetic mean ratio to the reference beam strength arithmetic mean value. According to the standard, the concrete called frost-resistant after certain cycle numbers if the frost resistance coefficient is not less than 75%.

Another frost resistance test, which is described in ČSN 73 1326 [ČSN 73 1326, 2003], is the concrete surface resistance determination against the water and chemical de-icing agents' action. The standard describes automatic cycling (A) and manual handling (B). Method A uses a device capable of cooling the sample surface from 20 °C to -15 °C in 45 to 50 minutes. Water saturated concrete samples are placed in a bowl with 3% NaCl solution submerged 5 ± 1 mm. Alternate sample surface freezing at -15°C for 25 minutes and thawing at 20 °C for 25 minutes is performed in the test area. After each 25th cycle, the samples are removed, and the amount of the depleted particles is determined after drying. The test is completed when the prescribed cycle number has been reached, or 500 g/m2 of waste has been exceeded. The result is given in the waste amount in g/m2 and behind the dash indicates the cycles number at which the waste amount was achieved.

1.9.   Fire resistance of geopolymers

According to studies conducted in this field, the refractoriness of the geopolymer and resistance to high temperatures should be noted. For example, fly ash-based geopolymers can be used as a material for the production of thermal insulation boards. From the fire resistance point of view, such geopolymers exceed metakaolin-based geopolymers. Unlike classic Portland cement, fly ash-based geopolymers have higher compressive strength and did not crack when heated. [Luna-Galiano Y. et al., 2015]

Most of geopolymers have excellent resistance to high temperatures due to the presence of a microporous ceramic structure. This structure allows physically and chemically bound water to evaporate and move without damaging the aluminosilicate network [Singh B. et al., 2015]. It was found, that fly ash-based geopolymers heated to 800 °C showed 6% higher strength than none heated and the metakaolin based GP 34%

lower strength [Daniel L.Y. Kong et al., 2007]. Geopolymers based on metakaolin using a potassium-based activator showed better strength characteristics than similar geopolymers using sodium activator [Singh B. et al., 2015]. So the choice of alkaline solution and the concentrations ratio are critical parameters which are important to optimize metakaolin-based geopolymers performance at high temperatures. Also, the presence of aggregates and fillers in the composite can have a significant impact on mechanical characteristics.

Testing of the geopolymer composites for high-temperature stability is interesting considering the main aim of this work - determination of the optimal proportions of the components to create a composite with the appropriate mechanical and chemical properties for subsequent use in the immersed tube segments production field. In accordance with a large amount of work and financial investment, subsequent research would be a logical continuation of this work.

Mostly, in laboratory experiments, a material sample is heated in a small furnace or on one side only. However, these are often small-sized samples, so the heat distribution inside the material is completely different in real conditions during a fire, for example, in a tunnel. Therefore, further testing should be performed on a modelled mock-up tunnel to get more accurate results.

1.10.   Shrinkage

The shrinking process is the process of the volume material reducing over time. Shrinkage mainly does not depend on external influences on the material. In total, there are several types of shrinkage: plastic, drying, chemical, and thermal shrinkage. Plastic shrinkage occurs when the material is in a plastic state due to evaporation or absorption of water into the environment. Plastic shrinkage can cause cracking during the curing process. This type of shrinkage also depends on the relative humidity of the environment and wind speed [Neville, 2011]. Drying shrinkage is a result of a material volume decrease during the drying process. This type is the most evident in concretes, where shrinkage depends on the ratio of water and cement, the type of aggregate and

its size, relative humidity, size and shape of the object being made. Chemical shrinkage occurs due to chemical reactions in the matrix, including hydration. Thermal shrinkage occurs in the process of heat release as a result of a chemical reaction during the interaction of material components [Neville, 2000]. The presence of aggregates in the material significantly reduces shrinkage [de Larrard et al., 1994; Neville, 2000].

Depending on the type of geopolymer, shrinkage indicators may vary. For example, the compressive strength of geopolymer concrete mixed with fly ash GGBFS increases simultaneously with an increase in the slag content. Shrinkage decreases with increasing slag percentage and decreasing SS/SH ratio. Shrinkage of the geopolymer during the solidification process at a laboratory temperature can be reduced within the range of calculated design values by increasing the slag content and reducing the SS/SH ratio *(Fig. 10.)*. R2.5S10 and R2.5S10 mixtures are differ from R2.5S20 and R2.5S20 in content of fly ash (360 to 320 grams respectively) and GGBFS content also (40 to 40 grams respectively). [Partha S.D. et al., 2015]. Also, studies have been conducted on the geopolymer shrinkage when creating reinforced concrete elements. It should be noted that in these studies, the reduction of shrinkage is achieved by thermal effects on geopolymer [Duxson P., Lukey G., 2007].

A
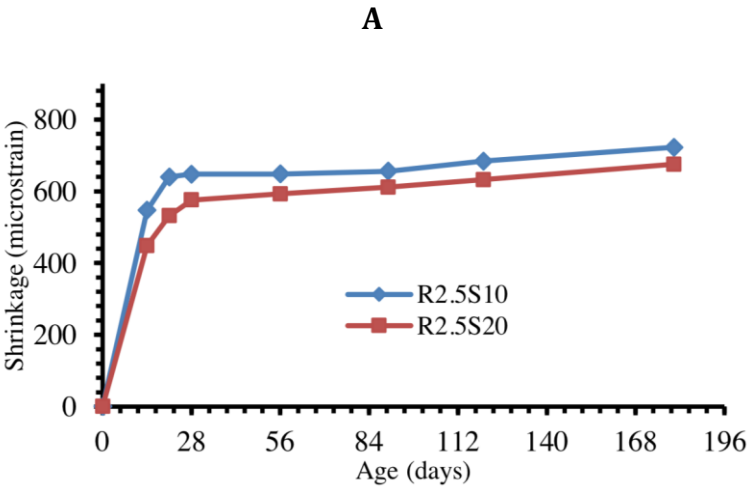
B
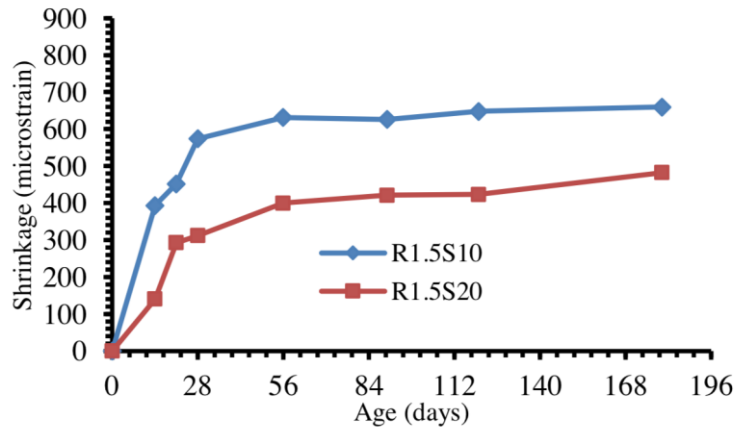
Fig. 10.: Drying shrinkage of geopolymer concrete with different slag content: (a) SS/SH ratio = 2.5, (b) SS/SH ratio = 1.5 [Partha S.D. et al., 2015]

1.11. Influence of raw kaolin on Czech produced geopolymer

The influence of basic constituents' composition on geopolymer strength, such as a variety slag-metakaolin ratio [Parthiban & Vaithianathan, 2015] or Si/Al metakaolin (MK) ratio [Duxson et al., 2006], is being studied. Even so, raw kaolin burning in industrial quantities can lead to the imperfect dehydration of kaolinite. So, the influence of kaolin remains in metakaolin Mefisto L05 (CLUZ Nove Straseci, Czech Republic) was also studied.

The main sources of aluminosilicates for geopolymers are metakaolin and fly ash [Davidovits, 1994]. Metakaolin is produced from kaolin, kaolinitic clay or claystone by continual burning. The quality of the burned product depends on the burned amount, particle size, thickness of the layer, and temperature. Therefore, the conversion of kaolinite to metakaolin could be not absolute, which affects further geopolymerization, such as other impurities [Autef et al., 2013; Wang et al., 2005].

A test series of compressive and flexural strength was conducted on samples with a variety of raw kaolin additions. Also, the mechanical properties of the geopolymers with and without the raw kaolin addition were further characterized by frost resistance. Due to 20nm-sized mesopores, the matrix behaves as a one-component

system with a homogeneous microstructure, but it is always tainted by microcracks [Drake, 1949]. Therefore, a sand aggregate was added in the amount of 60 wt% to avoid cracks and emphasize only the kaolin influence alone.

2. Aim of the work

The main aim of this work is to find the correlation between composition, components ratio, and mechanical properties, including frost resistance and resistance to aggressive environment of geopolymer composites under investigation. The filler content was monitored by its influence on the strength parameters. The results could be used to calculate the properties of materials usable in the building industry, mainly in the underground or in the other building industries, for example in the manufacturing of supporting structures and rehabilitation works.

The secondary aim was to find out how does the raw kaolin presence influences the mechanical properties of the final geopolymer product.

As a result of the work the best recipe with the optimal mechanical and resistant characteristics for subsequent use in the underground building, for example, immersed tube segments production, was found based on the raw materials available in the Czech Republic.

3. Experimental part

3.1. Methods

3.1.1. Work methods

The primary method to reach the goal of the work was measuring the properties of the samples prepared, so that their composition systematically represented the entire range of possible compositions of geopolymer based composites. The main tested sample composition includes the geopolymer Baucis LNa consists of two components: powder melted fly-ash metakaolin and liquid glass; two types of sand: Kaznejov sand for cement surfaces with grain sizes 0/4 mm and Zlosyn sand with grain sizes 0/4 mm; aggregates of 0/4 mm, 4/8 mm and 8/16 mm sizes; Fiberglass R63SX1 with a 4.5 mm length. In the future, it is also possible to add metal fibers and various improver additives. The wt. % ratios of the used materials are described in *Tab. 2*. The measurement was divided into three types: mechanical properties, chemical resistance, structural analysis. By comparison, the values of compositionally different composites and the relationship between the composite's composition and their mechanical properties can be evaluated.

Samples are made in three sizes: 10x10x10 cm, 40x10x10 cm and 15x15x15 cm. The sizes were chosen based on the CTU experimental Centre employees experience. Testing of produced specimens was performed at minimum one month after mixtures formation. This time is necessary for appropriate sample solidification.

Since it was impossible to prepare such a large number of samples for all types of testing compositions at once, it was decided to choose the two best mixtures based on the result of mechanical properties tests. Based on these mixtures, next series of samples were made for further testing for frost and the aggressive chemical environment resistance. For structural analyses, it was sufficient to use fragments from the samples after conducted compression tests.

For the kaolin influence describing the similar testing way was chosen. The main principle is gradual adding of raw kaolin in Mefisto L05 based metakaolin matrix. It is

important to note, that used Mefisto L05 was re-burned in a laboratory furnace before testing. After re-burning and before work start Mefisto L05 was tested for kaolinite presence, so the amount of kaolinite was under the detection limits.

3.2. Materials

3.2.1. Binder

As the basis of geopolymer composite Baucis LNa (CLUZ Nove Straseci, Czech Republic) was chosen. This material consists of two components that are packed separately. The first component is a slag-metakaolin powder, which is mixed with the second component of an alkaline sodium activator based on the water glass. The mixing ratio of the two components is determined by the manufacturer, and it is 5:4 respectively. The exact chemical composition of the components is not disclosed by the manufacturer.

For raw kaolin influence determination Mefisto L05, made by the Czech company CLUZ Nove Straseci (Czech Republic) was used with a declared metakaolin content of 95 wt% and impurities such as quartz and muscovite. To remove the residual kaolin in Mefisto L05, the powder was burned at 750 °C for 6 hours. The raw kaolin used was produced by Sedlec Ia (Czech Republic). The alkaline activator was prepared by dissolving NaOH (Lachner, Czech Republic) in sodium water glass from Vodni Sklo, a.s. (Czech Republic) in a ratio of 1 to 0.15, respectively.

3.2.2. Filler

Several types of material were chosen as a filler according to the main work task – applying geopolymer composite in the underground building industry:

- Two types of ordinary sand, which are widely used in civil building in the Czech Republic: Kaznejov sand for cement surfaces with grain sizes

0/4 mm obtained by floated kaolin production and Zosyn washed sand with grain sizes 0/4 mm, which is used in the concrete building industry. As an aggregate, silica sand Strelec ST 92 with 99 wt% of SiO_2 and a particle size of $D_{50} = 0.6$ mm was used for the samples made from Mefisto L05 metakaolin.

- Fiberglass R63SX1 with a 4.5 mm length was chosen on the basis of experiments conducted in the Academy of Sciences of the Czech Republic [Steinerova M. et al., 2017]. The purpose of the glass fibers was to improve the mechanical properties of the geopolymer composite and to reduce the binder percentage.

- Coarse aggregates of 0/4 mm, 4/8 mm, and 8/16 mm sizes. This size of aggregates is commonly used in the building industry, and it is easy to get them for the application in further experiments.

3.2.3. Reference material

The primary purpose of the work was to determine the optimal ratio of composite components for future use. In this regard, it was necessary to make a comparison with other materials already used in production - concrete. Attempts to get any information about the current compounding of concrete (composite) used by immersed tube manufacturers has not been successful. In this regard, for comparison, concrete based on a French-made Calcia Ultracem 52,5 HRC cement was chosen as a reference sample to its mechanical parameters.

3.2.4. Composition of geopolymer composites

In all conducted experiments the sand content in the mixtures was varied from 30 to 70 wt. %. Wet fresh mixture of geopolymer gel and sand loses porous water at

curing and drying processes to form a dry solid composite composed of geopolymer matrix and filler. In cases of high sand content ranging from 65 to 70 wt. %, during the mixing of the components, a small amount of water was added to increase the fluidity and solidification time. The full scale of the geopolymer composite's compositions is presented in the *Tab. 2*. A minimum of three samples of each composition were prepared for flexural strength testing and from three to six samples for compressive strength testing.

Metakaolin and an alkaline activator were mixed (Si/Al = 1.8; Na/Al = 1.0; $Na/H_2O = 0.7$) first for 5 minutes, and a basic geopolymer matrix was obtained. The amount of alkaline activator depended on the metakaolin and metakaolin+kaolin content. Then, kaolin and sand were added and stirred for 10 minutes. Sand formed 60% of the total mixture weight.

Tab. 2.: Scale of geopolymer composite compositions. Green color means tested recipes, red indicates the none-tested recipes. Aggreg. is used as an abbreviation for aggregate

Ratio Sand:GP wt. %	GP matrix	Zlosyn sand	Kaznejov sand	Aggreg. 0/4	Aggreg. 4/8	Aggreg. 8/16	Glass fibers
55:45 65:35 70:30	Green	Green	Green	Red	Red	Red	Red
50:50 55:45 65:35 70:30	Green	Green	Green	Red	Red	Red	Green
70:30	Green	Green	Green	Red	Red	Green	Red
30:70 55:45 65:35	Green	Green	Green	Red	Green	Red	Red
65:35	Green	Green	Green	Green	Red	Red	Red
50:50 55:45 65:35	Green	Green	Green	Red	Green	Red	Green
50:50 60:40	Green	Green	Green	Green	Red	Red	Green
0:100	Green	Red	Red	Red	Red	Red	Red

To ensure the homogenous distribution of a small amount of kaolin in the samples (5 wt% and lower) the appropriate amount of kaolin was dispersed in approximately 30 g of water, which was required for proper dilution of the alkaline activator. Then, the suspension was added into the already mixed geopolymer matrix. For samples with a kaolin content above 5 wt%, kaolin in the form of fine, dry powder was added with sand into a geopolymer matrix that helped activate the precursor mixture mechanically. The weight percentage of kaolin and metakaolin in the samples was 0 to 50 and 100 to 50, respectively. This form of writing was chosen to imitate the impurities percentage in the initial powder.

Tab. 3.: Prepared sample ratios of metakaolin substituted with kaolin

Kaolin (wt. %) (K)	Metakaolin (wt. %) (MK)
0	100
5	95
10	90
15	85
20	80
30	70
35	65
50	50

3.3.   Sample preparation

3.3.1. Preparation of geopolymer matrix

The geopolymer matrix consists of two components powder (metakaolin) and liquid (alkali activator) (*Fig. 11A*, *B*.). It has always been prepared in accordance with the recipe given by the manufacturer in the ratio of 5 to 4. This mixing ratio makes it

possible to achieve optimum rheological properties of the mixture and the optimum Si:Al ratio. Furthermore, the optimum mixing time under constant conditions, i.e., at a given fixed rotation speed of the mixer and at an optimum constant amount of metakaolin powder, in accordance with the mixer volume, was experimentally determined. The mixing time was depended on the increasing temperature of the suspension resulting from internal friction during the mixing process. In literature, this value was determined experimentally by taking samples during stirring each 5 minutes, from 0 to 20 minutes, and comparing the mechanical properties of the products after curing [Steinerova M., 2009]. In this way, a mixing time of 15 minutes was determined when the temperature of the slurry was increased by about 3 °C from the start of mixing. After this time, the strength of the samples began to decline. In order to ensure the constant rheological properties of the matrix, which rapidly hardened and gelled at 25 °C, the optimal volume of geopolymer gel was prepared at once for each series of samples.

3.3.2. Preparation of geopolymer composite

Mixing with the filler was carried out in a 40-liter tank. In some cases, a small amount of water was added to facilitate homogenization of mixture with a maximal filler amount. Mixing of the prepared matrix with a filler of different fractions proceeded in several phases depending on the filler type at 25 °C. The first was always added sand (*Fig. 11D, E.*) that, like all the other fillings were added gradually without the mixing process interruption. In the case of preparing samples with glass fibers (*Fig. 11C.*), it was added to the second. This was necessary so that the sand particles during the mixing process as a result of friction divided the faberglass into smaller filaments. Larger aggregate material (*Fig. 11F, G, H.*) was always added the last. This was due to the fact that their consistent distribution in the mixture requires less time as well as with a more significant load on the motor of the mixing machine.
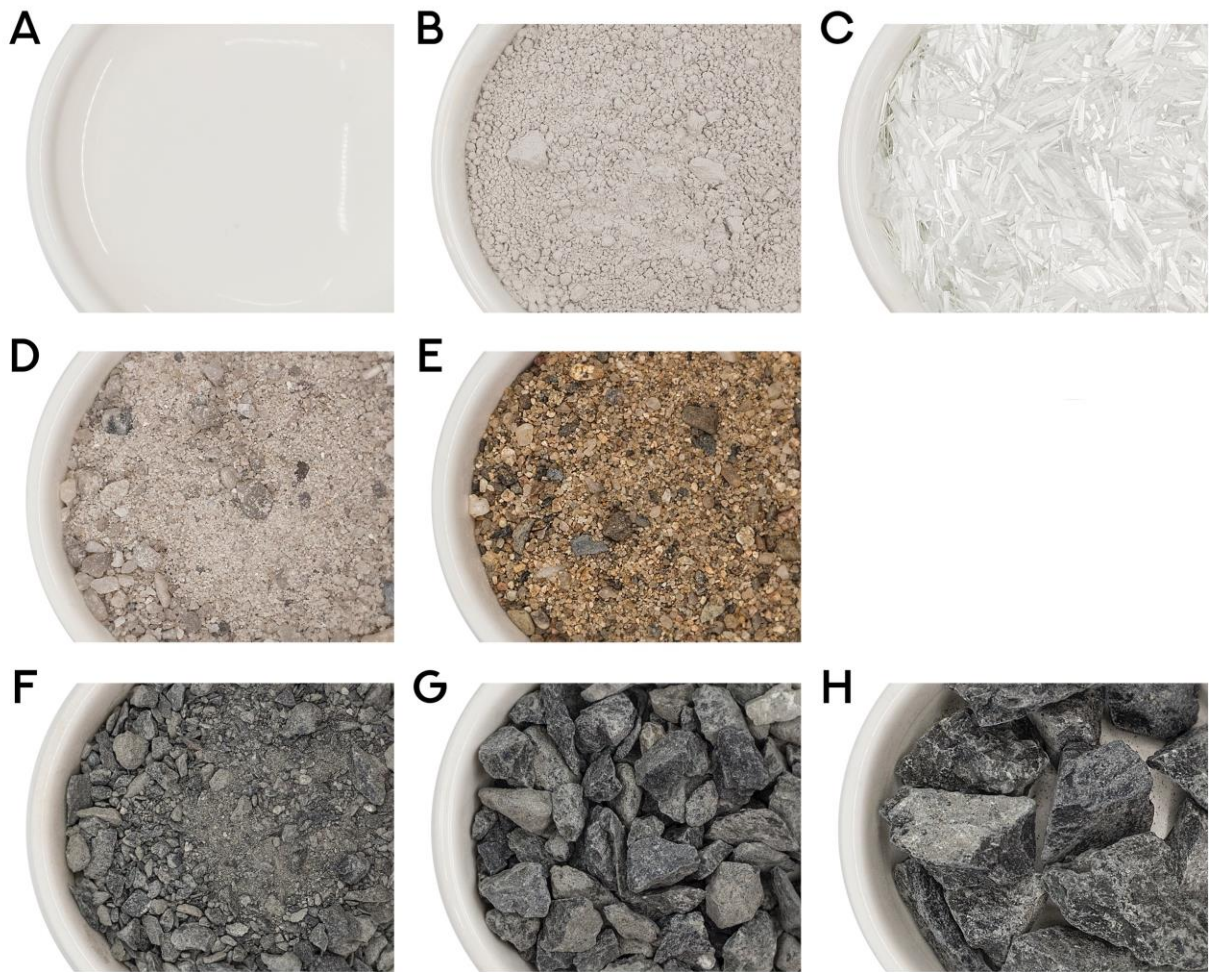
Fig. 11.: (**A**) Alkali activator, (**B**) Metakaolin, (**C**) Fiberglass, (**D**) Kaznejov sand size 0/4, (**E**) Zlosyn sand size 0/4, (**F**) Coarse aggregate 0/4, (**G**) Coarse aggregate 4/8, (**H**) Coarse aggregate 8/16

3.3.3. Preparation of reference concrete samples

The preparation of reference concrete samples was carried out under the similar temperature conditions as the geopolymer. French-made Calcia Ultracem 52,5 HRC cement (*Fig. 12A.*) was used as the main component. Ultracem 52,5 HRC cement from Calcia is purposed for the production of prestressed segments as well as for work where quick strength gaining is needed. Due to its properties, this cement is perfect for work in difficult conditions where it is necessary to achieve good strength characteristics, for example, in the cold. Silicon sand with a grain fraction of 0/4mm was used as a filler (*Fig. 12B.*). It is important to note that this composition was chosen on the basis of the mechanical properties testing of a series of geopolymer samples.

Fig. 12.: (**A**) Cement Calcia Ultracem 52,5 HRC, (**B**) Sand 0/4, (**C**) Mixing process, (**D**) Prepared samples covered with the PVC film

3.3.4. General conditions for sample preparation

Sample preparation was distributed in time due to their large number. Every time, the prepared mixture from the Baucis LNa and concrete was poured into molds of different sizes (depending on the type of mechanical testing) after accurate continual mixing of all components. After that, air bubbles were mainly eliminated from filled molds under vibration *(Fig. 13.)*. Then the samples were covered with a polyethylene foil and stored for 3-7 days at a laboratory temperature *(Fig. 13.)*. After this time, the foil was removed, and the samples were stored for at least 40 days before mechanical tests conducting. All samples were stored during the week in the same room where the test was conducted at temperature 20-25 °C.

Fig. 13.: Sample vibration process and film covering

The Mefisto L05 based mixture was poured into proper molds under vibration until air bubbles disappeared. The samples were stored in covered molds for 7 days. Then, the samples wrapped in polyethylene foil were cured at laboratory temperature for 28 days. All samples were prepared under the same conditions and stored for two months after curing before testing.

For XRPD and FTIR analyses dry mixtures of metakaolin (MK) and kaolin (K) were prepared in ratio MK:K = 95:5, 85:15, and 65:35.

3.4.   Methods of mechanical properties measurement

As the main methods of measuring the mechanical parameters of the material, two standard methods were chosen: flexural and compressive strength measuring. The recipes shown in *Tab. 2* were measured first. On the basis of the measurements obtained, two recipes with the best strength characteristics were choisen: 1. Kaznejov sand (55% + GP + 4/8 aggregates + fiberglass); 2. Zlosyn sand (70% + GP). Both recipes samples and concrete undergo aggressive environment and frost resistance tests, and then after drying mechanical were again tested.

3.4.1. Compressive strength

Compressive strength tests were performed:

a. for small samples prepared for frost resistance tests on a semi-automated press VEB Werkzeugmaschinenkombinat "Fritz Heckert", Leipzig according to Standard No. ČSN EN 1015-1116 using the halves of the standard samples with a 40 x 40 x 160 mm size.

b. for bigger samples prepared as reference samples and for choosing the best recipe on a VEB WMK "Fritz Heckert" Werkstoffprufmaschinen, Leipzig *(Fig. 14.)* according to ČSN EN 12390 - 3 using the appropriate sample size, i.e., 150 x 150 x 150 mm. Acid impact on the compressive strength was carried out on the halves of the standard samples with a 100 x 100 x 400 mm size.

Fig. 14.: The 150 x 150 x 150 mm sample under the press load

3.4.2. Flexural strength

Flexural strength test was performed:

a. for small samples prepared for frost resistance tests on a semi-automated press VEB Werkzeugmaschinenkombinat "Fritz Heckert", Leipzig *(Fig. 15.)* according to Standard No. ČSN EN 1015-1116 using the standard sample size, i.e., 40 x 40 x 160 mm.

b. for bigger samples prepared as reference samples, acid impacted samples and for choosing the best recipe on a semi- automated press VEB Werkzeugmaschinenkombinat "Fritz Heckert", Leipzig *(Fig. 16.)* according to ČSN EN 12390 - 5 using the appropriate sample size, i.e., 100 x 100 x 400 mm.

Fig. 15.: The 40 x 40 x 160 mm beam under the 3-point press load

Fig. 16.: The 100 x 100 x 400 mm beam under the 4-point press load

3.4.3. Fracture energy

Due to the fact that fiberglass was added to the samples, it was decided to test fracture energy. The measurement was carried out on the loading frame INOVA ZUZ 200 with a nominal maximum force of 100 kN *(Fig. 17.)*. The obtained values have been measured by the DEWETRON control panel. Loading was performed in according to the standard ČSN EN 12390-5 [ČSN EN 12390-5, 2009]. Testing was carried out only on the one type of samples made from geopolymer (K) (with a 60% of sand and 5% of glass fibers) due to the glass fibers presence.
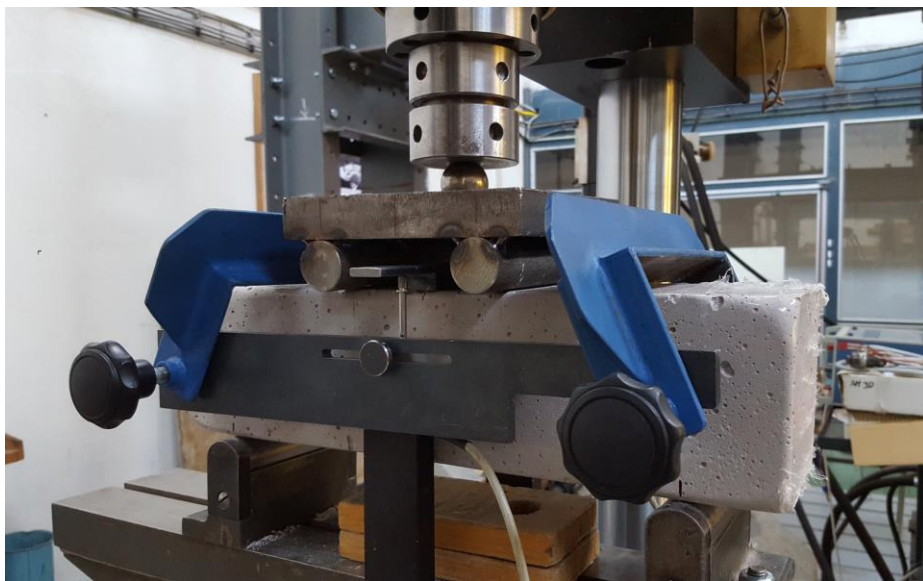
Fig. 17.: The 100 x 100 x 400 mm beam under the fracture energy measurement press load

3.4.4. Shrinkage

Measurement of volume changes was conducted by laser optoNCDT ILD1400-5 using optical triangulation method *(Fig. 18.)*. Depending on the distance, the scattering fraction of the reflection of the light spot is focused on the positioning element (CCD field) by an objective lens installed below a certain angle relative to the optical axis of the laser beam. Regulator senses the value measured from CCD field. The internally closed control loop allows to sensor make the measurement against various surfaces. The technical characteristics of the measuring laser are shown in the *Tab. 4*. Below is

shown a sample of a Baucis geopolymer with Zlosyn sand during the measurement *(Fig. 19.)*. The test was conducted for a month at constant laboratory temperature.
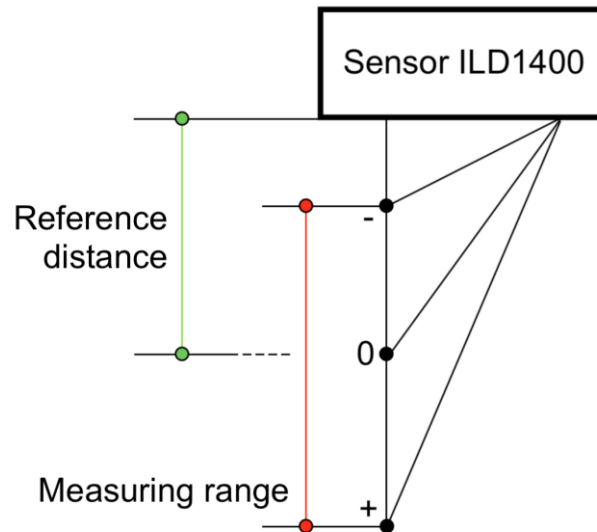
Fig. 18.: Schematic representation of the triangulation principle

Tab. 4.: Technical characteristics of the measuring laser

Measuring method	Optical, laser, triangulation
Measuring range	5 mm
Linearity from measuring range	± 0,2
Static resolution	0,6 μm
Sampling frequency	1 kHz
Allowable ambient light	4000 1x

Fig. 19.: Freshly prepared geopolymer (Z) cylinder in the shrinkage measuring device

3.4.5. Frost resistance

The mechanical properties of the composites were also compared in terms of the weathering resistance. The methodology for this measurement was to determine the water resistance of the sample at freezing and defrosting processes.

Following samples were tested:

- two optimal recipes of Baucis GP with Kaznejov and Zlosyn sand;

- whole range of samples with variative content kaolin in metakaolin (0-15% of kaolin).

Frost resistance tests were carried out according to the specific frost resistance standard for concrete CSN 73 1326 [CSN 73 1326., 2003]. It was tested by alternating freezing and defrosting of water-saturated samples with in 50 cycles (*Fig. 20.*). Testing of all 40x40x160 mm samples was conducted under the same conditions and the same

number of cycles. Freezing cycles were at temperature of -15 to -20 °C. One cycle consisted of 4 hours of freezing and 2 hours of defrosting in the water at 20 °C. Before the strength measurements were conducted, all samples were dried at laboratory temperature for 28 days.

Fig. 20.: Frost resistance measuring freezer. (**A**) loading room, (**B**) sample arrangement

3.5.   Acid resistance

One of the main parameters for determining the geopolymer suitability to the underground environment is the resistance to the aggressive waters. No universal standard was found on aggressive water tests, because the underground environment area is very different from each other depending on the location. In this regard it was decided to use hydrochloric acid and sulfuric acid based on the studied literature [Neetu Singh et al., 2013]. Hydrochloric acid imitates the most common underground water composition. Sulfuric acid is the main acid compound of acid rains and therefore could get in touch with underground constructions. However studied concentration imitates almost unrealistic conditions and therefore gives a clearer view of the geopolymer composition behavior under extreme conditions. Samples of geopolymer composite (*Fig. 21.*) and reference concrete (*Fig. 22.*) were immersed in pre-prepared acid solutions with pH 1. GE Whatman® Panpeha™ pH indicator strips were used to determine the acidity of the medium are highly accurate in pH determination indicator. In total, three series of samples from each recipe were prepared: Geopolymer (K); Geopolymer (Z), Calcia Ultracem based concrete. The time interval for soaking the

samples in the solutions was 1, 2, and 4 months. During this time, solutions pH was maintained at 1-4. Acidity measurements were taken every day during the first month, every three days for the next second month and once a week in the third and fourth months. Daily pH measurements were necessary due to the fast neutralization process during the first month and continual low pH maintenance. In the last two months, the pH changes were very slow. After the end of each time period, the samples were dried for two months at laboratory temperature and then tested for their mechanical properties. The average temperature of the environment during these tests was 27 °C.

Fig. 21.: Geopolymer (K) in the hydrochloric acid (HCl) solution
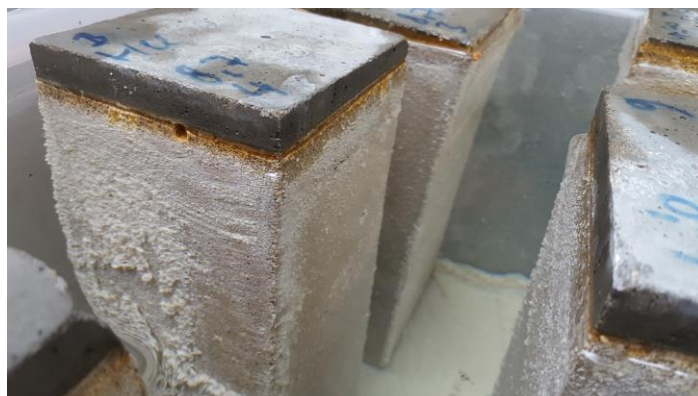
Fig. 22.: Reference concrete in the hydrochloric acid (HCl) solution

3.6. Structural measurement

3.6.1. XRPD

X-ray diffractograms were recorded using Rigaku MiniFlex 600 (Ni-filtered Cu-Kα1,2 radiation) *(Fig. 23.)* equipped with a NaI(:Tl) scintillation detector and were compared to the relevant records in the ICDD PDF-2 database [ICDD PDF-2 database, 2013].
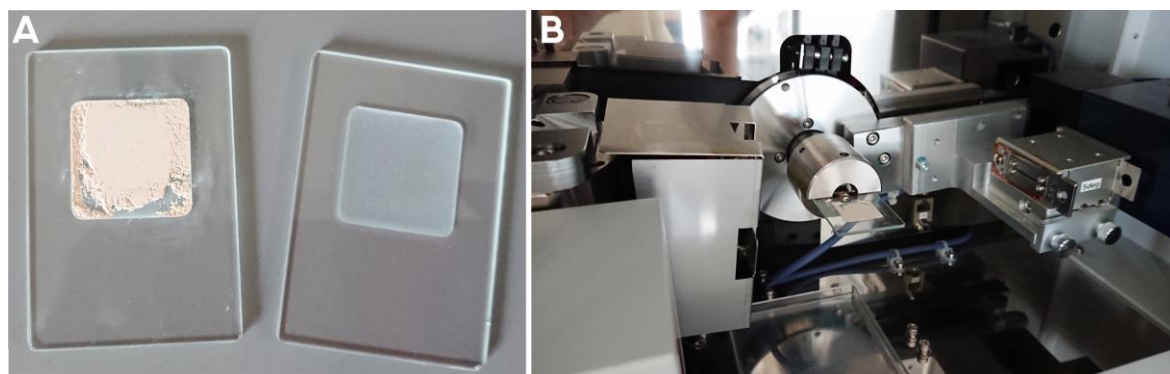
Fig. 23.: (**A**) Preparation of samples for XRPD measurements, (**B**) setup of XRPD measuring equipment

3.6.2. FTIR

The composition of samples was confirmed and studied with FTIR spectra recorded on Nicolet iS50 FTIR (ThermoScientific, USA) *(Fig. 24.)* in the middle infrared region at 400 – 4000 cm^{-1} with a resolution of 2 cm^{-1} on a ATR diamond crystal which were also compared to the relevant records in the database [HR Inorganics].
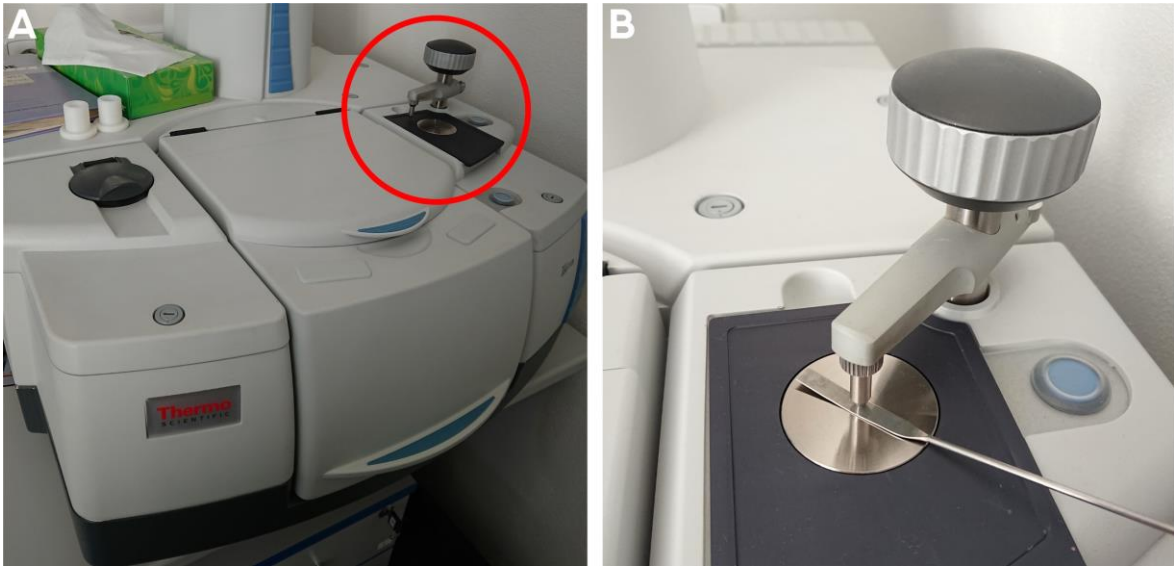
Fig. 24.: (**A**) Nicolet iS50 FTIR (ThermoScientific, USA), (**B**) FTIR-ART measuring process

3.6.3. SEM (Scanning Electron Microscope)

Conducting documentation of the measured samples was carried out on a Quanta 450 (FEI) SEM. The observations of the polished cross-sections were performed in backscattered electron (BSE) mode under high vacuum. The analytical conditions were: energy of the electron beam of 30 kV; spot size of 2 mm in a 10mm working distance. The samples were vacuum coated with gold to prevent localized charging of the specimen. The semi-quantitative chemical composition of the matrix was analyzed using an energy-dispersive X-ray microanalyzer (EDAX, Apollo X).

A detailed SEM was performed on a Phenom XL Desktop SEM under high-vacuum on the natural sample surface of the polished sections mentioned above with a voltage of 10 kV (SEM) and 15 kV (SEM/EDS).

3.6.4. Elasticity modulus measured by nanoindentation

To conduct the SEM study of the matrix, spot tests of the micromechanical properties on the polished sections were compared. The measurement was carried out with a nanoindentation tester by an NHTX S/N: 10-00039 from Anton Paar GmbH Austria. The settings were the maximal load of 2 mN, the loading rate of 30 nm/min,

the Poisson's ratio of 0.2. In the case of a sample containing kaolin, four consistent indents were conducted, while the sample without kaolin required numerous indents because of the varying results. The elasticity modulus was computed using the Oliver and Pharr method for the Mefisto geopolymer samples based only.

4. Results and discussions

4.1.   Compressive and flexural strength

Specimens preparation was carried out at the CLUZ company territory using dough kneader Alba Horovice *(Fig. 25.)*. Production and measurement of samples was carried out in three stages, each of which lasted a year due to the fact that in winter the temperature in the production area was below 15 °C, which dissatisfies the optimal conditions for mixing and subsequent storage of geopolymer composite samples. In this regard, all work was carried out in the summer period.
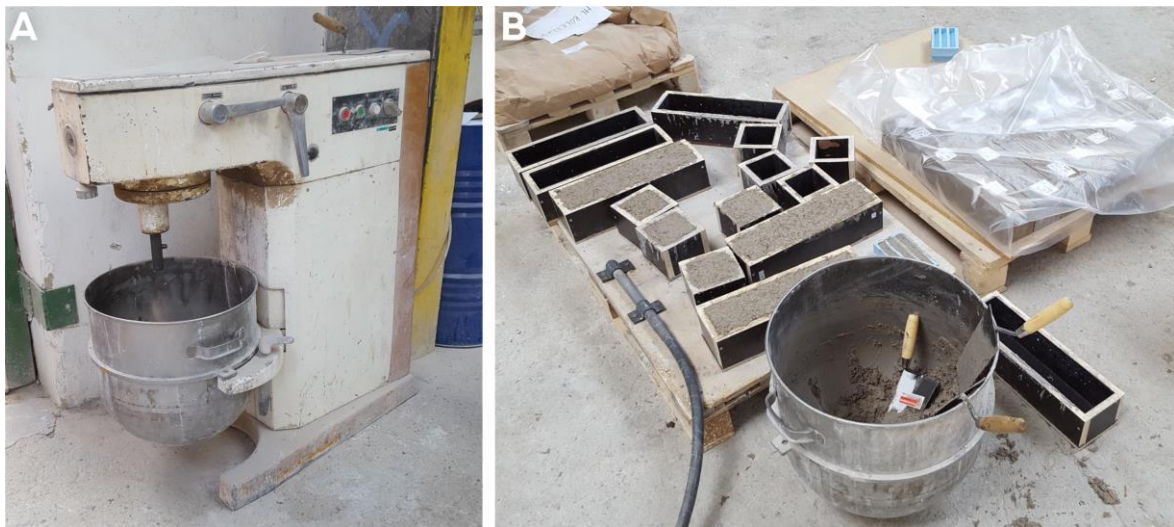
Fig. 25.: (**A**) Dough kneader Alba Horovice and (**B**) samples molding process

Stage 1 - Selection of the optimal component's ratio

At the first stage, all planned composite mixtures listed in the *Tab. 2.* were tested for compressive and flexural strength. The test results are presented in the graph below *(Fig. 26, and Fig. 27.)*. The specified percentage of sand is calculated from the volume of sand + GP without the other added components. The graph clearly shows two dominant composites - Zlosyn based geopolymer without adding additional components (blue line) and the Kaznejov based geopolymer with the addition of 4/8 mm coarse aggregates and fiberglass (light purple line). The Kaznejov based

geopolymer composite with fiberglass was chosen since the strength values are almost identical to composite without fiberglass. However, this mixture consists of a larger number of components, which makes it possible to study their behavior in further work.

Mixtures with zero strength value in the graphs were not prepared due to high fluidity and viscosity. The mixture with 8/16 aggregate has not been tested because of the mixer is not intended for the such aggregates size. In practice, it turned out that the 0/4 aggregate does not require the addition of sand and showed average values, so it was decided not to continue further experiments with this composite. Geopolymer matrix was also tested but due to its fragility, only compressive strength testing was performed, which showed very good results. However, the absence of aggregate fillers causes a strong fracturing of the matrix over time, which denies the possibility of its use in future.

Fig. 26.: Compressive strength values of all prepared samples
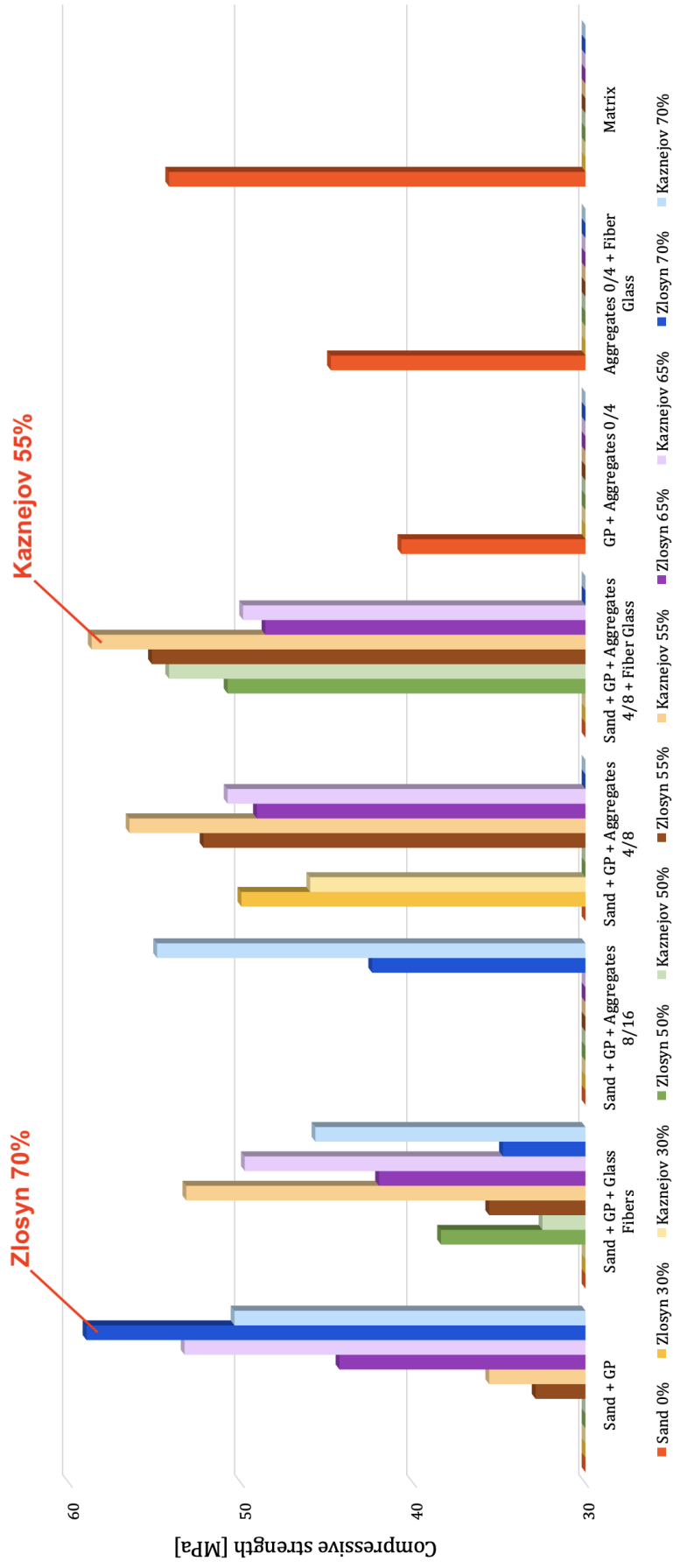
Fig. 27.: Flexural strength values of all prepared samples

Kaznejov (sand 55% + GP + 4/8 aggregates + fiberglass) and Zlosyn (sand 70% + GP) composites had almost 60 MPa for compressive strength and 12-18 MPa for flexural strength. It is important to note that for further research of the geopolymer composite, these two composite mixtures were taken as the basis.

Stage 2 – Reference sample

The number of samples needed for all further experiments was prepared, as well as reference samples for re-testing of mechanical characteristics after one year. At the same time, samples of concrete were prepared and tested. When comparing the results there is a noticeable difference in the values for different years *(Fig. 28.)*. This can be caused by two factors:

- Samples stored at different times before testing and some of them gained greater strength than the others.
- Used kaolin (metakaolin) was mined from different places of the mineral deposit.

However, these changes in strength values were in measurement tolerance and 2018-year samples were used as references.
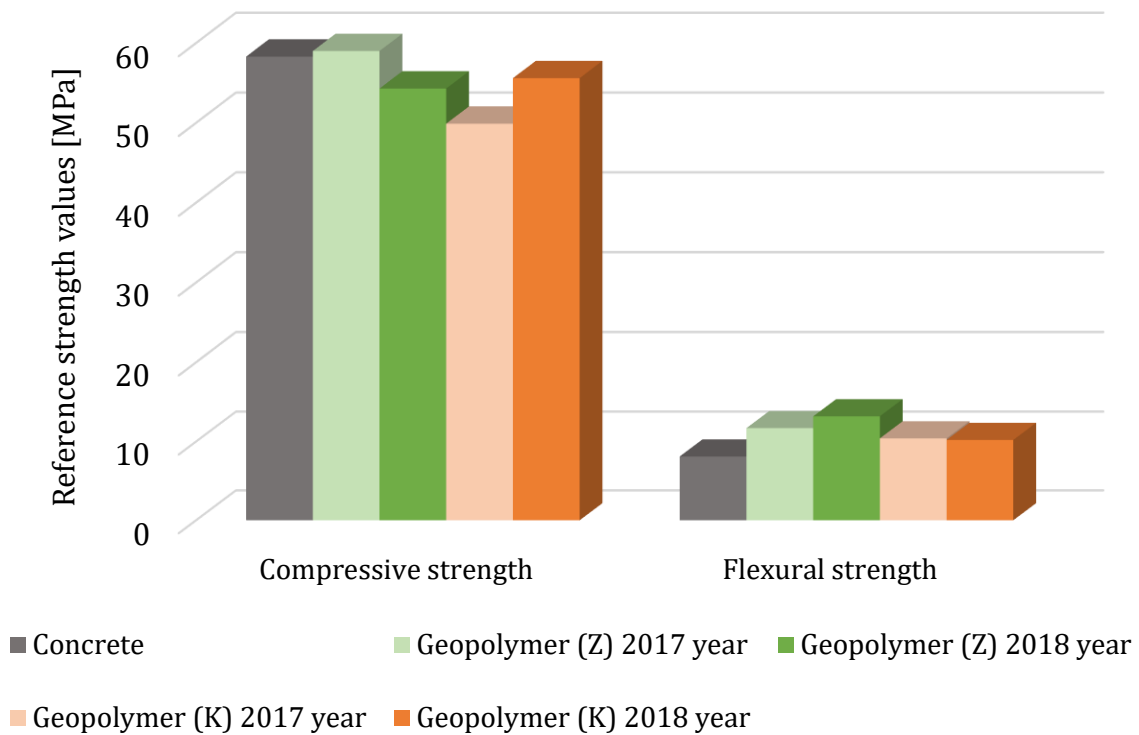
Fig. 28.: Comparison of mechanical strength properties of samples geopolymer different years of production and concrete

Stage 3 – Added kaolin influence

The resulting mechanical properties of the samples referring to the metakaolin substitution with kaolin are displayed in *Fig. 29.*
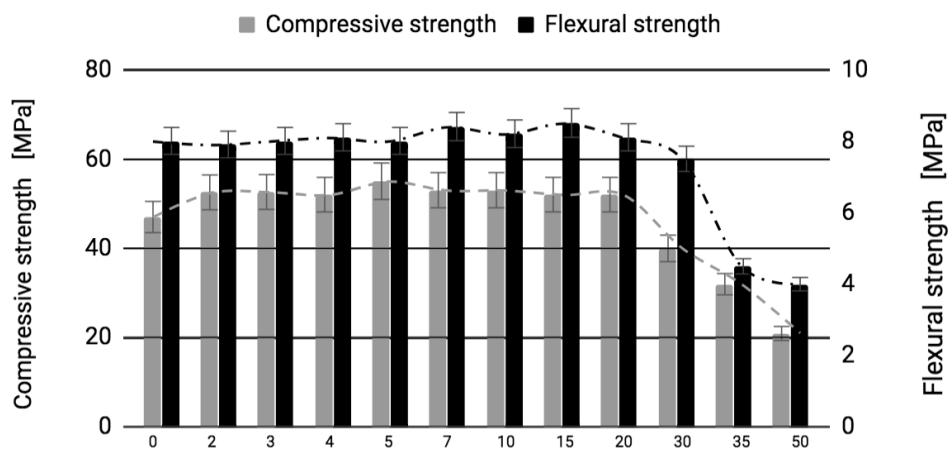
Fig. 29.: The compressive (grey) and flexural (black) strength values of the reference samples affected by kaolin input

The compressive strength of the tested samples with changing kaolin content ranged from 20 to 55 MPa. Samples with kaolin content in metakaolin up to 20 wt% showed slightly better compressive mechanical properties in comparison with samples made from the pure metakaolin. Changes in flexural strength due to varying kaolin content were negligible and within statistical error, while kaolin content was lower than 20 wt%. The addition of kaolin above 20 wt% led to a dramatic decrease in both the compressive and flexural mechanical strengths. The hardening time slowed down with the increasing addition of kaolin.

The addition of kaolin increased mixture viscosity and made mixing difficult, so the porosity of some samples could increase. This could influence the microstructure and thus decreased strength at higher kaolin concentrations.

4.2. Fracture energy

Geopolymer (K) composite with added glass fibers has been tested on fracture energy. Load-displacement curves of geopolymer (K) with 5% of glass fibers for 3 specimens are displayed in *Fig. 30*. Typical load-deflection plot comprises three stages of behavior. In the first phase (1) the deflection increases linearly with the load. A fracture process develops during the second phase (2) where microcracks form and slow crack growth is noticeable. In the third phase (3), known as strain softening, rapid crack growth is apparent. [Kozlowski M., et al 2015; Ulfkjaer J.P., Brincker R. 1995]

Fracture toughness was not determined, because the no-notch specimen was used. Bending tensile strength according to Bernoulli was determined to 13.51 ± 0.68 MPa and corresponded with flexural strength determined experimentally. Fracture energy was determined in three-point bending on un-notched beams according to the RILEM recommendation and calculated according to Ulfkjaer et al. (1995). The value of fracture energy was determined to 104.2 ± 5.2 N/m.

In compare with literature data [Ulfkjaer J.P., Brincker R. 1995; Ding, Y., et. al, 2018], Portland cement concrete with compressive strength about 50 MPa usually has

bending tensile strength 5 MPa and fracture energy 112 N/m. Fracture energy of tested GP was comparable.
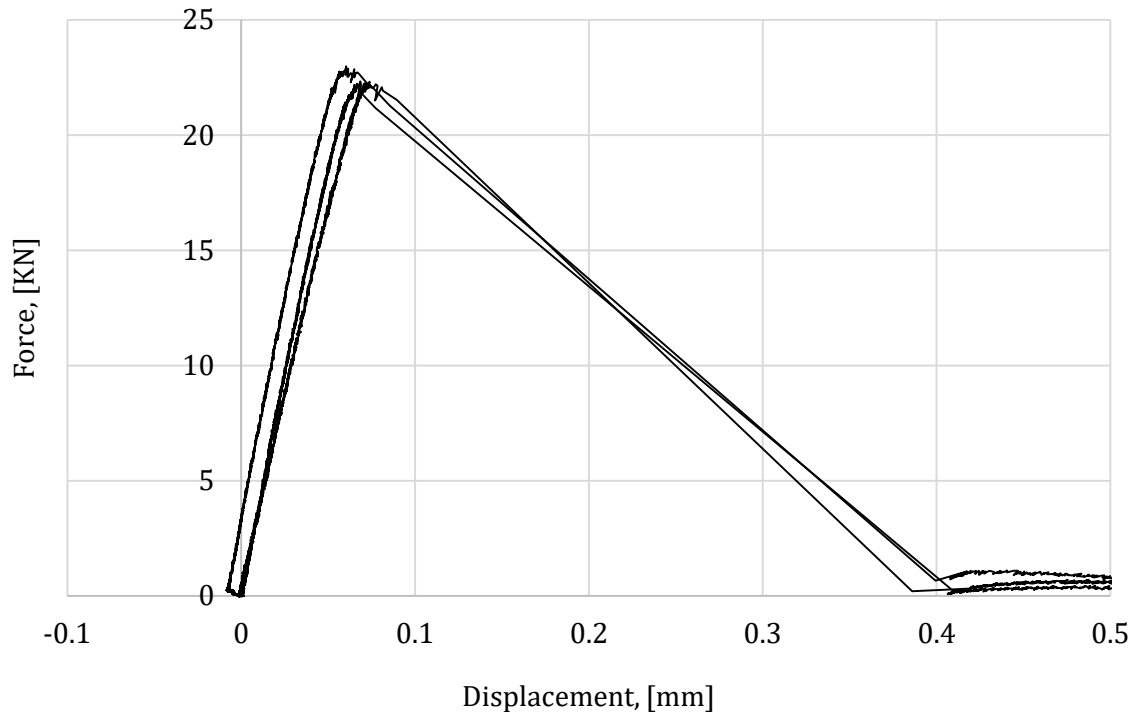
Fig. 30.: Load—displacement curves of geopolymer (K) with 5% of glass fibers for 3 specimens

4.3. Shrinkage

Testing the reduction of the volume of material during the solidification process was carried out on geopolymer (Z). It was chosen because it contains a smaller number of aggregates, in contrast to geopolymer (K), which means shrinkage process to be more active. After 20 days of testing under the constant temperature conditions, it was decided to stop the measurement. The *Fig. 31.* clearly shows that the strongest changes occurred in the first two days. Immediately after sample preparation increase of the volume was observed. It was probably caused by raising temperature of the sample because of ongoing geopolymerization Then, the next 12 days (288 hours) there was almost no shrinkage after which all samples showed a slight volume oscilation within two days. The average shrinkage value for this type of geopolymer composite was

equal to 1.10 ± 0.17 mm/m. Referring to studies on the shrinkage of concrete and Portland cements, it can be argued that the resulting value is little bit higher than that of some types of concrete with similar mechanical properties [N.A. Eroshkina, M.O. Korovkin, 2011]. It is possible to reduce the effect of shrinkage using aggregates with a size greater than 0/4 and other various additives. However, it is important to note that the components added to reduce shrinkage should not affect the flexural strength negatively.
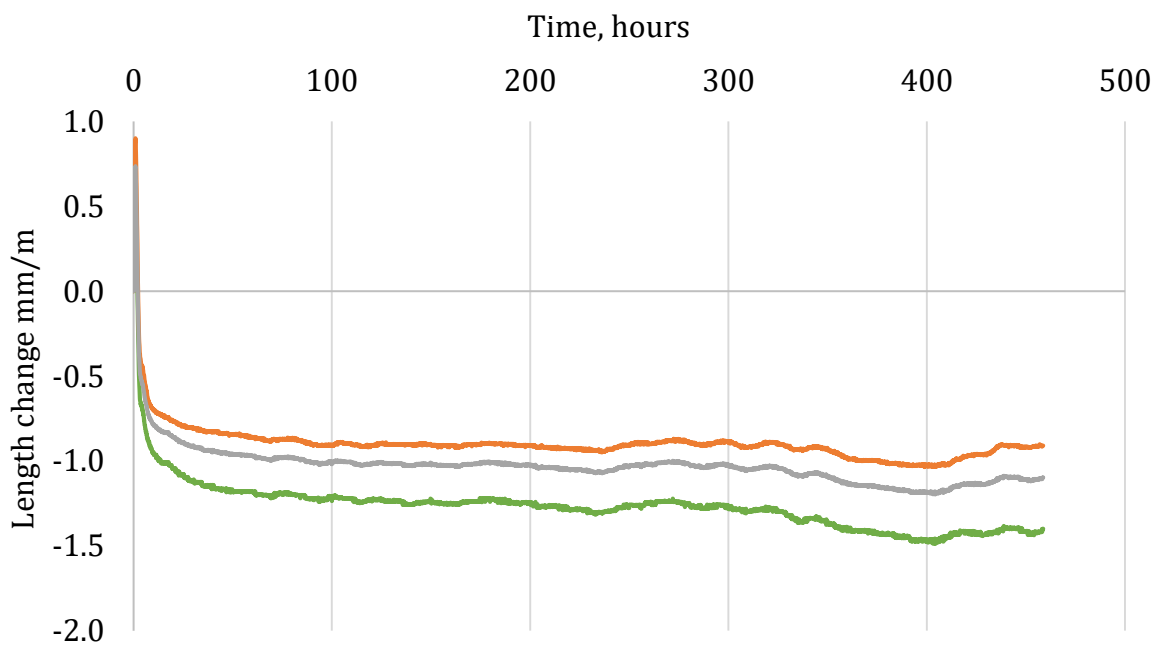
Fig. 31.: Changes in samples lengths over time during solidification of 3 samples.

4.4.   Frost resistance

For the first two stages, the frost resistance measurement was carried out in a laboratory freezer in accordance with the specific frost resistance standard for concrete CSN 73 1326 [CSN 73 1326, 2003]. The samples of the size 40x40x160 mm were prepared and stored 60 days before the tests.

Stage 1 – Geopolymer (K), geopolymer (Z) and reference concrete frost resistance evaluation

Samples of geopolymer (K), geopolymer (Z) and reference concrete were dried at laboratory temperature for two weeks, then weighed and placed in a freezer. After the first 25 cycles, the samples were monitored and none of the samples had external indicators of destruction. Therefore, it was decided to conduct the next 25 cycles of freezing and defrosting. After that, the samples were dried for a month at laboratory temperature and tested for the compressive strength and 3-point flexural strength *(Fig. 32.)* according to the standard CSN EN 1015-11 [CSN EN 1015-11, 1999]. The strength's results compared with the reference samples of the same size are shown in the graphs below *(Fig. 33., Fig. 34.)*.
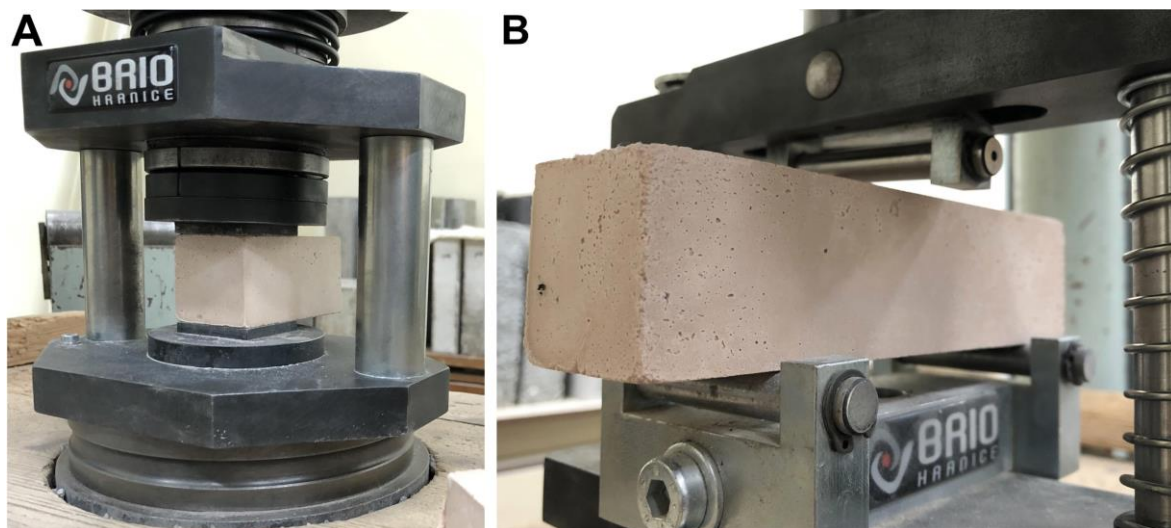
Fig. 32.: Geopolymer specimen measuring for compressive (**A**) and flexural (**B**) strength after 50 freezing cycles on EU 40 Werkstoffprufmaschien, Leipzig
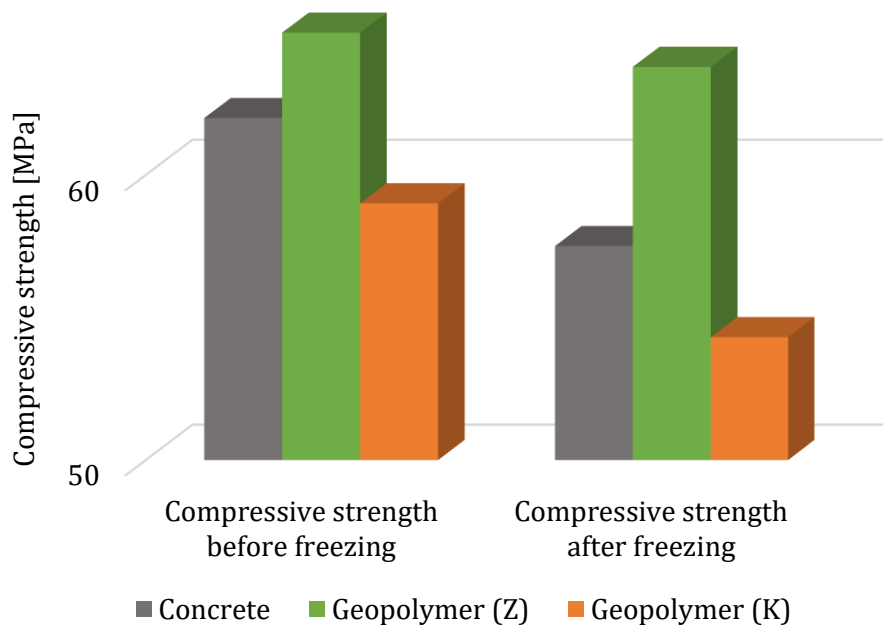
Fig. 33.: The compressive strength values of concrete, geopolymer (Z) and geopolymer (K) samples after 50 frost cycles

The percentage difference in compressive strength between reference samples and samples after 50 freezing cycles, is: 7% for concrete; 6% for Geopolymer (Z); 8% for geopolymer (K).
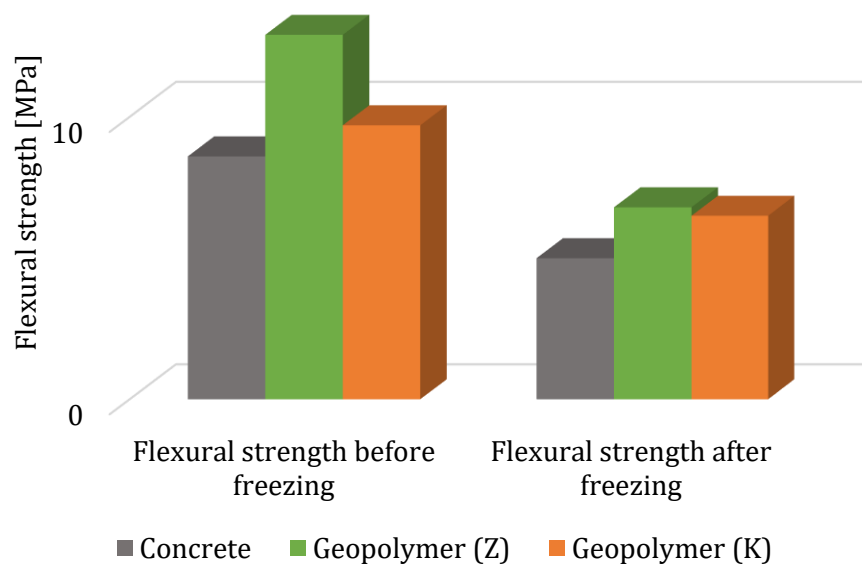
Fig. 34.: The flexural strength values of concrete, geopolymer (Z) and geopolymer (K) samples after 50 frost cycles

The percentage difference in flexural strength between reference samples and samples after 50 freezing cycles, is: 42% for concrete; 47% for Geopolymer (Z); 33% for geopolymer (K). Measurements have shown that freezing has a significant effect on flexural strength. Otherwise, for samples of all three materials, changes in the strength characteristics are almost the same.

The mass loss after 50 freeze-thaw cycles was less than 2% for all samples. The compressive strength of both geopolymer and concrete decrease after exposure to 50 freeze-thaw cycles. However, geopolymer (Z) exhibits a better frost resistance against freeze-thaw cycles than concrete. To provide an excellent resistance against freeze-thaw cycles micro-encapsulated phase change materials can be added [Shima Pilehvar et al., 2019].

Considering the intended use of geopolymer composites in the production of immersed tube segments, the final product will be practically not affected by frost and it could be supposed that the geopolymer composite is suitable for this building industry.

Stage 2 – Added kaolin influence on frost resistance

The compressive and flexural strength after the freeze-thaw cycles in water was compared with the values of the none-frost sample strength. Samples with 1 wt% of kaolin displayed visible cracks already after 25 freezing cycles. The cracks were probably caused by unsatisfactorily homogenized kaolin input and, therefore, were not measured. *Fig. 35* shows flexural and compressive strength after 50 cycles with the highest value reached by samples containing 2-3 wt% of kaolin. Here, the compressive strength even surpassed the highest values before freezing. The reason could be in the prolonged dwell in the proper conditions which supported the polycondensation process. Higher addition of kaolin deteriorated the frost resistance probably because of retaining water leading to dilatation inside the kaolin particles.
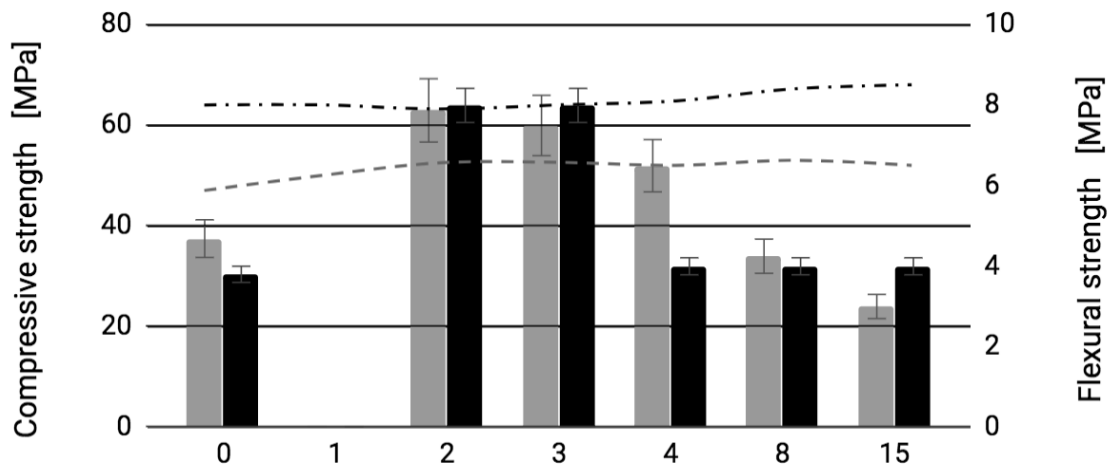
Fig. 35.: The compressive (grey) and flexural (black) strength values of samples affected by kaolin after 50 frost cycles. The grey dashed line shows the values of the reference sample's compressive strength, the black dash-dot line shows the flexural strength values of the reference samples

4.5.   Acid resistance

Testing the GP composite stability in acidic media was carried out on beams of size 100x100x400mm. This size was chosen due to the large number of required samples, as well as to ability to perform measurements for compressive and flexural strength on samples using beam halves. All samples were thoroughly dried at a laboratory temperature before testing. Two acid solutions were prepared - hydrochloric acid and sulfuric acid. These acids should stimulate unrealistic conditions in which the intended composite may be used. This allowed to understand the main trend of the influence of aggressive media on the material for a relatively short period of time. For more accurate results it needed much more time.

Both acid solutions were poured into six containers, three for each type of acid. Six samples were immersed into each container *(Tab. 5.)*.

After the first month of soaking, three samples were removed from each container and new three samples were added. During the whole period of testing, the measuring of pH solutions was carried out. The main task was to keep pH on the level of 1-4 during the whole time of the experiment. The trend of neutralizing solutions as a result of interaction with samples is shown in the graphs below *(Fig. 36., Fig. 37.)*.

Tab. 5.: List of materials and samples numbers prepared for testing

	HCl			H$_2$SO$_4$		
Container №	1	2	3	4	5	6
№ of samples	6+3	6+3	6+3	6+3	6+3	6+3
Material	Concrete	GP Kaznejov	GP Zlosyn	Concrete	GP Kaznejov	GP Zlosyn

During the first month, the process of acidic environment neutralization occurred due to interactions with 2-month-old samples' surface and was very active, especially in hydrochloric acid solution. Later, time required for neutralization increased and simultaneously decreased maxim reached pH value from 5 to 2-3 for all geopolymer samples in both acids. It means, that Na^{1+}, hydroxide anions presented on the surface and internal layer nearest to the surface, which had played the main role in the reaction in the beginning, were not available any more. Therefore, Na^{1+} and hydroxide from deeper layers of the samples were involved and its availability was lower. Interactions with the samples' surface is limited by diffusion speed and surface area. If diffusion speed can be affected by mixing, surface area of the sample including pores is defined by the sample material. So observed neutralization speed decrease of geopolymer samples could be caused by lower surface area due to smaller pores number and slower acid reactions with sample compounds.

Concrete, on the contrary, showed significant changes in pH value during the whole observation period. Neutralization stopped at pH 4 for sulphuric acid and pH 6 for hydrochloric acid every time, what means, that the availability of Na$^+$ or Ca^{2+} was always high probably due to higher porosity and faster reactions between concrete surface and acidic media. Since the acids had almost no influence on the geopolymers unlike concrete, it was decided not to change the pH during the last month to prevent the concrete samples disintegrations.
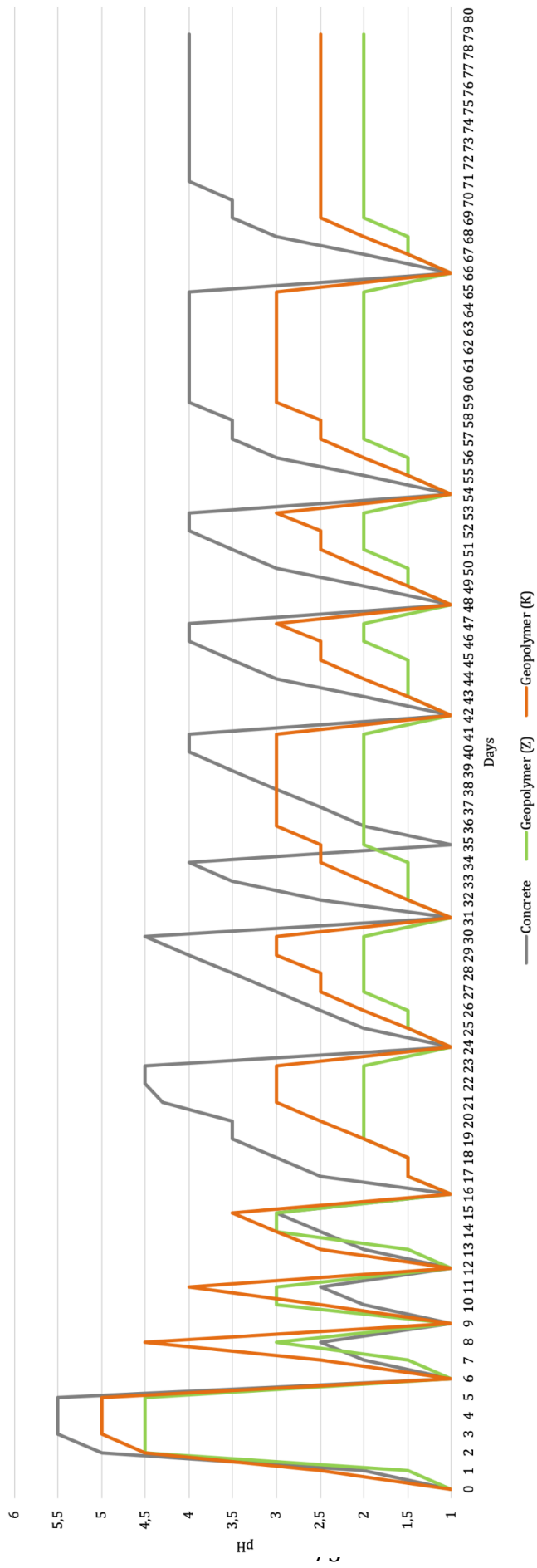
Fig. 36.: Maintaining of acidic H2SO4 environment during the 80 days
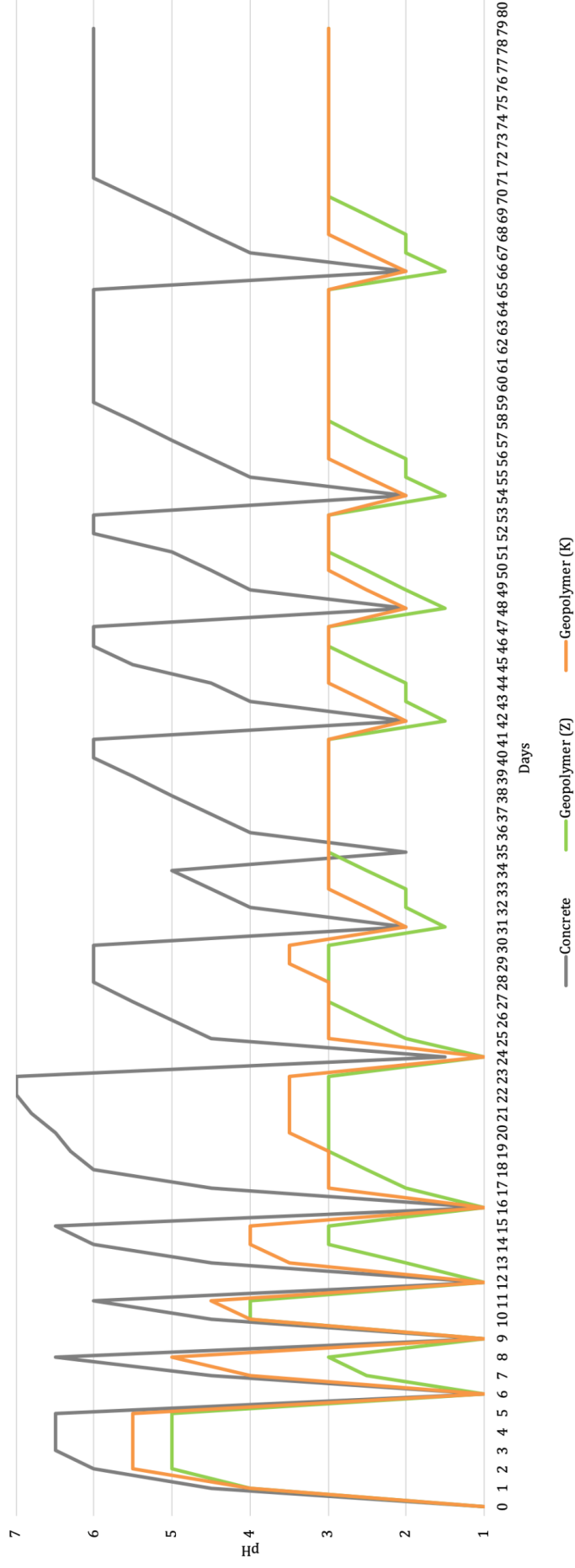
Fig. 37.: Maintaining of acidic HCl environment during the 80 days

At the end of each cycle of soaking in acids samples were thoroughly dried for two months, after that compressive and flexural strength was measured *(Fig. 38. and Fig. 39.)* In both cases from the compressing strength graphs it is obvious that concrete loses its strength in contrast to geopolymer, especially when exposed to sulfuric acid, which is quite expected since it is more active. Geopolymer specimens have shown no strength decrease and even significant strength increase in the case of geopolymer (Z) compressive strength measurements after immersion into sulphuric acid *(Fig. 38B.)*. This could be due to two factors. One of them is that specimens of a geopolymer harden over a longer period of time than concrete. The second is that the geopolymer has a closed pore structure, which minimizes the degree of influence of aggressive liquid medium [Steinerová M., 2009]. Concrete, unlike geopolymer, has an open pore structure and also contains chemically unbounded water which contributes to less effective resistance to aggressive water environments.

The samples of geopolymer showed *(Fig. 38A)* no noticeable increase in strength during the testing, which could be explained by its decrease as a result of the sulfuric acid influence. This means that in the case of both geopolymers (K and Z) the strength decreasing was a little active than its simultaneously increasing.

It is assumed that hydrochloric acid has a lesser effect on concrete than sulfuric, since it contains cement mixed with special additives that can directly affect test results [Pengfei Huang et al., 2005].

It is important to note that in *Fig's 38.A* and *39.A* the strength of concrete decreases over time for both types of testing of mechanical properties. On the other hand, in the *Fig. 38B* the strength indicator changes only during the first month, and in the *Fig. 39B* during the whole experiment time. This can be explained by the fact that chlorides have a greater solubility than sulfates, respectively, have a greater permeability. However, since the strength changes showed in *Fig. 38B* has a non-constant trend, therefore, it can be said that the influence of the chlorides solubility in the case of concrete has a slight effect. As for geopolymers, everything is obviously stable in all cases. Small changes of strength values may be due to the continued process of geopolymerization that was mentioned above.

A
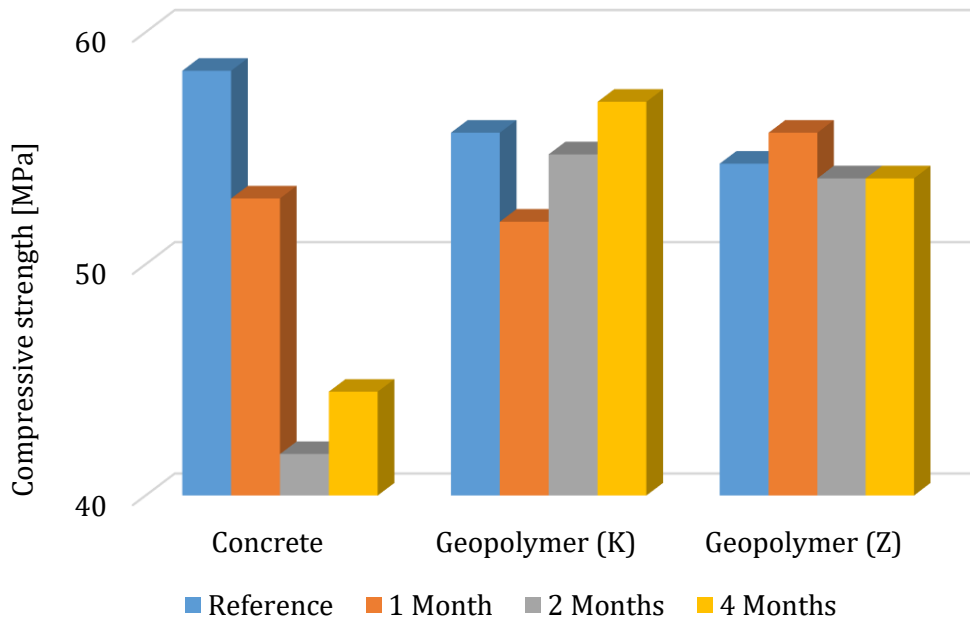
B
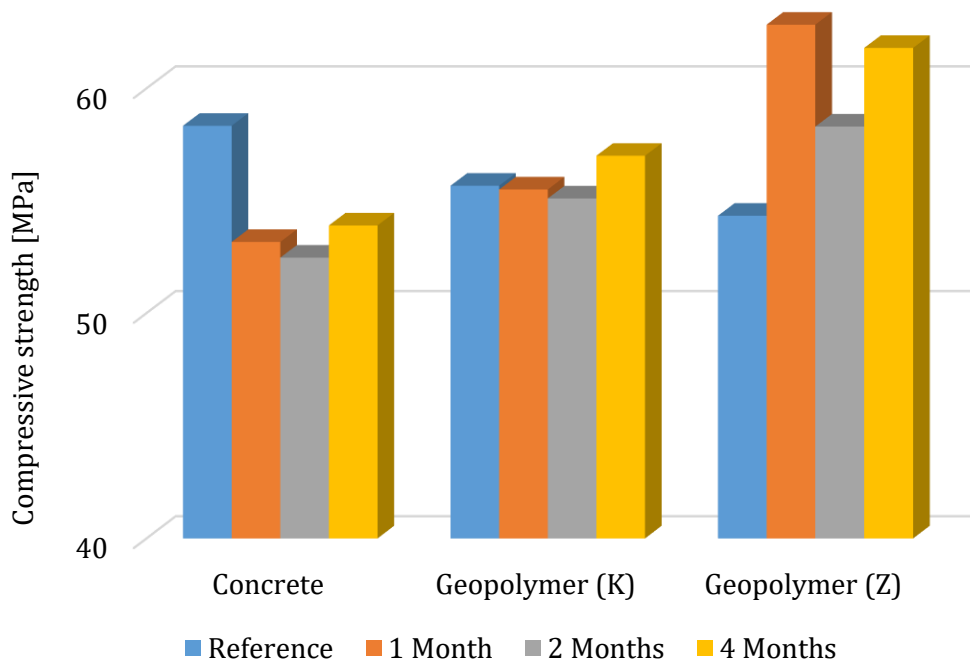
Fig. 38.: Compressive strength changing trend of concrete and geopolymer for three cycles soaking in H_2SO_4 (**A**) and HCl (**B**) compared with reference values
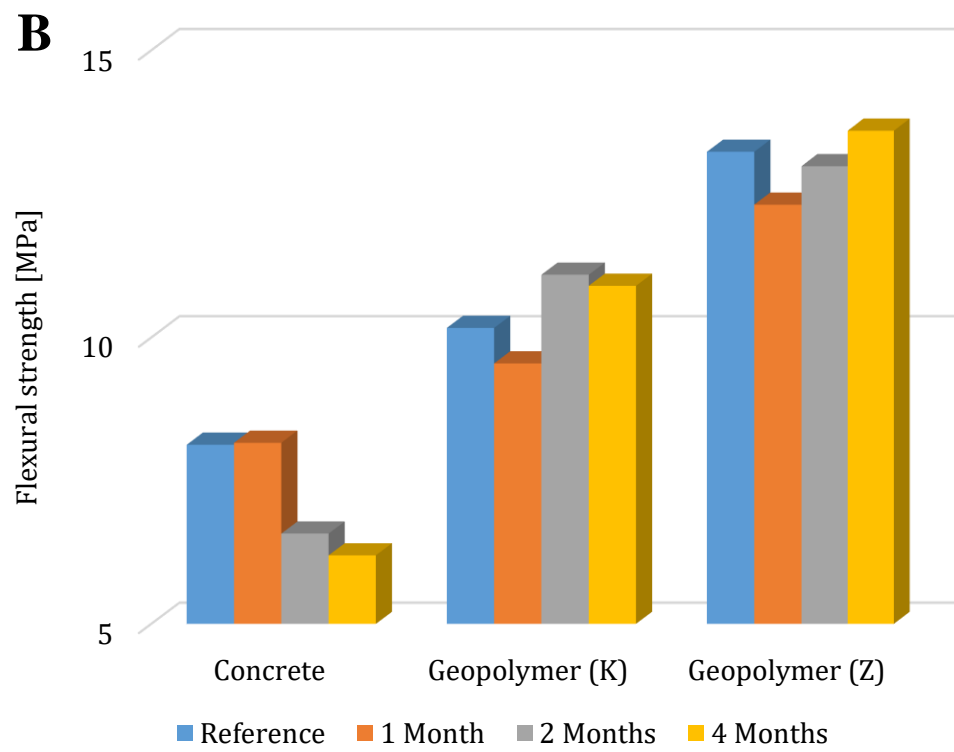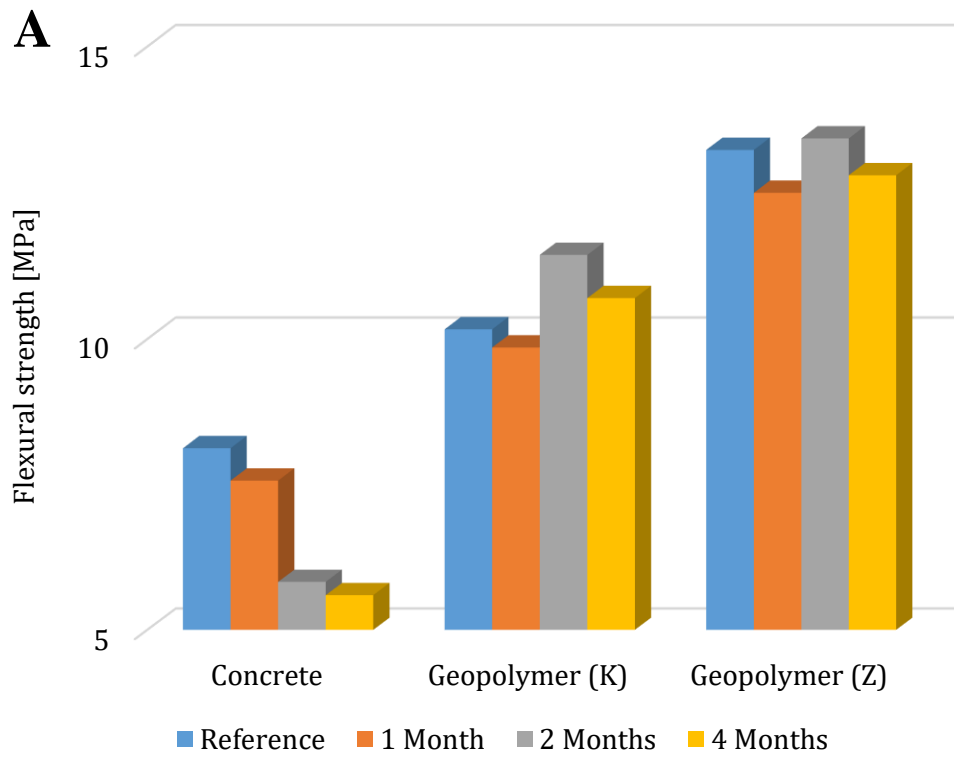
Fig. 39.: Flexural strength changing trend of concrete and geopolymer for three cycles soaking in H_2SO_4 (**A**) and HCl (**B**) compared with reference values

Upon closer inspection of the specimens' surface without using loupes or microscopes, it is noticeable that the concrete surface was the most damaged *(Fig. 40. and Fig. 41.)*. This was quite expected and met the results of the strength tests. Also visible mini cracks on the geopolymer (K) surface were observed. From the results of strength measurements, it follows that the strength was not affected by these cracks. However, it can be assumed that an increase in the depth of cracks requires a longer period of time for acidic medium to act on the sample surface. The geopolymer (Z) did not show any visible surface changes including efflorescence. For more detailed study of the acid spreading degree effect, it is necessary to conduct further research that was not the goal of this work.
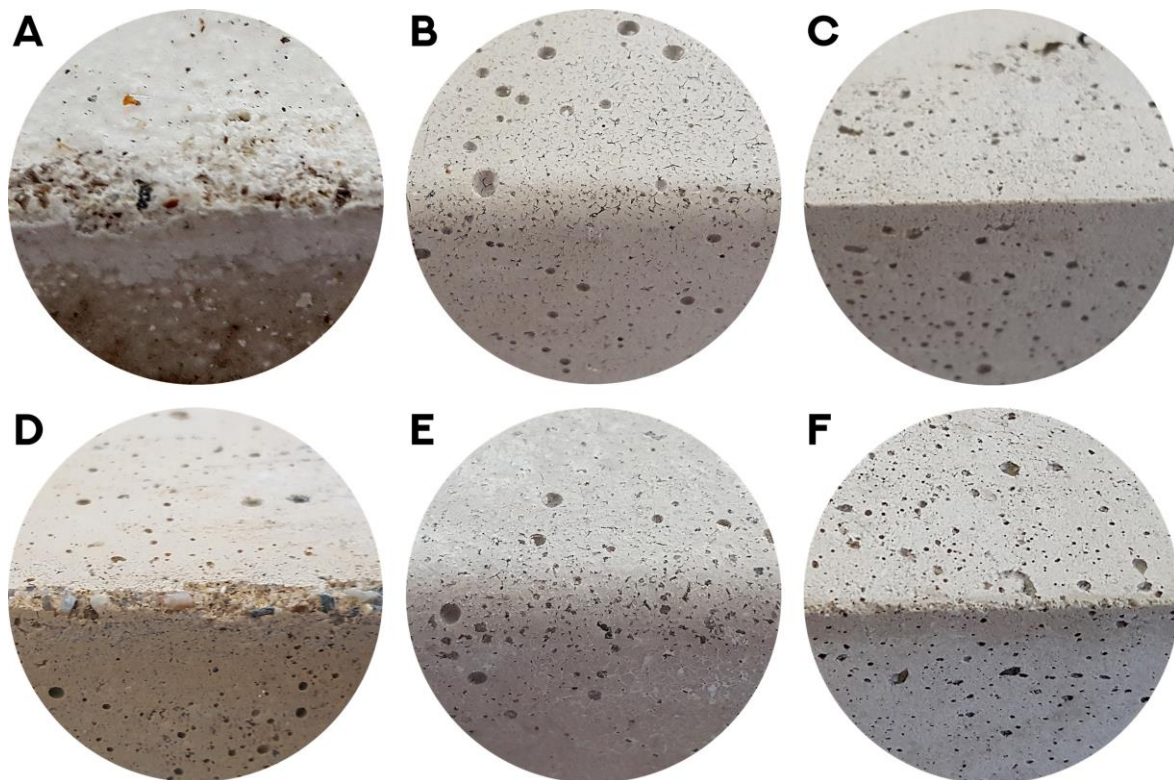
Fig. 40. The samples surface after two months in sulfuric acid (**A** – Concrete, **B** – Kaznejov, **C** – Zlosyn) and in hydrochloric acid (**D** – Concrete, **E** – Kaznejov, **F** – Zlosyn)

But yet, upon closer examination of the samples of concrete, it is clear that the surface was completely degraded into a few millimeters deep.

Fig. 41.: Visual comparison of geopolymer and concrete samples dried after 4 months in HCl and H₂SO₄ acids. (**A**) Photo of surface and inner structure of the samples, (**B**) detailed photo of dried samples' surface 4 month immersed in acids

According to visual observation, penetration depth of geopolymer and concrete samples after immersing into acids was very different. Surface colour changes were observed on concrete samples in both acids from grey to yellowish. Penetration depth caused by chemical reaction leaded to colour change in the case of sulfuric acid was about 1 mm and in the case of hydrochloric acid 3 mm *(Fig. 42B.)*. Changes on both geopolymer sample types were not observed without microscopic research *(Fig. 42A.)*.
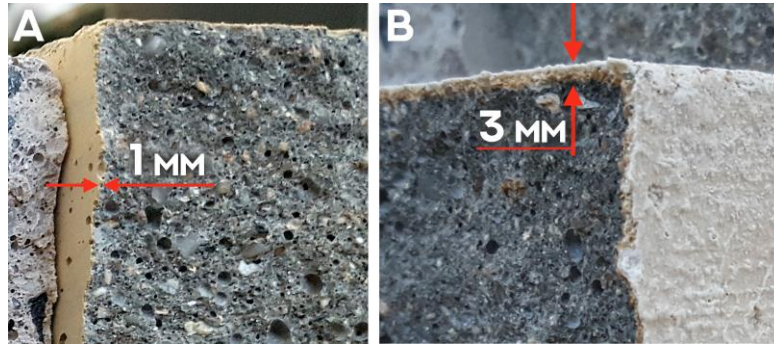
Fig. 42.: Photo visualizing depth of acid penetration on concrete. (**A**) sample immersed for 4 months in H_2SO_4, (**B**) sample immersed for 4 months in HCl

Tab. 6.: Solubility in water of chosen compounds at 25 ^{0}C [PubChem 2019]

Compound	g/100 ml	Compound	g/100 ml
Li_2SO_4	39,4	LiCl	84,3
Na_2SO_4	19,3	NaCl	36,0
K_2SO_4	12,0	KCl	25,4
$BeSO_4$	40,0	$BeCl_2$	15,1
$MgSO_4$	35,1	$MgCl_2$	52,9
$CaSO_4$	0,21	$CaCl_2$	74,5
$Al_2(SO_4)_3$	36,4	$AlCl_3$	46,3
$Fe_2(SO_4)_3$	Hydrolysis	$FeCl_3$	96,9
$FeSO_4$	26,3	$FeCl_2$	64,4

4.6. Structural properties measurement

4.6.1. XRPD

Stage 1 – Baucis geopolymer studies

Comparison between concrete and Baucis matrix samples' crystal phases is shown in *Fig. 43*. Evaluation of concrete diffractogram was complicated due to high amount of quartz and undefined composition of concrete after hardening. In Baucis matrix some nonreacted kaolin residua and low amount of quartz were found. Also,

quartz was found in raw Baucis, what means, that it enters during manufacturing process and its amount is undefined.
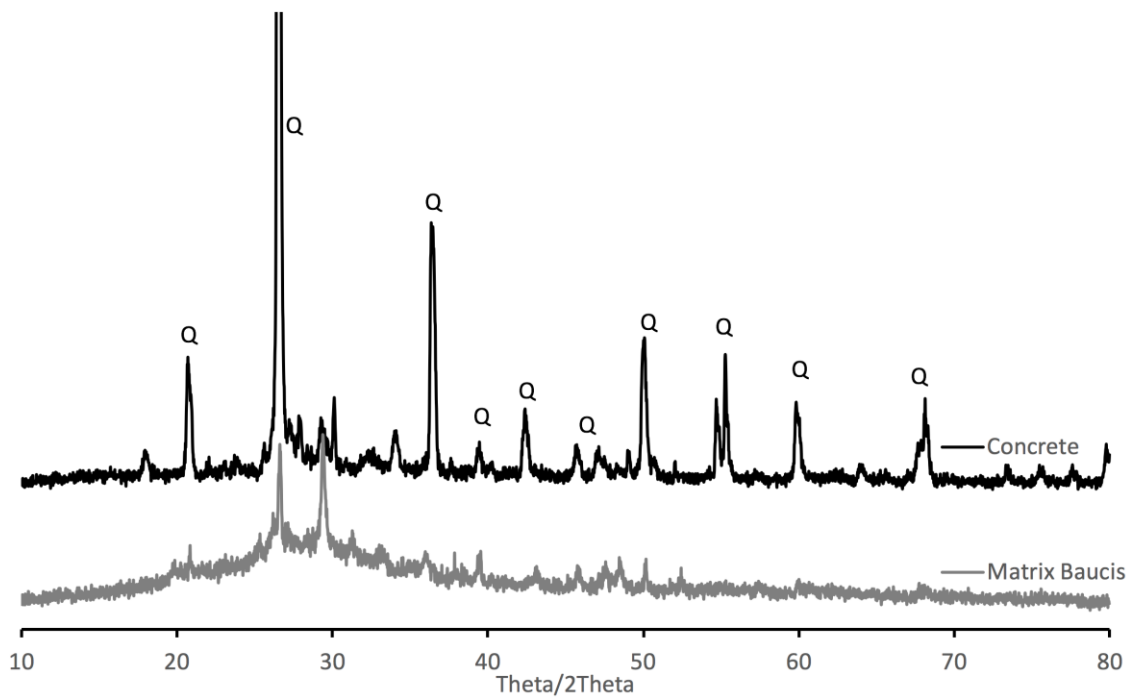
Fig. 43.: XRPD diffractograms of concrete and Baucis matrix samples. Q means quartz (#R040031, [RRUFF 2019]

During immersion in the sulfuric acid, on several samples on the non-immersed part white crystal efflorescence appeared. It was found, that the efflorescence was gypsum *(Fig. 44.)* with the chemical formula $CaSO_4 \cdot 2H_2O$, which water solubility is 0.2 g per 100 ml. The analogous compound, which can possibly appear in hydrochloric acid, $CaCl_2$, has solubility in water 74.5 g per 100 ml (*Tab. 6.*). Founded crystals provide the information, that saturated $CaSO_4$ solution appears during the reaction in sulfuric acid and no other phases were found on diffractogram. The same reaction probably occurs in HCl acid, however, solubility of hydrochloric acid salts and other sulfuric acid salts is higher and no other crystal formation occurred.
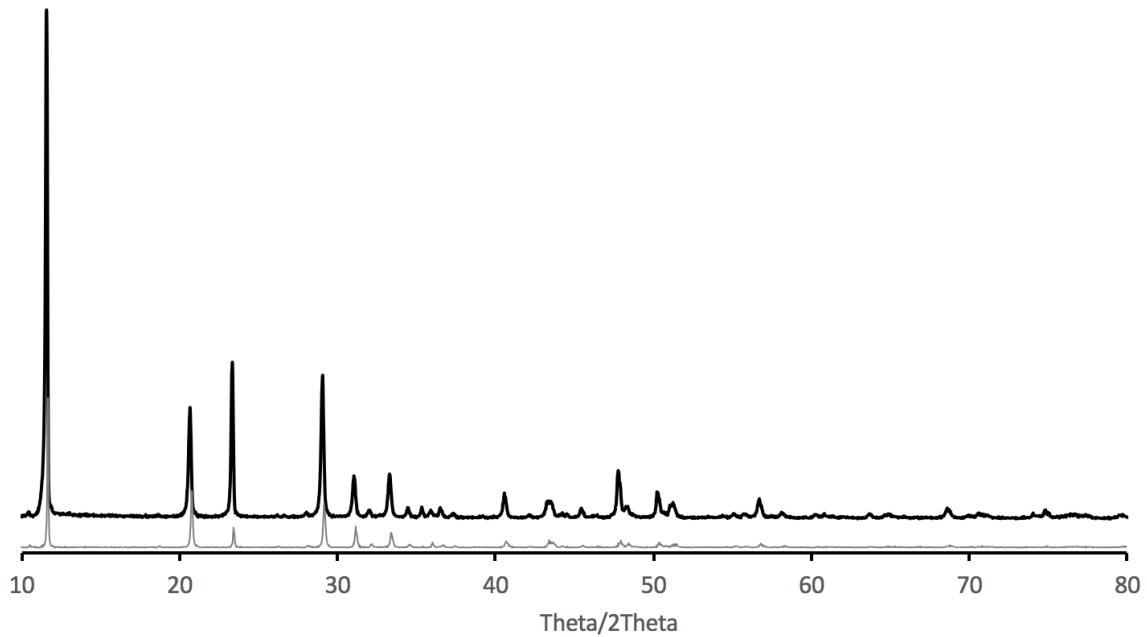
Fig. 44.: Diffractogram of a crystal precipitate collected on the geopolymer sample immersed into sulfuric acid. Black line - sample, gray line - gypsum database diffractogram #R040029.1 [RRUFF 2019]

Stage 2 – Added kaolin influence evaluation

CLUZ produced Mefisto L05 precursor and Baucis LNa and L110 geopolymers were compared *(Fig. 45.)*. Amorphous hump in the region between 20 and 30 degrees in Mefisto samples, which corresponds to amorphous metakaolin, the hump in both Baucis samples is not so well distinguished. It can correspond with lower amount of the metakaolin in Baucis samples. However, quantitative analysis could not be performed due to amorphous metakaolin and slag, which is supposed to be a filler in Baucis. Quartz was also found in all samples. The amount of quartz in Baucis L110 is sufficiently higher, than in the other samples. Therefore, for raw kaolin influence Mefisto as a pure metakaolin was chosen.
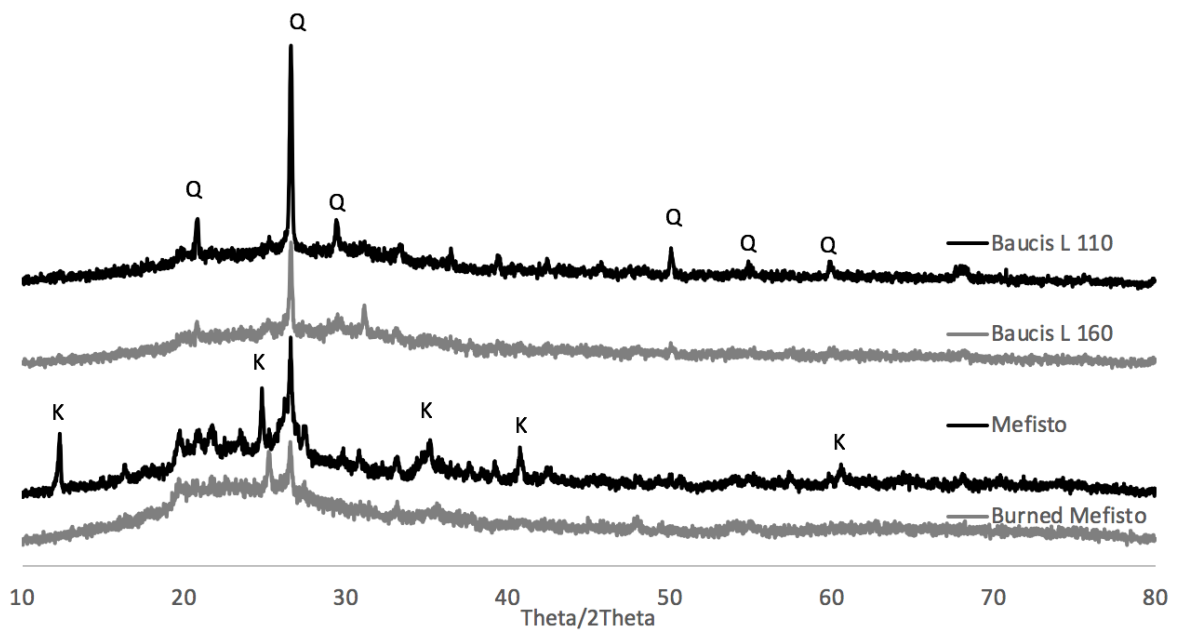
Fig. 45.: Diffractograms of Baucis L110 and L Na (L 160), Mefisto L05 and burned Mefisto L05 metakaolin. Q means quartz (#R040031, [RRUFF 2019]), K means kaolin
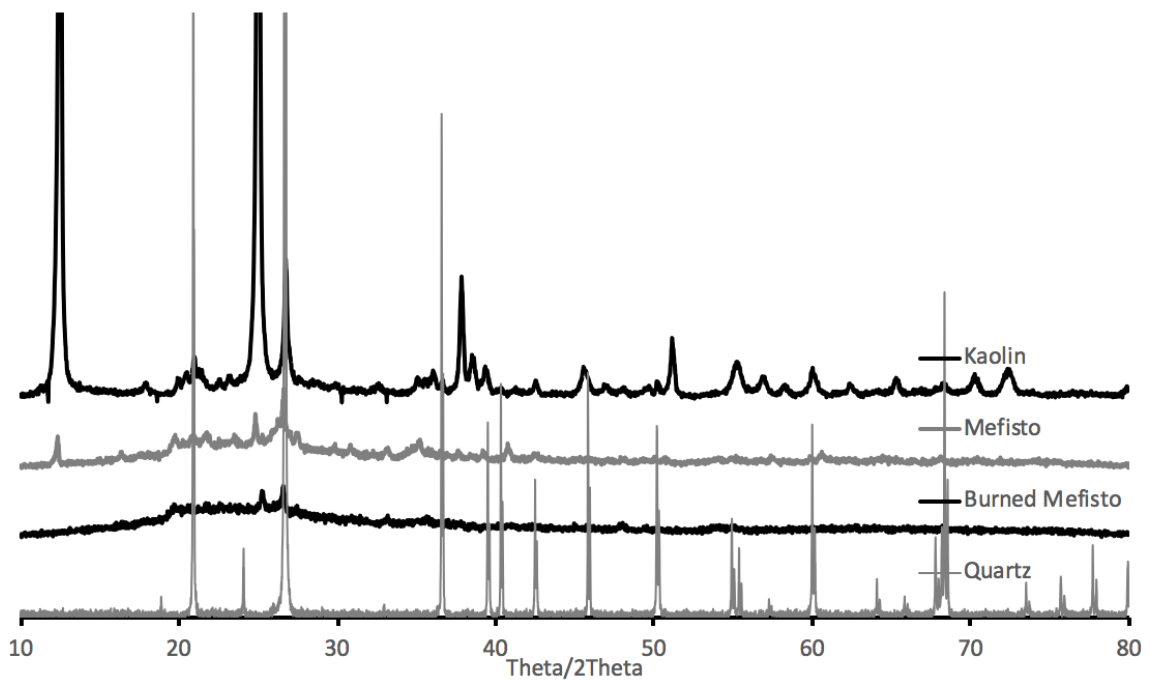
Fig. 46.: Diffractogram of kaolin, Mefisto L05 and burned Mefisto L05 samples and quartz database record (#R040031, [RRUFF 2019])
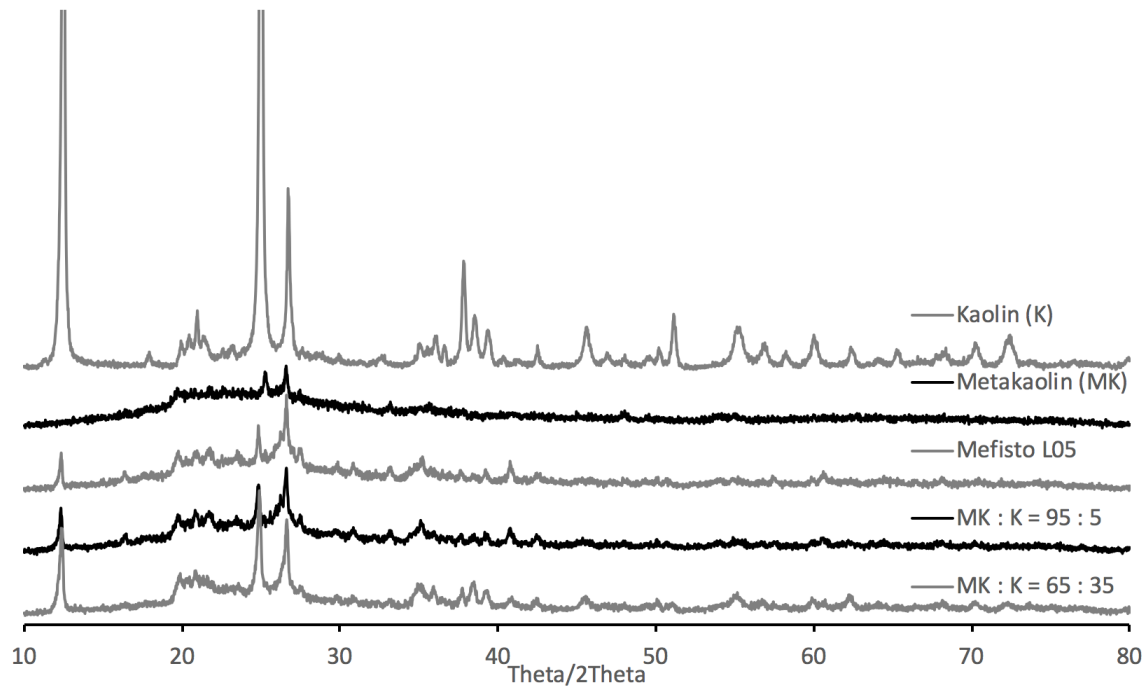
Fig. 47.: Diffractogram showing changes in peak intensity and interference in metakaolin and kaolin samples

The amount of raw kaolin in the industrial metakaolin precursor Mefisto L05 was determined based on two peak areas of kaolin at 12.3^0 and 24.8^0 *(Fig. 46.)*. According to calibration curves, the amount of unburned kaolin in Mefisto L05 was 3.5 ± 0.5 %. Presence of kaolin in Mefisto L05 is easily visible and its diffractogram looks similar to the record of the sample with 5% kaolin substitution (MK : K = 95 : 5) *(Fig. 47.)*. Kaolin was not found in the metakaolin sample burned in the laboratory kiln or its amount was under the detection limit. XRPD is a very sensitive method for the detection of crystal materials, as such it is possible to say that no kaolin was present in this burned metakaolin. Quartz was found in all samples (main peaks at 20^0 and 26,7^0, (#R040031, [RRUFF 2019]).

When comparing the two samples of hardened geopolymer matrix with and without the kaolin addition, the presence of kaolin after hardening was observed in the diffractogram *(Fig. 48., Matrix + 5% K)*. It means that kaolin did not participate in the polycondensation. Based on the kaolin calibration curve, its amount was calculated to 5.1 ± 1.0 wt.%, however these calculations could not be absolutely precise due to possible changes during polymerization process.
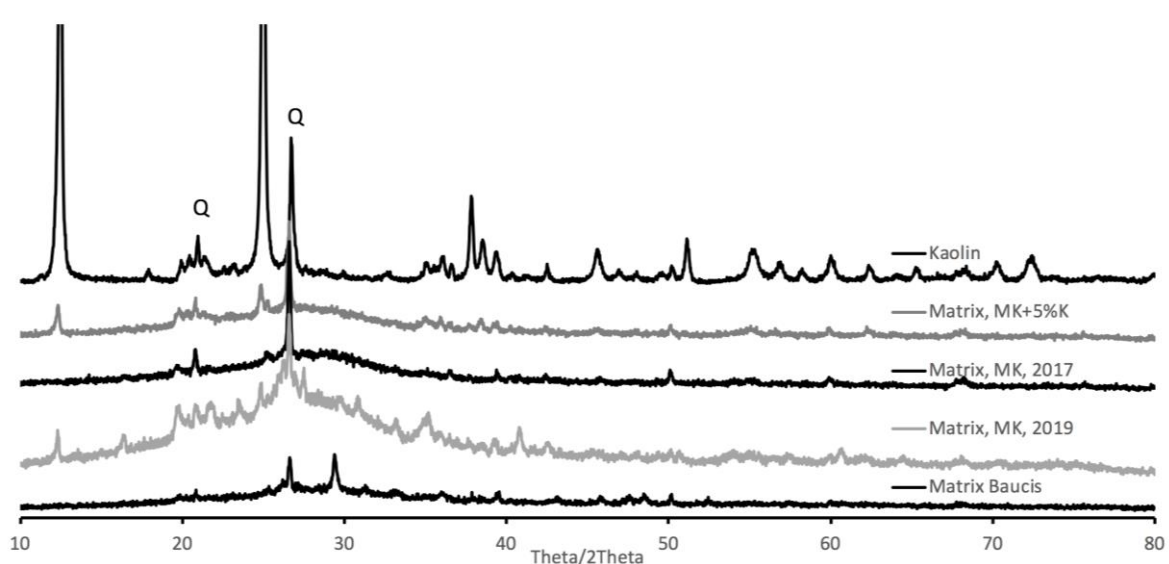
Fig. 48.: Diffractograms of matrix made of mixture metakaolin + kaolin = 95 + 5 %, metakaolin Mefisto 1 and 3 years old, Baucis LNa and raw kaolin sample to compare. Q means peaks of quartz. Sand (quartz) was not added to the samples in order to provide quality diffractograms

Geopolymerization reaction leads to shift of the amorphous hump from 20-30⁰ in metakaolin samples to 25-30⁰ in matrix samples (*Fig. 47.* and *48*). Also, in *Fig. 48.* is well seen, that Baucis Matrix provides smaller hump, which can means lower amount of metakaolin in Baucis precursor, what corresponds with observations of diffractograms in *Fig. 45.* The amorphous hump of metakaolin is shifted to higher angles and becomes narrower after polycondensation in matrix.

4.6.2. FTIR

Stage 1 – Baucis geopolymer studies

High intensity band (900-1100 cm⁻¹) of matrix samples *(Fig. 49.)* correspond to Si-O vibrations of geopolymer matrix. Also, right small shoulder of the band at 1100 cm⁻¹ correspond to Si-O vibrations in quartz. However, other characteristic vibrances of quartz Si-O are not well distinguished due to presence of Al-O-Si and Si-O bands of geopolymer *(Fig. 50.)*. Proper evaluation of concrete composition is possible only with deconvolution of bands and further evaluation. However, this was not done due to composition diversity of both metakaolin and cement samples. Therefore, general

changes and differences were studied only. In all matrix samples presence of water is evident due to hump at 3000-3500 cm^{-1}.

On pure metakaolin matrix is well seen time changes of the main geopolymer peak. It's become more intense, what could mean higher amount of studied compound and, therefore, continuation of polycondensation reaction occurred in older geopolymer sample (*Fig. 49.*).
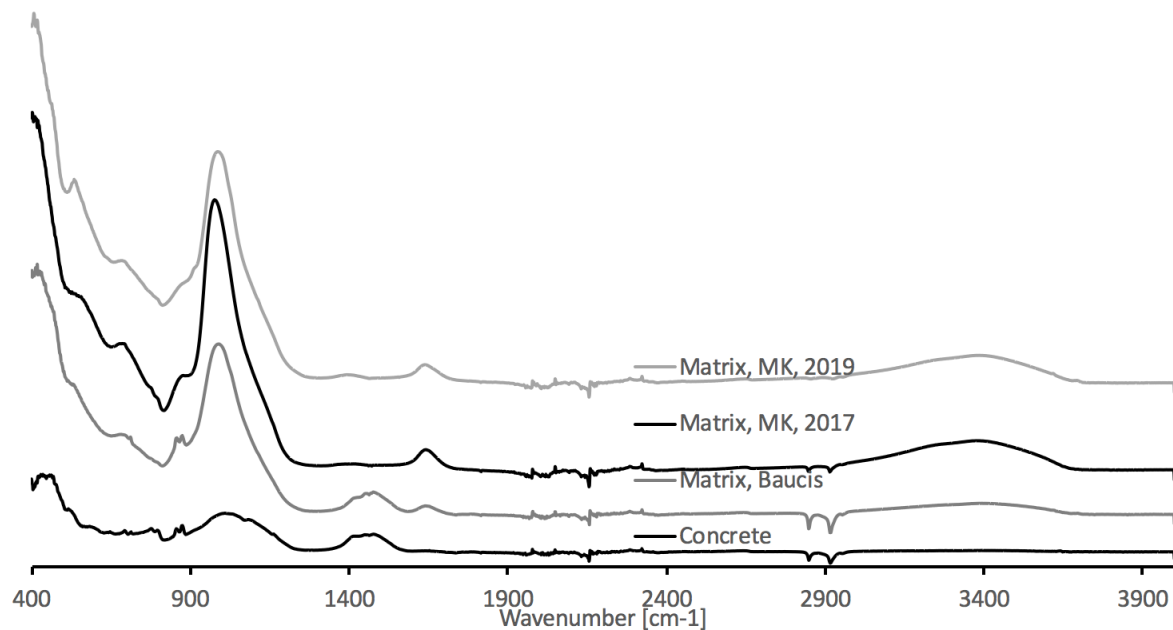
Fig. 49.: Comparison of FTIR records of metakaolin matrix samples, Baucis matrix and concrete

In *Fig. 50* comparison of Baucis based geopolymer with 2 types of sand (Kaznejov and Zlosyn), concrete and quartz are presented. Presence of quartz in all tested samples is obvious, however, bands at 850-900 cm^{-1} and 1400-1500 cm^{-1} do not belong to Si-O vibrations (*Fig. 50.*). They could be caused by impurities presented in samples in low quantities.

It should be also mentioned, that intensity of Al-O-Si and Si-O cumulative geopolymer bands at about 1000 cm^{-1} are higher, than Si-O shoulder of quartz at 1062 cm^{-1}. It is interesting, because presence of sand in each sample was 55 and 70 %, therefore it could be said, that amount of newly appeared Al-O-Si bonds was relatively high.
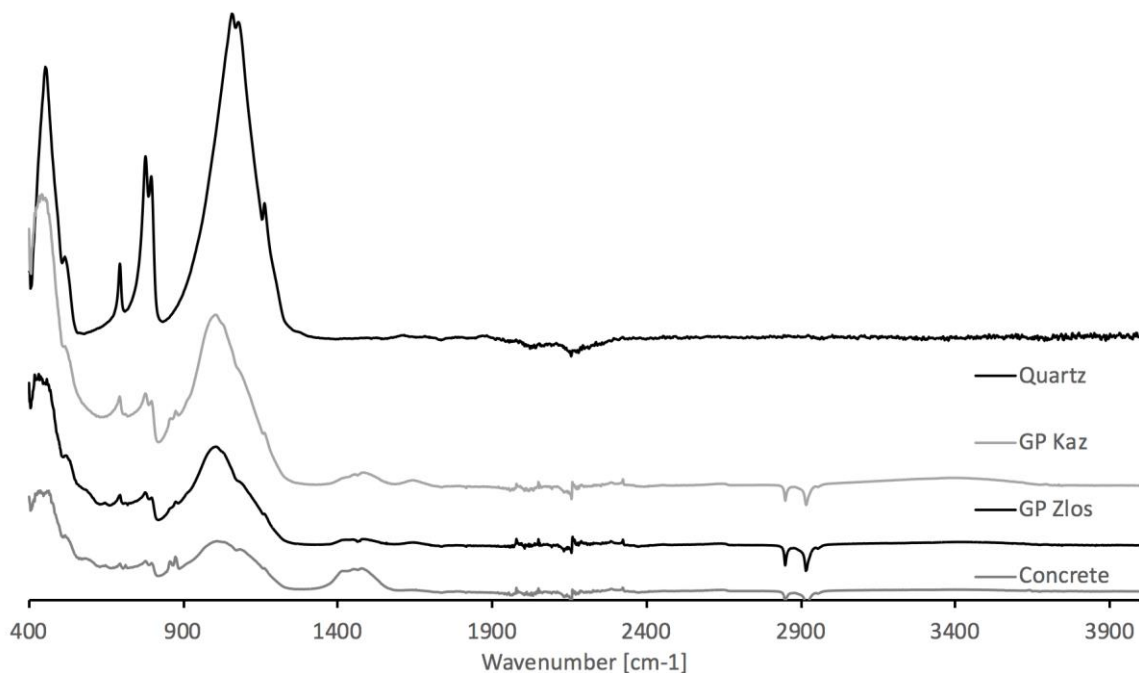
Fig. 50.: Comparison of FTIR records of Baucis based geopolymer with 2 sand types, concrete and quartz database record (#R040031, [RRUFF 2019])

Stage 2 – Added kaolin influence results

The content of kaolin in the industrial metakaolin Mefisto L05 was very low and thus a quantitative analysis based on FTIR spectra was not performed *(Fig. 51.)*. However, the addition of raw kaolin to the reference-scale samples is demonstrated by the bands of proportionally graduating height and by the shape with shoulders referring to the proper kaolin ratio.

The presence of kaolin in the matrix sample is well seen due to the OH deformation band linked to $2Al^{3+}$ at 911 cm^{-1} and the Si-O-Al stretching band at 524 cm^{-1} [Bhaskar J. S., Gopalakrishnarao P., 2010]. Furthermore, the kaolin and the reference-scale samples were compared to the database HR Inorganics I. record of kaolinite in order to confirm the composition. The metakaolin matrix (*Fig. 52.*, Matrix, MK) band at 930-1070 cm^{-1} with a maximum at 985 cm^{-1} is not so wide but shifted to a lower wavenumber in comparison to the metakaolin (*Fig. 51.*) main band at 960-1250 cm^{-1} with a maximum at 1035 cm^{-1}. The kaolin presence is visible in the main band of matrix

with kaolin (*Fig. 52.*, Matrix, MK : K = 95 : 5) as a shoulder at 1032 cm^{-1} and a maximum at 1008 cm^{-1}.

Al-OH stretching bands at 3500-3650 cm^{-1} were also observed in kaolin samples *(Fig. 52.)*. OH stretching bands of the physical bonded water at 3300-3500 cm^{-1} were observed only in both of the matrix samples, pure and with 5 wt.% of kaolin, where the slightly higher absorbance intensity induces water sorption by kaolin. Kaolin bands at 3610-3700 cm^{-1} shows that kaolin has well organized structure.

Presence of non-reacted kaolin in matrix after polymerization, as shoulders at 1115 cm^{-1} of Si-O and at 934 cm^{-1} of Al-OH in the mixture sample is well seen in *Fig. 53.* Matrix made of pure metakaolin did not show this vibration bands.
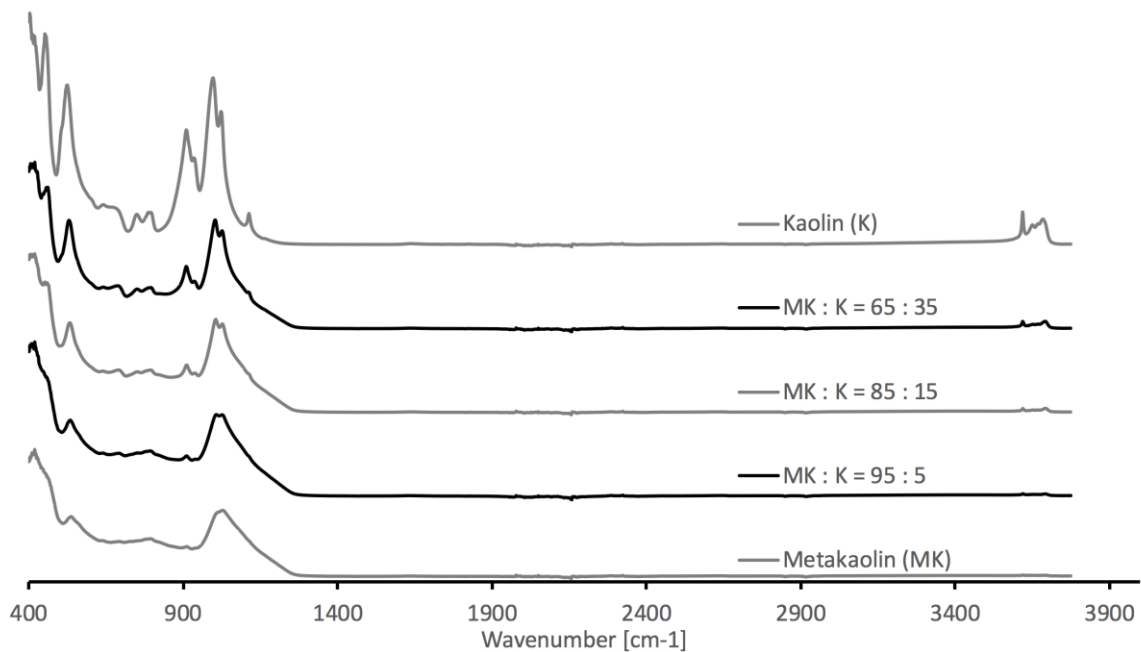
Fig. 51.: FTIR recordings of the industrial metakaolin (Mefisto L05) burned in laboratory (Metakaolin MK), kaolin (K), the reference mixtures (MK+5% K, MK+15% and MK+35% K)
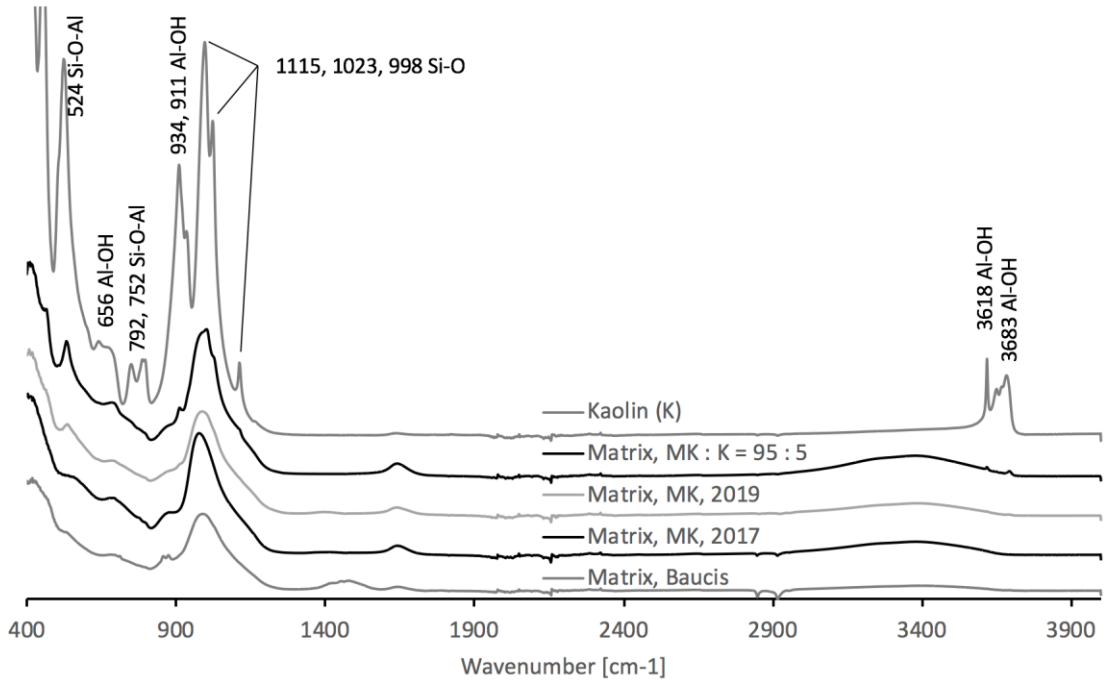
Fig. 52.: FTIR recordings of the resulting geopolymer matrix with and without kaolin produced in different years (MK : K = 95 : 5; MK) and Baucis's matrix
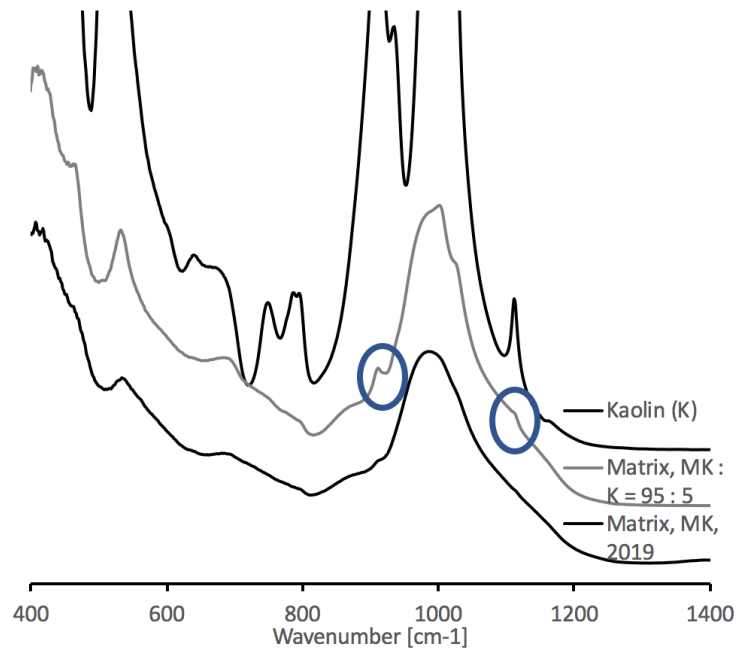
Fig. 53.: Closer look at raw kaolin, matrix with kaolin and matrix with pure metakaolin

4.7.   SEM analysis

Fig. 54. displays the differences between the two microstructures of the matrix with and without kaolin among quartz sand aggregates. The structures differ in their microcracks network. Whereas the matrix without added raw kaolin is more fragmented by numerous fine cracks (*Fig. 54. B*), the matrix with added kaolin shows fewer but wider cracks (*Fig. 54. A*). They demarcated the matrix in the areas of relaxed structural strain, unlike the crumbled matrix without raw kaolin. In this matrix, widespread light-grey crumbs were detected and identified by EDAX analyses as residual metakaolin particles (*Tab. 7.*). The residues of undissolved metakaolin created harder parts of the matrix. The liquid precursor alone hardened into a softer background matrix that surrounded all the objects. This is evidenced by the micromechanical properties measured by means of nanoindentation.

In *Fig. 54.* (C and D), the most common components of the microstructure are shown in detail: mesopores of the size of about 10-20 μm, under 10 μm and smaller particles such as metakaolin residues, kaolin residues, quartz, mica, and other impurities.

The added kaolin particles were difficult to detect because of their addition in the form of a colloid suspension. Some bigger kaolin floccules were detected by EDAX and are indicated in *Fig. 54. C*. The higher concentration of kaolin probably have slowed down the matrix chaining and setting, which was the reason for the delay in the products' hardening. The floccules reduced the internal strain and partly acted as a structural buffer hindering the spread of microcracks, which contributed to mechanical strength (at least up to the 20 wt% addition of kaolin in metakaolin). For the frost resistance, however, the higher concentration was less effective, probably because of the water retention.
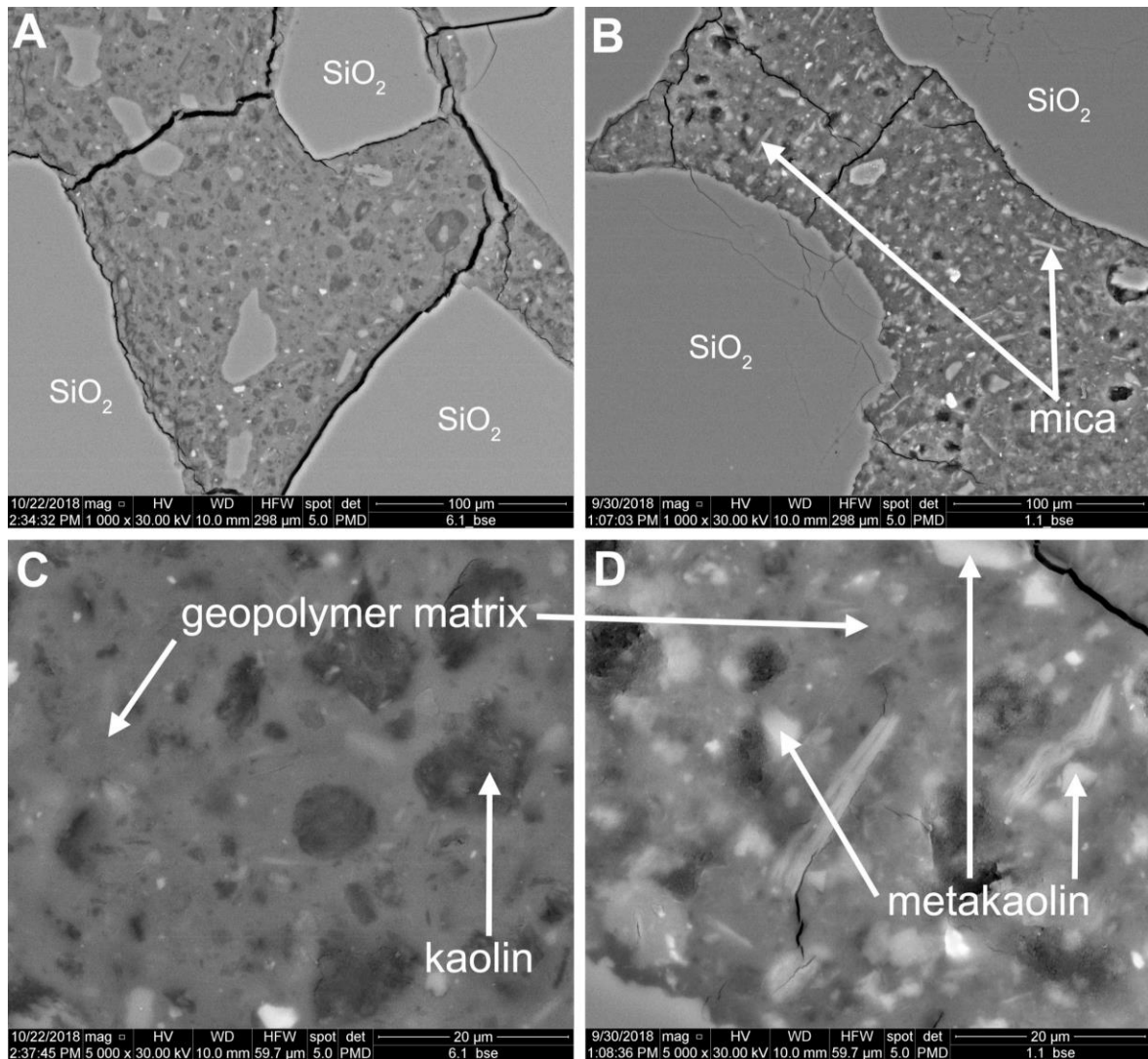
Fig. 54.: SEM micrographs of geopolymer made of metakaolin with kaolin (MK:K=95:5) (A; C) 306 and metakaolin (B; D) carried out on a Quanta 450 SEM in different scale.

The elasticity modulus (E) of the background matrix containing finely dispersed kaolin reached up to 15.2 GPa, unlike the pure matrix, where the results were split into the values of the background matrix (10 GPa) and the metakaolin residues (12 GPa). Both were of lower E than the matrix with kaolin. The differences among micromechanical properties are in accordance with the results of the mechanical properties. Samples with 5 wt% of kaolin added showed homogeneous microstructure. Strength increase could have been caused by the significantly delayed hardening of the samples with kaolin, however this is an observation only. During the prolonged dwell in the liquid alkaline medium, the metakaolin had more time to dissolve and react

without "freezing" its whole particles. This could increase monomer-precursor superiority. Thus, the metakaolin can participate in polycondensation towards the structure's densifying and strengthening.

Tab. 7.: EDAX spot analysis [wt. %] of the matrix-microstructure parts and objects (averaged results)

Spots in structure	Al_2O_3	SiO_2	Na_2O	K_2O	CaO	FeO	TiO_2
Matrix background	24	61	10	<1	2	<1	<1
Metakaolin residues	27	60	7	<1	3	<1	<1
Kaolin floccules	36	58	2	<1	<1	<1	<1

5. Conclusions

By the standards of science, geopolymer was not officially introduced until recently, although it has been probably used by humanity for several millennia. The active research in this field has been going on for almost 40 years now after it was started by Prof. Davidovits. This period of time was enough to gain a rather broad overview of the new material, but not to understand the nature of its behaviour as a building material thoroughly. Many corporations all over the world (Imerys Group/Ags Argil's & Minraux, Milliken & Company Inc., PCI Augsburg GMBH, DowDuPont, Rocla, Wagners, Universal Enterprise, Schlumberger Ltd, Murray & Roberts Cementation Co. Ltd, Banah UK Ltd, Zeobond Pty Ltd, Uretek, BASF, Corning Inc., Nu-Core, Pyromeral Systems, Airbus, etc.) already use various patented compositions based on geopolymer for successful solving of various engineering problems. However, this is only a small part of geopolymer's broad capabilities, according to numerous scientific publications on this matter until now.

According to the results of this work, it can be argued that the metakaolin-based geopolymer application in the underground building is promising. Immersed tube segments, as well as other similar construction elements, are manufactured indoors where it is possible to control various factors (for example, room temperature, relative humidity, etc.) during production. Thus, it is possible to achieve homogeneity of the geopolymer composite structure, and therefore, there will be no significant deviations of the mechanical properties. Conducted studies have shown that the Czech-produced geopolymer Baucis LNa has sufficient strength characteristics, even when used with ordinary building sand, such as Zlosyn or Kaznejov. An ordinary mixture with a high content of Zlosyn sand (up to 70 wt.% of GP:Sand ratio) and Baucis LNa geopolymer has better mechanical and resistant properties than the other tested recipes. Such a mixture is easy to prepare, which is a very important part of a building process, and it is more economically beneficial compared to the other tested mixture with the Kaznejov sand. The Kaznejov-based GP mixture also contains 5% of glass fibers (from GP mixture volume), which did not show much influence on mechanical or resistant properties, according to the

fracture energy and acid resistance tests. Additionally, it is important to keep in mind that the use of glass fibers increases the final product cost.

However, high resistance of both GP mixtures with Kaznejov and Zlosyn sand to aggressive water (compared to Portland cement with the similar mechanical properties) and the frost resistance are the most important parameters when choosing a material for the tunnel building purposes. The tested GP composites showed excellent resistance to the aggressive environment: HCl and H2SO4 acid solutions. After 4 months of being in these solutions with a 1÷3 pH, compressive and flexural strengths did not decrease and even increased slightly in some cases. Perhaps it was due to the closed pore structure, which protects liquids from deep absorption.

The most important result of this work is that despite the weakness of kaolin and although the raw kaolin is known to be non-convertible into geopolymer chains, it was found that kaolin spoiled neither the polycondensation nor the product solidification. Moreover, the solid did not crumble in water in a wide range of kaolin content (2–50 wt%). A further benefit of the measurement was the finding that a small amount of kaolin in metakaolin (up to 3 wt%) improved the geopolymer performance in compressive and flexural strength tests after frost-resistance tests in comparison with no-frost samples. Also, the presence of up to 20 wt% of kaolin did not affect the flexural strength of the geopolymer but slightly improved compressive strength. Based on the obtained results, monetary savings in large volume production can be achieved by either admixing raw kaolin into metakaolin or properly regulating the burning process.

In Geopolymer Market: Global Industry Trends, Share, Size, Growth, Opportunity and Forecast 2019-2024, it was mentioned that geopolymer has benefits, like its high strength, ultra-porosity, low drying shrinkage, low creep and acid resistance. That is why GP is used to substitute Portland cement as a binder in concrete. Also, GP is utilized for repairing bridges, buildings, underground tunnels, roads, and in the rehabilitation of pipes and structures in the civil infrastructure, oil and gas, and chemical industries. Moreover, geopolymers are cheaper than Portland cement, and GP production produces a reduced amount of carbon dioxide. With

rising environmental regulations and emission strain on the cement industry, the demand for geopolymer is increasing. Furthermore, factors such as technological developments and innovations in the construction sector are also contributing to the growth of the global geopolymer market. The market value is projected to reach US $16.2 billion by 2024, exhibiting a CAGR of around 27% from 2019-2024 (www.imarcgroup.com). All these facts indicate that the geopolymer has a great future, and it is necessary to master the areas of its application right now.

The results have expanded the understanding of the features of the slag-metakaolin geopolymer produced in the Czech Republic. However, this work was focused primarily on obtaining the optimal mixture of components for the immersed tube segments production. In the future, it will be necessary to carry out studies in the field of high-temperature resistance of the GP composite. Fire safety is one of the most important factors in building tunnels, so this study needs to be given special attention. It is also necessary to simulate the in-situ conditions of a tunnel built from segments that are made from selected recipes. It is best to use a Zlosyn-based recipe (GP:Sand ratio is 30:70) due to its good physical and mechanical characteristics as well as low cost. Moreover, according to microstructural data, the Czech raw materials that were studied have high quality and low impurity content, which prevents unexpected results in the future. Testing on more primitive construction elements such as road tiles, borders, and so on, can be done simultaneously. For example, during a study for this work, the obtained mixture was used to eliminate recesses in the road where heavy equipment passes through daily. Therefore, the more comprehensive study will be carried out, the more accurately it will be possible to determine the subsequent field of this GP composite application. So, the subsequent researches should be completed outside the laboratory and have an applied meaning.

6. References

Allouche E., Montes C., Geopolymer Coatings for Rehabilitation of Concrete-Based Wastewater Collection Systems, International Congress on modern Materials & Technologies, 12th International Ceramic Congress, 2010

Ancient concrete rises again, New Scientist, 2006, 192(2581), 10.1016/S0262-4079(06)61290-6

Barbosa V.F.F., Kenneth J.D. MacKenzie, Thermal behaviour of inorganic geopolymers and composites derived from sodium polysialate, Materials Research Bulletin, 2003, 319-331, 10.1016/S0025-5408(02)01022-X

Barsoum M. W., Ganguly A., Barsoum G., Microstructural Evidence of Reconstituted Limestone Blocks in the Great Pyramids of Egypt, Journal of the American Ceramic Society, 2006, 3788-3796, 10.1111/j.1551-2916.2006.01308.x

Bhaskar J. S., Gopalakrishnarao P., Fourier transform infrared spectroscopic characterization of kaolinite from assam and meghalaya, northeastern India, International Journal of Modern Physics, 2010, 206-210, 10.4236/jmp.2010.14031

Böcker J., Spectroscopie, 2009, 188, 978-3-80231-581-2

Bragg, W.l., Proc. Cambridge Phil. Soc., 1913, 17, 43

Brindley G. W., Nakahira M., Kinetics of dehydroxylation of kaolinite and halloysite, Journal of the American ceramic society, 1957, 346–350, 10.1111/j.1151-2916.1957.tb12549.x

Buchwald A., Weil M., Dombrowski K., Evaluation of primary and secondary materials under technical, ecological and economic aspects for the use as raw materials in geopolymeric binders, Proceedings of the 2nd Int. Symposium of Non-Traditional Cement and Concrete, 2005, 32-40, 80-214-2853-8

Chen J.J., Thomas J.J., Taylor H.F.W., Jennings H.M., Solubility and structure of calcium silicate hydrate, Cement and Concrete Research, 2004, 10.1016/j.cemconres.2004.04.034.

ČSN 73 1322, Stanovení mrazuvzdornosti betonu, Praha: Český normalizační institut, 1969

ČSN 73 1326, Zkoušky mrazuvzdornosti: Stanovení odolnosti povrchu cementového betonu proti působení vody a chemických rozmrazovacích látek., Praha: Český normalizační institut, 2003

CSN EN 1015-11, Zkušební metody malt pro zdivo - Část 11: Stanovení pevnosti zatvrdlých malt v tahu za ohybu a v tlaku, 1999

ČSN EN 12390-5, Zkoušení ztvrdlého betonu - Část 5: Pevnost v tahu ohybem zkušebních těles, 2009

Daniel L. Y. Kong, Jay G. Sanjayan, Kwesi Sagoe-Crentsil, Factors affecting the performance of metakaolin geopolymers exposed to elevated temperatures, Journal of Materials Science, 2008, 10.1007/s10853-007-2205-6

Daniel L.Y. Kong, Jay G. Sanjayan, Kwesi Sagoe-Crentsil, Comparative performance of geopolymers made with metakaolin and fly ash after exposure to elevated temperatures, Cement and Concrete Research, 2007, 10.1016/j.cemconres.2007.08.021

Davidovits J., 30 Years of Successes and Failures in Geopolymer Applications, Market Trends and Potential Breakthroughs. Geopolymer Conference, 2002

Davidovits J., Chemistry of Geopolymeric Systems Terminology, Geopolymer, 1999, 9–40, 10.4236/oalib.1100806

Davidovits J., Examples of geopolymer frameworks, [online], [cit. 17.3.2017], 2017, https://upload.wikimedia.org/wikipedia/en/archive/8/85/20130115154523%21Geopolymer_oligomer_molecules.jpg

Davidovits J., Geopolymer green chemistry and sustainable development, The Poly(sialate) terminology: a very useful and simple model for the promotion and understanding of green-chemistry proceeding of the world congress Geopolymer, 2005, 9–15, 2-9514820-0-0

Davidovits J., Geopolymers: Inorganic polymeric new materials, Journal of Thermal Analysis, 1991, 1633-1656, 10.1007/BF01912193

Davidovits J., High-Alkali Cements for 21st Century Concretes, Concrete Technology, Past, Present and Future: proceedings of Symposium, 1994A, 383–397

Davidovits J., Milestones in geopolymers, Concrete International, 1994B, 53-58

Davidovits J., X-ray analysis and X-ray diffraction of casting stones from the pyramids of Egypt and the limestone of the associated quarries, Science in Egyptology Symposia: Proceedings, 1984, 511-520

de Larrard F., Acker P., Roy R. L., Shrinkage creep and thermal properties, In S. P. Shah & S. H. Ahmad (Eds.), High Performance Concretes and Applications , 1994, 65-114

Dědeček J., Žilková N., Čejka J., Experimental study of the effect of Si/Al composition on the aluminum distribution in (Al)MCM-41, Microporous and Mesoporous Materials, 2001, 259-266, 10.1016/S1387-1811(01)00191-3

Deer W. A., Howie R. A., Zussman J., An Introduction to the Rock-Forming Minerals, Prentice Hall PTR, 2013, 277, 10.1180/DHZ

Demortier G., PIXE, PIGE and NMR study of the masonry of the pyramid of Cheops at Giza, Nuclear Instruments and Methods in Physics Research, 2004, 98–109, 10.1016/j.nimb.2004.02.024

Ding, Y., Shi, C.-J., Li, N., Fracture properties of slag/fly ash-based geopolymer concrete cured in ambient temperature. Construction and Building Materials, 2018, 190, 787–795, doi:10.1016/j.conbuildmat.2018.09.138

Divya Khale, Rubina Chaudhary, Mechanism of geopolymerization and factors influencing its development: a review, Springer Science+Business Media, 2005, 10.1007/s10853-006-0401-4

Drake L. C., Pore-size distribution in porous materials, Industrial & Engineering Chemistry, 1949, 780-785

Duxson P., Fernández-Jiménez A., Provis J.L., Lukey G. C., Palomo A., Van Deventer J. S. J., Geopolymer technology: the current state of the art, Journal of Materials Science, 2006, 2917–2933, 10.1007/s10853-006-0637-z

Duxson P., Lukey G. C., Van Deventer J. S. J., Evolution of Gel Structure during Thermal Processing of Na-Geopolymer Gels, American Chemical Society, 2006, 8750-8757, 10.1021/la0604026

Duxson P., Lukey G. C., Van Deventer J. S. J., Thermal evolution of metakaolin geopolymers: Part 2 – Phase stability and structural development, Journal of Non-Crystalline Solids, 2007 A, 2186–2200, 10.1016/j.jnoncrysol.2007.02.050

Duxson P., Lukey G., Physical evolution of Na-geopolymer derived from metakaolin up to 1000 °C, Journal of Materials Science, 2007 B, 3044–3054, 10.1007/s10853-006-0535-4

Duxson P., Mallicoat S. W., Lukey G. C., Kriven W. M., Van Deventer J. S. J., The effect of alkali and Si/Al ratio on the development of mechanical properties of metakaolin-based geopolymers, Colloids and Surfaces A: Physicochem. Eng. Aspects, 2007 C, 8-20, 10.1016/j.colsurfa.2006.05.044

Duxson P., Provis J. L., Lukey G. C., Mallicoat S. W., Kriven W. M., Van Deventer J. S. J., Understanding the relationship between geopolymer composition, microstructure and mechanical properties, olloids and Surfaces A: Physicochem. Eng. Aspects., 2005, 47–58, 10.1016/j.colsurfa.2005.06.060

Eroshkina N.A., Korovkin M. O., Study deformation and strength properties of concrete based on mineral-alkaline binder, Scientific and Engineering Monthly, MGSU National Research University, 2011, 314-319, 2304-6600

Friedrich W., Knipping P., Laue M., Sitzungsberichte der Mathematisch-Physikalischen Klasse der Koniglich Bayerishen Akademie der Wissenschaften zu Munchen, 1912, 303

Gabovich E., Concrete buildings of romans, Celts and Egyptians, IX International conference on the civilization problems, 200

Grutzeck M., Kwan S., Dicola M., Zeolite formation in alkali-activated cementitious systems, Cement and Concrete, 2004, 949-955, 10.1016/j.cemconres.2003.11.003

Hanykýř V., Kutzeddörfer J., Koroze keramiky kapalinami, Technologie keramiky, 2002, 142, 80-900860-6-3

Hanykýř V., Kutzeddörfer J., Technologie keramiky. Mechanické vlastnosti keramiky., 2002, 124-126, 80-900860-6-3

Hanzlíček T., Analysis of the Czech translation of Vitruvius II. books from ten architecture books from the building chemistry perspective, Listy filologické, 2004, 3–4

Hanzlíček T., Steinerová M., Immobilization of Toxic Metals in Solidified Systems of Siloxo-Sial Network, Journal of the American ceramic society, 2005, 968-970, 10.1111/j.1551-2916.2005.00822.x

Hanzlíček T., Steinerová M., Studie rozpouštění aluminium-silikátů ve vodném prostředí za laboratorních podmínek, Ceramics-Silikáty, 2002, 81-120

Hermann E., Kunze C., Gatzweiler R., Kießig K., Davidovits J., Solidification of various radioactive residues by geopolymer with special emphasis on long-term-stability, Geopolymere proceedings, 1991

Hongkong W., Haihong L., Fengyuan Y., Synthesis and mechanical properties of metakaolinite-based geopolymer, Colloids and Surfaces A: Physicochem, Eng. Aspects, 2005, 10.1016/j.colsurfa.2005.01.016

HR Inorganics I, Minerals database – FTIR, Thermo Scientific™ OMNIC™, USA

https://www.imarcgroup.com/geopolymer-market, Geopolymer Market: Global Industry Trends, Share, Size, Growth, Opportunity and Forecast 2019-2024, [online], [cit. 10.6.2019], 2019, Conclution, https://www.imarcgroup.com/geopolymer-market

Husbands T. B., Malone P. G., Wakeley L. D., Performance of concretes proportioned with Pyrament blended cement, Technical Report, Waterways Experiment Station, U.S. Army Corps of Engineers, 1994, 3619, 103, CPAR-SL-94-2

ICDD, PDF-2 database, version 2013, ISDD, USA

Korovkin Mark Olympievich, Kalashnikov Vladimir Ivanovich, Eroshkina Nadezda Aleksandrovna, Influence of high-calcious ash-drop on the properties of self-laying concrete, Regional architecture and construction, Penza State University of Architecture and Construction (Penza), 2015, 49-53, 2072-2958

Kozłowski, M., Kadela, M., Kukiełka, A., Fracture Energy of Foamed Concrete Based on Three-Point Bending Test on Notched Beams. Procedia Engineering, 2015, 108, 349–354, doi:10.1016/j.proeng.2015.06.157

Ksandr Z., Infračervená spektroskopie, [online], VŠCHT Praha [cit. 2017-04-22], http://lms.vscht.cz/Zverze/Infrared.htm

Kubátová D., Studium povrchového náboje vysokodisperzních soustav na bázi silikátů, [online], [cit. 2016-11-24], 2004, http://www.fch.vut.cz/minimovky/kubatova.pdf

Liefke E., Industrial applications of foamed inorganic polymers, Geopolymers 2002 Conference, 2002, 189–199

Liritzis I., Sideris C., Vafiadou A., Mitsis J., Mineralogical, petrological and radioactivity aspects of some building material from Egyptian Old Kingdom monuments, Journal of Cultural Heritage, 2008, 1-13, 10.1016/j.culher.2007.03.009

Luna-Galiano Y., Cornejo A., Leiva C., Vilches L. F., Fernández-Pereira C., Properties of fly ash and metakaolín based geopolymer panels under fire resistance tests, Materiales de Construcción, 2015, 10.3989/mc.2015.06114

Müller-Römer F., F. Pyramidenbau im Alten Ägypten über Rampen und mit Seilwinden, Bautechnik, 2008, 696-704, 10.1002/bate.200810053

Murty B.S., Shankar P., Baldev Raj, Rath B. B., James Murday, Springer Science & Business Media, 2013, 150

Neetu Singh, Sameer Vyas, Pathak R. P., Pankaj Sharma, Mahure N. V., Gupta S. L., Effect of aggressive chemical environment on durability of green geopolymer concrete, International Journal of Engineering and Innovative Technology, 2013, 2277-3754

Neville A. M., Properties of Concrete (Fifth ed.), Essex, England: Pearson Education, Longman Group. , 2011, 978-0-273-75580-7

Paiva, Helena & Velosa, Ana & Cachim, Paulo & Ferreira, Victor, Effect of pozzolans with different physical and chemical characteristics on concrete properties, Materiales de Construcción, 2016, 66. 10.3989/mc.2016.01815

Partha Sarathi Deb, Pradip Nath, Prabir Kumar Sarker, Drying shrinkage of slag blended fly ash geopolymer concrete cured at room temperature, Procedia Engineering, 2015, 594 – 600, 10.1016/j.proeng.2015.11.066

Pengfei Huang, Yiwang Bao, Yan Yao, Influence of HCl corrosion on the mechanical properties of concrete, Cement and Concrete Research, 2005, 584-589, 10.1016/j.cemconres.2004.06.027

Petránek J., Usazené horniny jejich složení, vznik a ložiska. Zvětrávání, 1963, 573-574

Prost R., Dameme A., Huard E., Driard J., Leydecker J. P., Infrared study of structural oh in kaolinite, dickite, nacrite, and poorly crystalline kaolinite at 5 to 600 k, Clays and clay minerals, 1989, 464-468

PubChem, [online], [cit. 2019-6-18], https://pubchem.ncbi.nlm.nih.gov

Puyam S. Singh, Mark Trigg, Iko Burgar, Timothy Bastow, Geopolymer formation processes at room temperature studied by 29Si and 27Al MAS-NMR, Materials Science and Engineering, 2005, 392–402, 10.1016/j.msea.2005.02.002

Pytlík P., Technologie betonu. Fyzikální vlivy na trvanlivost, 2000, 359-366, 80-214-1647-5

Ramer G., Lendl B., Attenuated Total Reflection Fourier Transform Infrared Spectroscopy, Encyclopedia of Analytical Chemistry, 2013

Ramer G., Thermo Fisher Scientific ATR, [online], FTIR Sample Techniques: Attenuated Total Reflection (ATR) [cit. 2019-06-15]

RRUFF database, [online], [cit. 2019-6-18], http://rruff.info/

Sanz J., Madani A., Serratosa J. M., Moya J.S., Aza S., Aluminum-27 and Silicon-29 Magic-Angle Spinning Nuclear Magnetic Resonance study of the kaolinite-mullite transformation, Journal of the American ceramic society, 1988, C418 - C421, 10.1111/j.1151-2916.1988.tb07513.x

Šatava Vl., Fyzikální chemie silikátů, SNTL, 1986

Shima Pilehvar, Anna M. Szczotok, Juan Francisco Rodríguez, Luca Valentini, Marcos Lanzón, Ramón Pamies, Anna-Lena Kjøniksen, Effect of freeze-thaw cycles on the mechanical behavior of geopolymer concrete and Portland cement concrete containing micro-encapsulated phase change materials, Construction and Building Materials, 2019, 94-103, 10.1016/j.conbuildmat.2018.12.057

Shmakov N., Основы рентгеноструктурного анализа рентгеноструктурный анализ поликристаллических материалов на синхротронном излучении, ИК СО РАН им. Г.К. Борескова, 2012

Singh B., Ishwarya G., Gupta M., Bhattacharyya S. K., Geopolymer concrete: A review of some recent developments, Construction and Building Materials, 2015, 10.1016/j.conbuildmat.2015.03.036

Škvára F., Alkali activated materials or geopolymers? Ceramics - Silikáty, 2007, 173–17

Škvára F., Alkalicky aktivované materiály: geopolymery, Informátor, Česká společnost pro výzkum a využití jílů, 2008, 37

Škvára F., Geopolymer Concrete: An Ancient Material Too? Ceramics Silikáty, 2008, 296-298.

Slížková Z., Metody konzervace porézních stavebních historických materiálů, Disertační práce, 2007, 17

Steenie Edward Wallah, Drying Shrinkage of Heat-Cured Fly Ash-Based Geopolymer Concrete, Modern Applied Science, 2009, 10.5539/mas.v3n12p14

Steinerová M., Geopolymer - alternativa cementu, Lafarge Journal, 2007, 6-7

Steinerova M., Matulova L., Vermach P., & Kotas J., The Brittleness and Chemical Stability of Optimized Geopolymer Composites, Materials, 2017, 10.3390/ma10040396

Steinerová M., Vliv složení a textury geopolymerních kompozitů na jejích mechanické vlastnosti, PhD thesis, 2009, 13-14

Supriya K., X-Ray Fluorescence: Principle, Working and Application, [online], X-Ray Fluorescence: Principle, Working and Application [cit. 2019-06-15], 2019, http://www.environmentalpollution.in/pollution/regulation-and-monitoring/x-ray-fluorescence-principle-working-and-application/1910

Teplý B., Rovnaník P., Účinky mrazu na beton, Beton technologie konstrukce sanace, 2007, 42-45

Theory of XRD, [online], Arya electron optic © [cit. 2019-06-15], http://www.aryaeo.com/en/cat/71-1/theory-of-xrd.aspx

Tironi, Alejandra, Trezza M.A., Irassar, Edgardo, Scian A.N., Thermal Treatment of Kaolin: Effect on the Pozzolanic Activity, Procedia Materials Science, 2012, 343–350, 10.1016/j.mspro.2012.06.046

Trutnova V., Рентгенофлуоресцентный элементный анализ с использованием синхротронного излучения, [online], [cit. 2017-5-3], https://fen.nsu.ru/xoc/lab/lab6.html

Ulfkjrer J.P., Brincker R., Fracture Energy Of Normal Strength Concrete, High Strength Concrete And Ultra High Strength Ultra Ductile Steel Fibre Reinforced Concrete. Fracture Mechanics Of Concrete Structures, Proceedings FRAMCOS-2, D-79104 Freiburg, 1995

Weil M., Buchwald A., Dombrowski K., Development of geopolymers supported by system analysis, Proceedings of the 2nd Int. Symposium of Non-Traditional Cement and Concrete, 2005, 25-31, 80-214-2853-8

Weil M., Buchwald A., Dombrowski K., Sustainable Design of Geopolymers – Integration of Economic and Environmental Aspects in the Early Stages of Material Development, GDCH-Monograph, 2006, 297-306, 10.1007/978-1-84628-935-4_49

Weil M., Dombrowski K., Buchwald A., How to assess the environmental sustainability of geopolymers for building products? A live cycle perspective. 12th

International Conference on Modern Materials and Technologies, 2010, 10.4028/www.scientific.net/AST.69.186

Weil M., Dombrowski K., Buchwald A., Sustainable design of geopolymers – evaluation of raw materials by the consideration of economical and environmental aspects in the early phases of material development, Materials Design and Systems Analysis, 2007, 57-76, 978-3-8322-6311-9

Weil M., Ecological and economic analyses of geopolymer concrete mixes for external structural elements, BFT International, 2011, 34-42, 1865-6552